Investigating aprataxin function: roles in DNA single strand break repair and functional cellular effects

Jean Carroll

DPhil Biochemistry

University of Sussex

April 2013

Summary

Aprataxin protects nuclear and mitochondrial DNA against genotoxic stress, and loss-of-function mutations in the APTX gene cause the autosomal recessive cerebellar ataxia, Ataxia Oculomotor Apraxia 1 (AOA1) in humans. In an effort to extend current understanding of aprataxin function, this thesis examines the roles of aprataxin, especially in response to oxidative damage. Firstly, involvement of aprataxin during the gap-filling as well as the end-processing steps of single strand break repair were demonstrated using an in vitro single strand break repair assay using synthetic DNA substrates, cell-free lysates and/or recombinant proteins. Next, loss-of-function studies were conducted in $Aptx^{-/-}$ mouse embryonic fibroblasts (MEFs) and tissues from adult mice harbouring a toxic gain-of-function mutant form of superoxide dismutase1 ($SOD1^{G93A}$). Expression of the mutant $SOD1^{G93A}$ enhanced sensitivity to oxidative damage in aprataxin-deleted cells and revealed an accelerated senescence and attenuated somatic growth phenotype. Together these findings suggest that aprataxin function is involved in optimal repair of single strand breaks and is therefore critical in maintaining cell function in situations of elevated oxidative stress.

Declaration

I hereby declare that this thesis has not been and will not be submitted, in whole or in part to another university for the award of any other degree.

Jean Carroll

Acknowledgements

"Hofstadter's Law: 'Everything takes longer than you expect..
Even when you take into account Hofstadter's Law'"

Douglas Hofstadter

I first heard this quote about half way through my PhD and it really resonated with me and my experience at the time of data collecting. It has since become something of a mantra of mine. It has served me well and will continue to do so, as a reminder of the planning and perseverance necessary to succeed in the most worthwhile tasks.

There were many moments during the course of my project when completion seemed quite unimaginable, so it is with great pleasure and relief that I submit the completed version. The help of the many knowledgeable scientists of the Genome Damage and Stability Centre and the Hafezparast laboratory has been invaluable. Especially I have to thank my supervisors, Sherif El-Khamisy and Majid Hafezparast for their guidance and support.

I am especially grateful to Tony Carr for going above and beyond the call of duty to advise and encourage me.

Finally I'd like to express my deep gratitude to my mother, Petra Carroll, who has supported me in all the most practical of ways. Living with her again as an adult in order to complete my PhD has been an absolute joy: her zest for life, sweet nature and wisdom are a constant source of inspiration to me.

Funding for this project was gratefully received from Ataxia UK (grant c346).

Dedication

I would like to dedicate this thesis to the memory of my father, Jonathan Carroll, who died several years before I embarked on this project. My father encouraged me to pursue my fascination for science and taught me the importance of self-application and standing up for one's principles. He was an intelligent, hard-working man who could always be relied upon for sound advice. The many challenges I have faced during the course of this project have in the short term heightened my sense of loss at having lost my father too soon. But in the end they have revealed the constant presence of his spirit within me.

"Stop bloody procrastinating and get on with it!"

Contents

List of Figures and Tables

Appendix 1

Abbreviations

Alkaline comet assay = Alkaline single-cell agarose-gel electrophoresis

ALS = Amyotrophic lateral sclerosis

AMP = Adenosine monophosphate

AOA1 = Ataxia oculomotor apraxia 1

AOA2 = Ataxia oculomotor apraxia 2

AP site = Apurine/Apyramidine

Approx. = Approximately

APS = Ammonium persulfate

APTX = Aprataxin

$Aptx^{+/+}$ = Aprataxin competent

$Aptx^{+/-}$ = Aprataxin heterozygous

$Aptx^{-/-}$ = Aprataxin knockout

AT = Ataxia Telangiectasia

ATLD = Ataxia telangiectasia - like disorder

ATM = Ataxia telangiectasia mutated

ATP = Adenosine triphosphate

BER = Base excision repair

bp = Base pair

BRCT = Breast cancer associated protein 1 C-terminal domain

BSA= Bovine serum albumin

Ci = Curie

CHK2 = Checkpoint kinase 2

cDNA = Complementary DNA

CK2 = Casein kinase 2

CPT = Camptothecin

CS = Cockayne syndrome

CSA = Cockayne syndrome A protein

CSB = Cockayne syndrome B protein

C-terminus = Carboxyl terminusgoo

DDB1 = DNA damage binding protein 1

DDR = DNA damage response

ddH2O = double distilled H_2O

DMEM = Dulbecco's Modified Eagle's Media

DMSO = Dimethyl sulfoxide

DNA = Deoxyribonucleic acid

DNA PK = DNA dependent protein kinase

DNA PKcs = DNA dependent protein kinase catalytic subunit

dNTP = Deoxynucleoside triphosphate

DPBS = Dulbecco's phosphate buffered saline

dRP = 5'-deoxyribose phosphate

DSB = Double strand break

DSBR = Double strand break repair

DTT = Dithiothreitol

E.coli = Escherichia coli

ECL = Enhanced chemiluminescence

EDTA = Ethylenediaminetetraacetic acid

EGTA = Ethylene glycol tetraacetic acid

ERCC1 = Excision repair cross-complementing 1

FACS = Fluorescent activated cell sorting

FCS = Foetal calf serum

FEN1 = Flap endonuclease 1

FHA = Fork-Head Associated Domain

GFP = Green fluorescent protein

GGR = Global genomic repair

Gy = Gray

^{3}H = Tritium (hydrogen-3)

H2AX = Histone H2A variant X

H_2O_2 = Hydrogen peroxide

HCl = Hydrochloric acid

HDR = Homology directed repair

His = Histidine

HIT = Histidine Triad Domain

HJ = Holliday junction

HMGN1 = High mobility group nucleosome binding domain 1

HNT3 = Histidine triad Nucleotide-binding 3

hr = Hour

HR = Homologous recombination

IMAC = Immobilised metal affinity chromatography

IP = Immunoprecipitation

IPTG = Isopropyl β-D-1-thiogalactopyranoside

IR = Ionising radiation

Kb = Kilobase

KCl = Potassium chloride

kDa = Kilo dalton

LB = Luria-Bertani medium

L = Litre

LigI = DNA ligase I

LigIIIα = DNA ligase III α

M = Molar

MCSZ = Microcephaly, early-onset, intractable seizures and developmental delay

MDC1 = Mediator of DNA damage checkpoint protein 1

MEF = Mouse embryonic fibroblasts

$MgCl_2$ = Magnesium chloride

MLS = Mitochondrial localisation signal

MMS = Methyl methanesulfonate

MPG = N-methylpurine-DNA glycosylase

Mre11 = Meiotic recombination 11

MRN = Mre11/Rad50/Nbs1

NAD(P)H = Nicotinamide adenine dinucleotide phosphate

NBS1 = Nijmegen breakage syndrome 1

NEIL1 = Endonuclease VIII-like 1

NEIL2 = Endonuclease VIII-like 2

NLS = Nuclear localisation signal

N-terminus = Amino-terminus

nt = Nucleotide

NTase = Nucleotidyltransferase

OD = Optical density

OGG1 = 8-oxoguanine DNA glycosylase

OH = Hydroxyl

ORF = Open reading frame

P = Phosphate

p53 = Tumour protein 53

PAGE = Polyacrlyamide gel electrophoresis

PAR = Poly(ADP-ribose)

PARG = Poly(ADP-ribose) glycohydrolase

PARP1 = Poly(ADP-ribose) polymerase 1

PBS = Phosphate buffered saline

PCNA = Proliferating cell nuclear antigen

PCR = Polymerase chain reaction

PG = Phosphoglycolate

pI = Isoelectric point

PIKK = Phosphoinositide-3-kinase-related protein kinase

PLD = Phospholipase D

PMSF = Phenylmethanesulfonylfluoride

PNK = Polynucleotide kinase phosphatase

Pol = Polymerase

Pol β = DNA polymerase beta

Pol δ/ε = DNA polymerase delta/epsilon

Pol ι = DNA polymerase iota

Pol λ = DNA polymerase lambda

RAD50 = Radiation sensitive 50

Rad27 = Radiation sensitive 27

RFC1 = Replication factor C 1 (large subunit)

RPA = Replication protein A

ROS = Reactive oxygen species

RNA = Ribonucleic acid

RNA Pol II = RNA polymerase II

RNF8 = Ring finger protein 8

RNF168 = Ring finger protein 168

rpm = Rotations per minute

SCAN1 = Spincocerebellar axonal neuropathy 1

SD = Standard deviation

SDS = Sodium dodecyl sulphate

SDSA = Synthesis dependent strand annealing

siRNA = Small interfering RNA

SOD1 = Superoxide dismutase 1

SOD2 = Superoxide dismutase 2

SOD3 = Superoxide dismutase 3

S-phase = Synthesis phase

SSA = Single-strand annealing

SSB = Single-strand break

SSBR = Single-strand break repair

TAE = Tris base, Acetic acid, EDTA

TBE = Tris base, Boric acid, EDTA

TBST = Tris-buffered saline / Tween 20

TCR = Transcription coupled repair

TDG = Thymine-DNA glycosylase

TDP1 = Tyrosyl-DNA phosphodiesterase 1

TDP2 = Tyrosyl-DNA phosphodiesterase 2

TdT = terminal deoxyribonucleotidyltransferase

TEMED = Tetramethylethylenediamine

TLS = Translesion synthesis

TOP1 = DNA topoisomerase 1

TOP2 = DNA topoisomerase II

TTD = Tricothiodystrophy

U = unit

Ub = Ubiquitin

UNG2 = Uracil- N-glycosylase 2

UV = ultraviolet

UVDE = Ultraviolet DNA endonuclease

V = Volt

V(D)J recombination = Variable (Diverse) Joining recombination

v/v = Volume per volume

VZ = Ventricular zone

SVZ = Subventricular zone

Wt = Wild type

w/v = Weight per volume

XAB2 = pre-mRNA splicing factor gene

XLF = XRCC4-like factor

XP = Xeroderma pigmentosum

XPA = Xeroderma pigmentosum complementation group A

XPB = Xeroderma pigmentosum complementation group B

XPC = Xeroderma pigmentosum complementation group C

XPD = Xeroderma pigmentosum complementation group D

XPE = Xeroderma pigmentosum complementation group E

XPF = Xeroderma pigmentosum complementation group F

XPG = Xeroderma pigmentosum complementation group G

XRCC1 = X-ray cross complementing 1

XRCC4 = X-ray cross complementing 4

ZnF = Zinc finger motif

Chapter One

Introduction

1.1 DNA Damage and Repair

DNA encodes the genetic instructions for the development and functioning of all known forms of life. Whilst this remarkable macromolecule is of fundamental importance in all living organisms, it is also extremely sensitive to damage. Damaging agents from several sources cause a wide array of damages, or lesions, at an estimated rate of 1000 to 1,000,000 molecular lesions per cell per day. Although this constitutes only 0.000165% of the human genome, unrepaired lesions can be highly problematic for the cell, by stalling transcription, and/or leading to genetic instability (mutation) and/or cell death (Figure 1.1) (Lindahl 1993a, Limoli et al. 1998).

Sources of DNA damage may be either endogenous or exogenous. Endogenous sources include metabolic by-products such as reactive oxygen species (ROS), and errors made during replication. Exogenous sources include ionizing radiation (X-ray and γ rays), chemotherapeutic agents, and industrial chemicals such as polycyclic hydrocarbons, vinyl chloride and hydrogen peroxide, to name just a few. Further DNA damage is sustained independent of a distinct causative agent, because of the tendency of some chemical bonds in DNA to spontaneously hydrolyse, even under physiological conditions. Glycosidic bonds can hydrolyse, leading to abasic (AP) sites; and the spontaneous deamination of cytosine, adenine, guanine or 5-methylcytosine can result in uracil, hypoxanthine, xanthine and thymidine respectively (Figure 1.2) (Lindahl 1993).

Discontinuities in the sugar-phosphate backbone may be in one strand only, known as a single-strand break (SSB) or both strands, known as a double-strand break (DSB). SSBs, although not considered to be genotoxic themselves, can be converted into DSBs by collision with a replication or transcription fork (Kuzminov 2001, Hoeijmakers 2001, Kouzminova and Kuzminov 2006). DSBs are considered to be the most genotoxic lesion that can arise and if left unrepaired or repaired inappropriately can lead to a variety of chromosomal aberrations and/or mis-segregation of chromosomes during mitosis (Hoeijmakers 2001).

A complex network of biochemical systems has evolved in order to counter this threat by limiting the extent of damage sustained, detecting damage and mediating its repair. DNA damage response (DDR) impacts on a wide range of cellular events and is of particular interest to medical science as these processes are implicated in diverse human diseases. Despite the wide array of lesions and the plethora of components involved in their repair mechanisms, the DNA repair process in general remains a highly ordered, sequential one. First the lesions must be detected by sensor proteins, which recruit repair complexes. Various components of the repair complex are responsible for specific end processing, gap filling and ligation roles. Depending on the nature of the initial lesion, and to some extent the nature of the surrounding DNA (ie newly transcribed or not, hypermethylated or not), repair pathways can have elaborate and often overlapping roles. For example damage to transcribed regions of DNA are sensed and repaired preferentially in a process called transcription coupled repair (TCR).

The system demonstrates widespread redundancy: structurally and functionally distinct components compensate for one another under conditions where an activity is lost or suppressed, thus providing robustness against component or pathway failure.

Over the last half century research into the DDR has revealed it to be a remarkably complex yet elegant system that coordinates countless proteins to detect and repair myriad lesions with remarkable speed and efficiency. This is necessarily done in concert with many other DNA-dependent processes such as DNA restructuring, transcription and replication. The focus of this thesis is aprataxin – the DNA repair protein product of *APTX*, the gene mutated in the neurodegenerative cerebellar ataxia, Ataxia Oculomotor Apraxia 1. First I will introduce the major forms of DNA repair, before discussing pathologies associated with defective DNA damage response. Finally I will discuss the current understanding of aprataxin, before presenting and discussing my findings.

1.2 DNA Single-Strand Breaks

SSBs are the most frequent type of DNA lesion, arising at a rate of approximately 10,000 SSBs per cell per day (Lindahl and Nyberg 1972, Lindahl 1993a, Limoli et al. 1998, Beckman and Ames 1997). Although SSBs are not considered to be very toxic themselves, if left unrepaired and allowed to convert into DSBs via collision with replication or transcription machinery, the volume of breaks would soon overwhelm the double strand break repair (DSBR) capacity of the cell (Kuzminov 2001, Deckbar et al.

2007). Consequently, cells have evolved rapid and efficient repair pathways collectively known as single-strand break repair (SSBR) (Reviewed in (Caldecott 2008)).

The assembly of repair complexes and the progression of repair is dependent on the nature of the break - the size of the 'patch' required to fill the gap (a one-nucleotide patch is referred to as short-patch, multiple-nucleotide patches are referred to as long-patch) and the chemical nature of the break termini. Structures of the most common 3' and 5' break termini are shown in Figure 1.3 and Figure 1.4, respectively.

SSBs may result directly from damage or they may result indirectly, from excision of damaged or mismatched bases. Indirect SSBs may arise following the excision step of base excision repair (BER), nucleotide excision repair (NER) or mismatch repair (MMR). The processes by which these breaks are repaired are similar in some respects and distinct in others (Figure 1.5).

Endogenous SSBs can also arise via the abortive action of the enzyme topoisomerase I (Top1). Top1 relaxes supercoiled duplex DNA during transcription and DNA replication by nicking one strand of the DNA double helix, thereby allowing it to unwind (Roca 1995, Wang 2002). A transient cleavage complex is formed, in which Top1 becomes covalently linked via a 3' phosphotyrosyl bond to the DNA, before the nick is resealed. These nicks are usually resealed rapidly. However if a DNA or RNA polymerase collides with Top1 before the nick is resealed, then the cleavage complex can become trapped as a Top1-associated single strand break (Top1-SSB), and the SSB cannot be

religated as usual (Pommier et al. 2003). Top1-SSBs can also become trapped if the cleavage complex occurs in close proximity to another DNA lesion (Pourquier et al. 1997). In this case the Top1 peptide bound to the 3' terminus of the break must be degraded and the tyrosine residue removed. A phosphodiesterase called Tyrosyl-DNA phophodisterase 1 (TDP1) is stabilised at the SSB site via interaction with LigIIIα and performs this end processing function (Figure 1.6) (Chiang, Carroll, and El-Khamisy 2010). Mutation of the *TDP1* gene leads to the autosomal recessive cerebellar ataxia, spinocerebellar ataxia with axonal neuropathy 1 (SCAN1) (El-Khamisy et al. 2005). This disease shares some common features with AOA1 and is discussed in section 1.5.2.

The Top1 inhibitor camptothecin (CPT) increases the half-life of Top1 cleavage complexes and is used experimentally to increase the level of Top1-SSBs (Pourquier et al. 1997)). CPT treatment and TDP1 deletion have been used experimentally to stabilize single strand breaks in order to examine processes of repair (El-Khamisy et al. 2009).

1.2.1 DNA Single-Strand Break Repair

The various overlapping repair pathways dedicated to repairing SSBs are collectively known as single-strand break repair (SSBR) and proceed through three key stages of repair; detection of the break, processing of damaged termini (and gap filling if necessary), and DNA ligation (Figure 1.5). Again, the repair process selected depends upon nature of the break. The SSB may arise directly due to the action of a damaging agent, in which case it is referred to as a ‘direct’ SSB, or they may be as a result of the

excision of nucleotides as part of the Nucleotide Excision Repair (NER), Mismatch Repair (MMR) and Base Excision Repair (BER) pathways in which case it is referred to as an 'indirect' SSB and is repaired differently (i.e. Figure 1.5).

The distinction between these pathways is beginning to fade as evidence grows of multi-functional repair proteins, active across what were previously thought to be distinct pathways, and the condition-specificity of pathway election. These findings challenge the notion that specific lesions are repaired by specifically dedicated repair pathways. The redundancy and versatility of the system confound its categorization. Hence, it is perhaps more useful to discuss SSBR in terms of functionalities and mechanisms rather than ill-defined pathways. First, I will introduce the precursor processes of indirect SSBR - BER, NER, and MMR. Then I will discuss each of the steps of SSB repair in a little more detail.

1.2.2 Base Excision Repair

BER resolves DNA base damage, including oxidation and alkylation. It also repairs abasic sites, which may arise directly due to the action of a damaging agent - as accounts for an estimated 20% of all damage induced by ionizing radiation (Von Sonntag 1987, Demple and DeMott 2002) or due to the hydrolysis of bases in aqueous solution. It is estimated that 2000-10000 depurination events occur per cell per day (Lindahl and Nyberg 1972, Lindahl 1993a).

One noteworthy example of base damage is the spontaneous deamination of cytosine to uracil, which can result in the mis-incorporation of adenine and a CG→TA point mutation. Spontaneous cytosine deamination events are estimated to occur 60-500 times per cell per day (Krokan, Drabløs, and Slupphaug 2002, Barnes and Lindahl 2004). Cytosine deamination can also be caused by ROS-induced oxidative damage resulting from ionising radiation (Bjelland 2003). The most common reason for base loss is oxidation following nucleophilic attack by ROS (Ward et al. 1987, Limoli et al. 1998) - for example the formation of 8-oxo-G and thymine glycol from guanine and thymine, respectively (Figure 1.7). The oxidised form of guanine, 8-hydroxyguanine, is a commonly occurring oxidative lesion and is the most frequently used marker for oxidative base damage (Kasai, Tanooka, and Nishimura 1984; Lindahl 1993). This oxidative lesion is particularly mutagenic as adenine can be inserted opposite an 8-oxo-G lesion with the same efficiency as cytosine during DNA replication, resulting in a GC → TA point mutation (Figure 1.8) (Shibutani, Takeshita, and Grollman 1991). The continuous generation of ROS during normal cellular metabolism mean that offsetting this threat is of major importance to preserving genomic integrity and cell survival (Beckman and Ames 1997, Cadet 2003, Sander et al. 2005). A detailed discussion of oxidative damage and mechanisms for its prevention and repair is provided in section 1.4.3.

During BER, detection of base damage is achieved in a different manner to that of direct SSBs. Altered bases cause minor perturbations in the DNA helix, which are recognised and cleaved by specific DNA glycosylases. PARP1 accumulates at sites of base damage

although there is some question over whether its recruitment role here at indirect SSBs is as important as at direct SSBs (Durkacz et al. 1980, El-Khamisy et al. 2003, Campalans et al. 2013, Campalans et al. 2005). Independent of PARP1, XRCC1 (X-ray cross complementing 1) can interact with the DNA glycosylases: oxoguanine glycosylase (OGG1), nei endonuclease VIII-like 1 (NEIL1), nei endonuclease VIII-like 2 (NEIL2), methylpurine-DNA glycosylase (MPG) and apurinic/apyrimidinic endonuclease 1 (APE1) (Vidal et al. 2001, Marsin et al. 2003, Das et al. 2006, Campalans et al. 2005) enabling subsequent co-ordination of the repair complex and execution of the next necessary repair step. See Figure 1.5 for a graphic outline of the processes and components involved in the repair of a SSB arising as a BER-intermediate. A detailed account of each process is provided in section 1.2.5-1.2.8.

1.2.3 Nucleotide Excision Repair

Nucleotide excision repair (NER) is a highly versatile DNA repair pathway that resolves a wide array of DNA lesions, including bulky DNA adducts that distort the DNA double helix (Nouspikel 2009). UV radiation, especially UVB which is a component of sunlight, can cause such bulky, helix distorting adducts referred to as photodamage (Jean Cadet, Sage, and Douki 2005). Cyclobutane pyrimidine dimers (CPD) and (6-4) pyrimidone photoproducts ((6-4)PPs) are the most commonly occurring type of lesion sustained (Jean Cadet, Sage, and Douki 2005). Other bulky DNA adducts that are repaired by NER include those induced by polycyclic aromatic hydrocarbons, commonly found in air, food, drinking water and tobacco smoke (Peltonen and Dipple 1995).

NER is highly versatile by virtue of excising a short patch of DNA surrounding the lesion, bypassing the need for particular DNA repair enzymes specific to the type of damage. There are two pathways that operate within NER; global genome NER (GGR), which recognises and repairs DNA adducts that cause major distortions of the double helix anywhere in the genome, and transcription coupled repair (TCR), which repairs transcription-blocking lesions and is associated with the transcription machinery (Figure 1.9) (Gillet and Schärer 2006, Tornaletti 2009, Nouspikel 2009, Cloney 2011).

Two major damage detection complexes are involved in GGR. The XPC complex is involved in the recognition of major helix distorting lesions, such as (6-4)PPs (Kusumoto et al. 2001, Sugasawa et al. 2001, Araki et al. 2001), but is unable to recognise lesions which cause minor distortions in the double helix, such as CPDs. Recognition of these minor helix distorting lesions is performed by the XPE/XPC complex (Kim, Patel, and Choi 1995, Payne and Chu 1994). In TCR, the lesion is encountered by an elongating RNA polymerase, causing stalling of the transcription bubble (Payne and Chu 1994). Cockayne syndrome A and cockayne syndrome B proteins (CSA and CSB) are recruited to the stalled transcription complex and are required for efficient TCR (Tu, Bates, and Pfeifer 1997, Van Gool et al. 1997). Following distinct mechanisms for detection of the lesion, the GGR and TCR pathways converge (Nouspikel 2009).

The next step of NER is the unwinding of the DNA helix to form a 'bubble' around the lesion. This is carried out by the transcription factor TFIIH, a large complex consisting of 10 subunits, including the two ATP-dependent DNA helicases XPB and XPD, which have complementary 3' - 5' and 5' - 3' helicase activities respectively (Tapias et al. 2004, Wang et al. 1996). At this point the proteins XPA, XPG and the ssDNA binding protein RPA are recruited via interactions with TFIIH (Tapias et al. 2004, Volker et al. 2001). The coating of RPA on the undamaged DNA strand is essential for the incision and DNA synthesis steps (Coverley 1992). XPA is essential for NER to proceed although its precise role at this early step has not yet been determined (Tanaka et al. 1990, Gillet and Schärer 2006). One potential role it could perform is strand discrimination to ensure that RPA coats only the undamaged DNA strand, allowing proper assembly of the pre-incision complex (Sugasawa et al. 2001). Finally, ERCC1-XPF is recruited to the pre-incision complex via interaction with XPA (Park and Sancar 1994, Nagai et al. 1995).

Following formation of the denaturation 'bubble' and assembly of the pre-incision complex, dual incisions are made at the 3' and 5' ends of the 'bubble', at the ssDNA-dsDNA junctions, by the structure-specific endonucleases XPG and ERCC1-XPF respectively (Park et al. 1995, O'Donovan et al. 1994, Matsunaga et al. 1995). Following excision, the gap is filled by the replicative polymerases Pol-δ and Pol-ε in association with PCNA, and the remaining nick is ligated by LigIII, which is stabilized at the break by forming a complex with XRCC1 (Popanda and Thielmann 1992, Shivji, Kenny, and Wood 1992, Moser et al. 2007).

1.2.4 Mismatch Repair

Classical Watson-Crick base pairing - in which cytosine (C) forms hydrogen bonds with guanine (G), and thymine (T) forms hydrogen bonds with adenine (A) - is a key feature of double stranded DNA and allows for the error-free replication and maintenance of genetic information (Watson and Crick 1953).

However, occasionally during replication mismatches can occur in which non-Watson-Crick combinations of bases form bonds. The bases may both be undamaged, or an undamaged base may pair with uracil or an undamaged base may bond with a damaged base, such as 8-oxo-G with A (Fig 1.8) (Shibutani, Takeshita, and Grollman 1991).

DNA mismatches arising from base damage are generally recognised and repaired by specific DNA glycosylases during BER, while other DNA mismatches are generally recognised and repaired by a highly conserved repair pathway known as DNA mismatch repair (MMR), reviewed in (Kunkel and Erie 2005). In both cases, strand discrimination (identification of the nascent strand from the parental strand) is crucial to maintain genomic stability. In gram-negative bacteria transient hemimethylation is exploited to distinguish the strands - in the minutes following replication the parental (template) strand is methylated and the daughter strand is not (Hare and Taylor 1985). In other prokaryotes and eukaryotes the exact mechanism of strand discrimination is not clear but evidence suggests that the nicks present on the newly synthesized strand are sites for

replication factor C (RFC)-dependent loading of the DNA sliding clamp protein PCNA, in an orientation-specific manner, thereby identifying the nascent strand and recruiting repair proteins accordingly (Pluciennik et al. 2010), and that SUMOylation of PCNA acts to stabilise the replication fork (Gali et al. 2012).

In humans, MMR is initiated after replication by the recognition of mismatches by two heterodimers, MSH2-MSH6 and MSH2-MSH3 (Kunkel and Erie 2005). Next, MLH1/PMS2 is recruited to form a ternary complex, which is necessary for the completion of MMR in human cells (Kunkel and Erie 2005). PCNA appears to play a role in the recruitment of MMR proteins in the vicinity of a replication fork via interaction with MSH6 and MSH3 (Clark et al. 2000). Once the MMR machinery has been assembled at the site of damage, a nick is introduced 5' to the mismatch by PMS2 in a reaction that is dependent on PCNA. The 5' -> 3' exonuclease EXO1 then degrades the nicked strand (Genschel, Bazemore, and Modrich 2002). The single strand gap is then rapidly bound by RPA, which facilitates Pol-δ or Pol-η dependent DNA synthesis. Finally the nick is ligated by DNA ligase I (Kunkel and Erie 2005). Non-canonical variations on replication-coupled MMR are discussed in (Kunkel and Erie 2005) but will not be described here.

The foremost consequence of defective MMR is an increased abundance of point mutations across the genome. In prokaryotes this elevated mutation rate acts to improve the survival fitness of colonies under stress. In humans the improved survival fitness of sub-populations of cells can result in cancer (Kunkel and Erie 2005).

1.2.5 Single-Strand Break Detection and Signalling

Detection of direct SSBs is carried out by the enzyme poly (ADP-ribose) polymerase 1 (PARP1) (D'Amours et al. 1999, Kim, Zhang, and Kraus 2005) (Figure 1.5). Of the seventeen PARP proteins identified by homology searching of the human genome database, three (PARP1, PARP2, and PARP3) have characterized roles in DNA repair. PARP1, the most abundant of the PARP proteins, is a multi-functional DNA repair protein that binds DNA breaks with high affinity. Once bound, it catalyses the polymerisation of long branched poly(ADP-ribose) chains, predominantly upon itself, but also onto other target molecules . These include histones, DNA topoisomerases I and II, and DNA helicases (Benjamin and Gillg 1980, Bramson et al. 1993). Accumulation of PAR at DNA breaks leads to an accumulation of negative charge and the recruitment of XRCC1 (Caldecott et al. 1996, El-Khamisy et al. 2003, Masson et al. 1998), a scaffold protein which serves as an assembly platform for repair complexes comprising of several repair proteins, including PNK, DNA ligase III-α, DNA polymerase-β, APE1 and aprataxin (Marintchev et al. 2000, Loizou et al. 2004, Luo et al. 2004, Vidal et al. 2001) DNA ligase III-α and DNA polymerase-β appear to be present in all XRCC1 complexes, other factors are variable. Once maximally autoribosylated, the PARP1 molecule disassociates from the break (Ferro, Higgins, and Olivera 1983, Zahradka and Ebisuzaki 2005) and is rapidly targeted by the enzyme poly(ADP-ribose) glycohydrolase (PARG) which catalyses the degradation of the poly(ADP-ribose) polymers, allowing PARP1 to be recycled (Figure 1.5) (Cortes et al. 2004, Fisher et al. 2007).

PARP1 depletion, deletion or inhibition results in decreased rates of SSBR (Fisher et al. 2007, Le Page et al. 2003, Godon et al. 2008), as does depletion of PARG. XRCC1-dependent recruitment of repair factor complexes to SSBs facilitates rapid repair, both by concentrating repair proteins at the site of damage, and stimulating their activity and is essential for efficient repair (Vidal et al. 2001, Whitehouse et al. 2001). $Xrcc1^{-/-}$ mice do not survive past embryonic day 6.5 (Tebbs et al. 1999; Tebbs, Thompson, and Cleaver 2003). Furthermore, four Chinese hamster ovary (CHO) cell lines that harbour mutations in XRCC1 display global SSBR defects and hypersensitivity to DNA damaging agents (Caldecott 2003).

During BER, detection of base damage is achieved in a different manner to that of direct SSBs. Altered bases cause minor perturbations in the DNA helix which are recognised and cleaved by specific DNA glycosylases. PARP1 accumulates at sites of base damage although there is some question over whether its recruitment role here at indirect SSBs is as important as at direct SSBs (Durkacz et al. 1980, Campalans et al. 2013). Independent of PARP1, XRCC1 can interact with the DNA glycosylases OGG1, NEIL1, NEIL2 and MPG and APE1 (Vidal et al. 2001, Marsin et al. 2003, Campalans et al. 2005, Das et al. 2006) enabling subsequent co-ordination of the repair complex and execution of the next necessary repair step.

1.2.6 Single-Strand Break End Processing

As previously mentioned, the majority of SSBs have 'damaged' termini. For successful gap filling and DNA ligation to take place the conventional 3'OH and 5'-P chemistries have to be resolved. Consequently a wide array of DNA end-processing factors have evolved to repair the various different moieties present at damaged termini (see Figures 1.3 and 1.4 for the structure of various different moieties present at damaged termini.) The importance of DNA end-processing is highlighted by the elucidation of three human neurological disorders, found to be associated with mutations in SSBR proteins and defective end-processing since the turn of the millennium. These serious genetic disorders are; ataxia oculomotor apraxia 1 (AOA1), X-linked mental retardation (XLMR), spinocerebellar ataxia with axonal neuropathy 1 (SCAN1) and microcephaly early-onset intractable seizures and developmental delay (MCSZ), in which aprataxin, Cul4 E3 ubiquitin ligase, TDP1 and PNK are mutated respectively (Kerzendorfer et al. 2010, Date et al. 2001, Moreira et al. 2001, Takashima et al. 2002, Shen et al. 2010).

APE1 is an important SSBR factor involved in the repair of both direct and indirect SSBs. In addition to its AP lyase activity it can also process damaged 3' termini - 3'-phosphoglycolate (3’PG) with high affinity and 3'-hydroxyl (3’OH) (Figure 1.3) with low affinity (Chen, Herman, and Demple 1991, Demple and Harrison 1994; Izumi et al. 2000). APE1 is essential in mammalian cells and $Ape1^{-/-}$ mice do not survive past embryonic day 4-5 (Xanthoudakis et al. 1996, Tadahide Izumi et al. 2005).

Aprataxin is a member of the Hint-like histidine triad (HIT) superfamily (Clements et al. 2004, Brenner 2002, Kijas et al. 2006) (Figure 1.10). The forkhead associated domain at the N-terminus of aprataxin is homologous to that of PNK and mediates interactions with CK2-phosphorylated XRCC1 and XRCC4 (Figure 1.11) (Sano et al. 2004, Clements et al. 2004, Luo et al. 2004, Date et al. 2004, Gueven et al. 2004). Aprataxin and PNK have been confirmed to bind to the same CK2-phosphorylated cluster on XRCC1, and are present in two mutually exclusive complexes (Luo et al. 2004). Aprataxin has also been reported to co-immunoprecipitate with PCNA (Hirano et al. 2007), PARP1 and p53 (Gueven et al. 2004). During normal ligation 5’ adenosine monophosphate (5’AMP) is a transient intermediary (Figure 1.12). In a process called abortive ligation, 5’AMP can persist at unligated SSBs (Figure 1.13). This process is described in detail in section 1.2.8. Aprataxin catalyses the hydrolysis of 5'-AMP (the product of abortive ligations) to release AMP and restore the correct 5' terminus for ligation, a 5'P (Figure 1.14). It has also been reported that aprataxin can remove 3'P and 3'PG with very low efficiency (unlikely to compete with APE1 or PNK in vivo) (Takahashi et al. 2007). Mutations in aprataxin result in the neurodegenerative disorder AOA1 in humans, but deletion produces no phenotype in mice, suggesting that its functions are only crucial in maintaining the long-term health of the nervous system in long-lived mammals.

Tdp1 resolves DNA-peptide adducts which occur as a result of abortive topoisomerase I reactions (El-Khamisy et al. 2005) (Figure 1.6). SCAN1 is a late onset autosomal recessive ataxia caused by mutations in the TDP1 gene. SCAN1 patient cells display

elevated levels of DNA-peptide adducts and hypersensitivity to camptothecin, a chemotherapeutic drug that causes abortive topoisomerase I reactions (Miao et al. 2006). Camptothecin and Tdp1-deletion have both been used as strategies to study SSBs experimentally (El-Khamisy et al. 2009).

PNK is a bi-functional protein that possesses both 3' phosphatase and 5' kinase activity (Jilani et al. 1999, Karimi-Busheri et al. 1998, Whitehouse et al. 2001, Bernstein et al. 2005). PNK has an N-terminal FHA domain, via which it interacts with CK2-phosphorylated XRCC1 and XRCC4, and phosphatase and kinase catalytic domains (Loizou et al. 2004, Whitehouse et al. 2001, Bernstein et al. 2005). PNK is considered to be a critical protein in SSBR due to the large proportion of 3'-P termini at SSBs. This is the predominant terminus produced following excision and cleavage of base damage by a bi-functional DNA glycosylase in a β-δ-elimination reaction and following TDP1 activity during the repair of TOP1-SSBs (Figure 1.6) (Caldecott 2001, Limoli et al. 1998, O'Connor and Laval 1989, Interthal, Pouliot, and Champoux 2001). Although other proteins (e.g. APE1) possess 3' phosphatse activity, PNK function is necessary for efficient repair in humans. Mutations in PNK result in the human developmental disorder known as 'microcephaly, early-onset, intractable seizures and developmental delay' (MCSZ) (Shen et al. 2010). As a secondary role, PNK can also phosphorylate 5' OH termini, which may arise as the result of ROS-induced sugar disintegration or as a product of TDP1 activity (Ward et al. 1987, Caldecott 2001, Interthal, Pouliot, and Champoux 2001).

1.2.7 Single-Strand Break Gap Filling

Since most SSBs have at least one missing base, a gap-filling step usually follows end-processing. Depending on the extent of the gap, one of two sub-pathways will be taken. Short-patch repair is the term applied to the process in which a one-nucleotide gap is filled with a single nucleotide (Dianov, Price, and Lindahl 1992) and long-patch repair refers to the process whereby a patch of 2 or more nucleotides is synthesized, displacing a 5' single-stranded flap which is then cleaved by flap endonuclease 1 (FEN1) (Figure 1.15) (Frosina et al. 1996, Klungland and Lindahl 1997, Kim, Biade, and Matsumoto 1998, Mosbaugh and Linn 1984, Singhal, Prasad, and Wilson 1995). These processes described are reviewed in (Caldecott 2001).

Numerous reports of defective short-patch repair using cell-free extracts from Pol-$\beta^{-/-}$ MEFs strongly suggest an important role for Pol-β in short-patch repair (Singhal, Prasad, and Wilson 1995, Sobol et al. 1996, Kubota et al. 1996, Klungland and Lindahl 1997, Karimi-Busheri et al. 1998, Fortini et al. 1998, Winters et al. 1999, Dianov et al. 1999, Whitehouse et al. 2001, Podlutsky et al. 2001, Pascucci et al. 2002, Dianova et al. 2004, Vens, Hofland, and Begg 2007). While these reports demonstrate Pol-β to be the most efficient gap-filling agent at single-nucleotide gaps, it is most certainly not the only one. Quiescent Pol-$\beta^{-/-}$ MEFs are sensitive to γ-irradiation, while their cycling counterparts are not (Niedernhofer et al. 2006, Vermeulen et al. 2007, Vermeulen et al. 2008) suggesting that replication-coupled pathways can adequately compensate for loss of Pol-β function. Another member of the X-family of polymerases, Pol-λ, has 5-dRP lyase

activity and can also carry out single nucleotide incorporation during short-patch repair in the absence of Pol-β, as can Pol-ι - a member of the Y-family of polymerases (Bebenek et al. 2001, Rajendra Prasad et al. 2003, Vens, Hofland, and Begg 2007). The Y-family polymerases are low-fidelity polymerases, which are involved in the bypass of DNA lesions during translesion synthesis (Reviewed in (Prakash, Johnson, and Prakash 2005)), the importance of which is highlighted by the hypersensitivity of Pol-ι $^{-/-}$ fibroblasts to hydrogen peroxide (Petta et al. 2008).

The whole system exhibits extensive redundancy - where one function is missing or depleted, there are generally several others capable of compensating. This is especially true of gap-filling as a wide array of proteins possess overlapping DNA polymerase activity. Several polymerases have been implicated in long-patch repair. Some reports suggest that Pol-β carries out strand displacement synthesis during long-patch repair in a reaction that is stimulated by the presence of PARP1 and FEN1 (Dianov et al. 1999, Prasad et al. 2001, Prasad et al. 2000, Liu et al. 2005, Balakrishnan et al. 2009), while some reports suggest that Pol-β is only responsible for the initiation of synthesis and other polymerases carry out the strand displacement reaction (Parlanti et al. 2004, Podlutsky et al. 2001, Dianov et al. 2001, Dianov et al. 1999). In vitro repair experiments using extracts from Pol-β$^{-/-}$ MEFs show that the replicative polymerases Pol-δ and Pol-ε can also carry out strand displacement synthesis in a reaction that is dependent on the presence of proliferating cell nuclear antigen (PCNA) (Dresler and Lieberman 1983a, Dresler and Lieberman 1983b, DiGiuseppe and Dresler 1989, Frosina et al. 1996, Klungland and Lindahl 1997, Stucki et al. 1998, Fortini et al. 1998, Parlanti

et al. 2004).

1.2.8 Single-Strand Break Ligation

Once the gap has been filled, the final stage of SSBR is DNA ligation, whereby the sugar-phosphate backbone of DNA is resealed. This process is carried out in mammalian cells by two DNA ligases; DNA Ligase III-α (LigIIIa) and DNA Ligase I (LigI) (Reviewed in (Ellenberger and Tomkinson 2008). The ligase most associated with short-patch repair is LigIIIα (Brookman, Tebbs, and Allen 1994, Caldecott et al. 1994, Cappelli et al. 1997, Sleeth, Robson, and Dianov 2004). LigIIIα is one of three polypeptides generated by the LIG3 gene; the nuclear version that interacts with XRCC1 (LigIIIα), a mitochondrial version (mtLigIIIα), which differs to the nuclear version only by the presence of an N-terminal mitochondrial localisation signal (MLS), and a germ-line specific isoform called LigIIIβ, which is generated by an alternative splicing event and lacks the C-terminal BRCT domain (Lakshmipathy and Campbell 1999, Perez-Jannotti, Klein, and Bogenhagen 2001, Mackey et al. 1997).

LigIIIα binds XRCC1 via a constitutive interaction between each of their BRCT domains that is required for stability of the ligase in vivo (Caldecott et al. 1994, Caldecott et al. 1995, Nash et al. 1997, Taylor et al. 1998, Dulic et al. 2001). LigIIIα can also ligate DSBs, an activity which requires both the N-terminal ZnF and the catalytic core (Cotner-Gohara et al. 2008).

LigI is the ligase most associated with long-patch repair (Karimi-Busheri et al. 1998, Matsumoto et al. 1999, Pascucci et al. 1999, Prasad et al. 1996, Winters et al. 1999, Sleeth, Robson, and Dianov 2004). Its role here is dependent on its interaction with PCNA (Levin et al. 1997, Levin et al. 2000). Aside from its role in SSBR, LigI also plays an essential part in the maturation of Okazaki fragments during DNA replication (Waga and Stillman 1998).

The roles of LigI and LigIIIα have mostly been elucidated as a result of in vitro repair assays and two recent studies in vivo suggest there may be greater cross-over between ligase functionalities than previously appreciated (Simsek et al. 2011, Katyal and McKinnon 2011, Gao et al. 2011). DNA ligases are nucleotidyltransferases (NTases) that exploit a high energy cofactor (ATP) to catalyse phosphodiester bond formation in a universal three-step reaction mechanism (Figure 1.12).

In the first step of DNA ligation, the ligase reacts with ATP to produce a ligase-adenylate intermediate in which AMP is covalently linked to the active site lysine via a phosphoamide bond, and a pyrophosphate molecule is released (Olivera et al. 1968, Harvey et al. 1971, Weiss, Thompson, and Richardson 1968, Bernard Weiss and Jacquemin-Sablon 1968, Gumport and Lehman 1971, Lehmann 1978). This reaction is very energetically favourable and therefore very rapid. During this step an oxygen of the 5'P group attacks the phosphorus of the AMP group, dispelling the lysine and transferring the adenylate group onto the 5'P, forming a 5'-AMP DNA intermediate (Odell et al. 2000, Nair et al. 2007). This is accompanied by a conformational change in

the ligase and a possible reconfiguration of metal ions in the active site (Odell et al. 2000, Nair et al. 2007).

The final step of ligation is the resealing of the phosphodiester backbone (Lehmann, 1978). During this step the non-adenylated ligase catalyses the nucleophilic attack of the 5'AMP by the 3'OH, thereby displacing the AMP and joining the two polynucleotides by formation of a phosphodiester bond (Odell et al. 2000; Crut et al. 2008; Nair et al. 2007). This step is very rapid - the rate of phosphodiester bond formation is much faster than the adenylation of the DNA (Crut et al. 2008).

Under certain circumstances, such as a premature attempt to ligate a SSB with a damaged 3' terminus, the ligation reaction will stall and a stable abortive ligation intermediate (5'-AMP) will persist (Figure 1.13). Aprataxin can cleave 5’-AMP to restore the ligatable 5’-P terminus (Ahel et al. 2006). The discovery of the neurodegenerative disorder AOA1, a disease caused by mutations in APTX and resulting loss of function in the gene product aprataxin - the protein that cleaves 5'-AMP - suggests that the persistence of abortive ligation intermediates is toxic (Date et al. 2001, Barbot et al. 2001).

1.2.9 Replication-Coupled Single-Strand Break Repair

The SSBR pathways described previously are very rapid and seem to operate throughout the cell cycle and are therefore known as 'global' SSBR (Reviewed in (Caldecott 2008)).

However there is some evidence that alternative SSBR pathways operate at different times throughout the cell cycle, specifically during S-phase. It has been shown that XRCC1 co-localises with PCNA at replication foci (Fan et al. 2004) and a complex consisting of APE1, uracil N-glycosylase 2 (UNG2), XRCC1 and Pol-β, replicative polymerases Pol-α, Pol-δ/ε and DNA ligase I co-associates with DNA replication proteins in human cycling cells (Parlanti et al. 2007, Otterlei et al. 1999). It has also been shown that the BRCT domains within XRCC1 have a role in the repair of SSBs during S-phase (Taylor et al. 2000). It may be that a core SSBR complex associates with the replication fork during S-phase and repairs SSBs that hit the replication fork. This hypothetical pathway has been termed replication-coupled SSBR (RC-SSBR) (Caldecott 2008, Caldecott 2001, Caldecott 2003). It is considered likely that this hypothetical pathway would resemble long-patch repair due to the fact that many of the proteins involved in long-patch repair, such as Pol-δ/ε, PCNA, FEN1 and LigI, are also present in the replication machinery (Fan et al. 2004, Parlanti et al. 2007, Otterlei et al. 1999) but may differ in detection mechanisms.

Confirmation of the existence of this pathway would help to explain the lack of cancer predisposition in SSBR-defective disorders, as unrepaired SSBs repaired by a RC-SSBR before the encountering the replication fork would avoid conversion into a double strand break. It has also been suggested that this pathway could operate in conjunction with the DSBR pathway homologous recombination (HR), due to the fact that SSBs converted into DSBs upon collision with the replication fork are substrates for HR (Kouzminova and Kuzminov 2006, Kuzminov 2001).

1.2.10 Single-Strand Breaks and Transcription

The continuing function of a cell depends on the unperturbed transcription of the coding regions of the genome and therefore DNA lesions within these transcribed regions of the genome can result in a number of deleterious effects. Transcribing past the damage can result in mutations due to incorrect base insertion opposite the lesion, the presence of the lesion can affect the rate of transcription, altering the expression level of the damaged gene, and finally transcription can be completely blocked, leading to loss of the transcript (Zhou and Doetsch 1994, Tornaletti 2009).

The existence of dedicated repair pathways, termed transcription-coupled repair (TCR), to recognise and repair transcription-blocking lesions is well established (Tornaletti 2009, Nouspikel 2009, Lagerwerf et al. 2011). Human disorders, such as the microcephalic cockayne syndrome, which are associated with defects in the repair of DNA lesions in transcribed genes, highlight the cytotoxicity of unrepaired transcription-blocking lesions (Lehmann 2003). Cyclobutane pyrimidine dimers (CPD) and intrastrand crosslink are confirmed transcription-blocking lesions that can be repaired by TCR. There is evidence that SSBs can also block RNA polymerases and that SSBR has a role in protecting against transcription-blocking DNA damage.

Upon collision with transcription machinery Top1 cleavage complexes convert into abortive Top1-SSBs (Kroeger and Rowe 1989, Wu and Liu 1997). A significant portion of the accumulating abortive Top1-SSBs seen in TDP1-defective cell lines following incubation with camptothecin (CPT), a Top1 poison that increases the half-life of Top1 cleavage complexes, is dependent on the presence of active transcription as demonstrated by their disappearance following incubation with the RNA polymerase inhibitor α-amanitin (Miao et al. 2006, El Khamisy et al. 2005). Moreover, CPT-induced SSBs still accumulate in TDP1-defective cell lines in the presence of the replication inhibitor aphidicolin showing that TDP1-dependent SSBR has a role in protecting the cell against transcription blocking lesions (Miao et al. 2006, El Khamisy et al. 2005). Furthermore, the DNA glycosylase NEIL2 has also been shown to associate with RNA polymerase II and to preferentially repair oxidised bases within transcribed genes, further supporting a role for SSBR in the repair of transcription-blocking lesions (Banerjee et al. 2011).

1.3 DNA Double-Strand Breaks

DNA double strand breaks (DSB) are discontinuities in both strands of the DNA double helix and may arise from both endogenous and exogenous sources. Although these lesions are rare: only ten DSBs are estimated to arise per cell per day based on experiments performed on early passage primary human fibroblasts (Lieber et al. 2003, Lieber and Karanjawala 2004, Martin et al. 1985), DSBs are considered to be

particularly genotoxic. A single unrepaired DSB can be sufficient to induce apoptosis (Rich, Allen, and Wyllie 2000). Failure to repair these breaks correctly can lead to chromosomal rearrangements, including translocations and deletions, chromosomal mis-segregation during mitosis and/or cell death (Hoeijmakers 2001).

DSBs can be generated directly by the formation of two direct SSBs nearby but on opposite strands, by ionizing radiation or radiomimetic chemicals. Free radical attack of the sugar-phosphate backbone of the DNA double helix results in the disintegration of two closely located oxidised sugars on anti-parallel DNA strands (Ward et al. 1987, Limoli et al. 1998).

Ionising radiation is a major source of DSBs as the IR particles create localised clusters of ROS as they pass through the cell, mostly from water, increasing the chance that two closely spaced lesions will arise. Indeed, whilst hydrogen peroxide induces one DSB for every ~2000 SSBs, IR generates one DSB for every 25 - 40 SSBs (Ward et al. 1987, Limoli et al. 1998). Endogenous DSBs can arise from a number of sources; as the result of the abortive activity of type II DNA topoisomerases which transiently nick both strands of the duplex in nearby loci, by the collision of a replication fork with a SSB during DNA replication, or from mechanical stress on chromosomes such as during chromosomal segregation in mitosis (Adachi et al. 2003, Kuzminov 2001, Hoeijmakers 2001, Kouzminova and Kuzminov 2006).

1.3.1 DNA Double-Strand Break Repair

The efficient repair of double strand breaks is of prime importance for the maintenance of genomic integrity. DNA double strand break repair can be divided into two major sub-pathways: Non-Homologous End Joining (NHEJ) and Homology Directed Repair (HDR). These pathways involve different repair complexes, have different levels of repair rate and fidelity and take place preferentially at different stages of the cell cycle.

1.3.2 Double-Strand Break Signalling

DSB detection, signal transduction and activation of checkpoints in controlled by two crucial kinases, ATM and ATR. ATM detects DSBs and disruptions in chromatic structure, whereas ATR acts primarily in response to stalled replication forks. Both kinases phosphorylate downstream targets in a signal transduction cascade, eventually leading to cell cycle arrest (Bakkenist and Kastan 2003, Goodarzi et al. 2006).

ATM belongs to a family of serine-threonine kinases, which possess structural homology to phosphoinositide I (PI3) kinases, known as the PI3 kinase-like-kinase (PI3KK) family which include DNA PK, and plays an important role in the coordination of events that take place during DSBR (Abraham 2004). ATM is rapidly recruited to DSBs whereupon it phosphorylates serine 139 on the histone variant H2AX to produce γ-H2AX (Burma et al. 2001). ATM activity is partially dependent on the presence of MRN, another DSB sensor that is believed to act in concert with ATM to promote

efficient DSBR (Uziel et al. 2003, Lavin 2007, Williams, Williams, and Tainer 2007).

Upon formation of γ-H2AX, the mediator of DNA damage checkpoint protein 1 (MDC1) is recruited to the break, is phosphorylated by ATM, and binds to the phosphorylated histone (Manuel Stucki and Jackson 2004; Lukas et al. 2004), where it is thought to acts as a protein platform to help stabilise DDR proteins at the lesion. It also acts to propagate the γ-H2AX signal by recruiting more ATM to the break via its FHA domain, which then phosphorylates H2AX further away from the break to produce more γ-H2AX (Lou et al. 2006). H2AX phophorylation can spread for up to 2 megabases either side of the DSB, which is important for orchestrating the DDR (Celeste et al. 2002; Harper and Elledge 2007).

A cascade of ubiquitin modification at DSB sites signals recruitment of many more effectors of the DDR. The E3 ubiquitin ligase ring finger protein 8 (RNF8) interacts with phophorylated MDC1 at the break and ubiquitinates H2A and γ-H2AX in the vicinity of the break (Huen et al. 2007, Kolas et al. 2007, Mailand et al. 2007). A second and third E3 ligase are then recruited - RNF168 and HERC2, to stimulate further ubiquitination (Doil et al. 2009; Grant S Stewart et al. 2007). The spreading ubiquitin chains promote the recruitment of RAP80, BRCA1 and 53BP1 (Huen et al. 2007; Kolas et al. 2007; Lavin 2008). 53BP1 plays an important role in the DDR although it is not yet clearly understood. Cells from patients with loss-of-function mutations in ATM do not arrest at the S phase checkpoint following irradiation (Painter 1981) and are consequently hypersensitive to it (Littlefield et al. 1981).

1.3.3 Non-Homologous End Joining

NHEJ is the primary method of DSBR in non-proliferating or G1-phase cells (Takata et al. 1998). It is high-fidelity DSBR pathway and since NHEJ does not require a homologous sequence for accurate repair it operates throughout the cell cycle and is of particular importance during G0, G1 and early S-phase when a sister chromatid is not available for use as a template (Takata et al. 1998, Sonoda et al. 2006, Delacôte and Lopez 2008).

Classical NHEJ

The poly (ADP) ribose polymerase protein PARP3 is activated upon detection of a break, ribosylating itself and other substrate proteins such as histones to signal the break (Rulten et al. 2011). Ku70/80 heterodimers rapidly bind both ends of the DSB and form a ring-like structure that encircles the DNA and translocates along the strands, making the ends of the DNA accessible for recruitment of DNA-dependent protein kinase catalytic subunit (DNA PKcs), which in concert with Ku and DNA forms the active holoenzyme DNA PK (Jin et al. 1997, Uematsu et al. 2007, Suwa et al. 1994). XRCC4, the scaffolding protein, facilitates recruitment of repair factors and provides a platform for the activated DNA PK to align the broken ends and form a 'synaptic complex' (DeFazio et al. 2002). The synaptic complex acts to tether the ends of the DSB to each other and to offer protection against unwanted processing by nucleases. The assembly of the DNA PKcs/Ku/DSB synaptic complex also stimulates the serine/threonine protein kinase activity of DNA PK. Among other proteins, it also targets itself - causing a

conformational change that allows end-processing enzymes to access the ends of the double-strand break (Meek et al. 2007).

The next stage of NHEJ is the processing of the DNA termini at the ends of the DSB to restore ligatable 3'-OH and 5'-P termini. Like SSBs, DSBs can have a multitude of different chemistries at the DNA ends, depending on the source of the damage, and therefore require a diverse set of end-processing enzymes for repair. The Werner protein (WRN) plays an important role here - highlighted by the clinical manifestation of the progeroid syndrome, Werner syndrome - wherein the protein cannot be appropriately transported to the damage site (Delacôte and Lopez 2008). Artemis is a key NHEJ end processing factor that is reported to possess a number of different repair activities, including 5' -> 3' exonuclease and 3'-PG processing activity as well as the ability to resolve DNA hairpins (Goodarzi et al. 2006, Ma et al. 2002). Artemis is recruited to DSBs via an interaction with DNA PKcs, and is only activated for end-processing upon phosphorylation by the DNA damage inducible protein kinase ataxia telangiectasia mutated (ATM) (Ma et al. 2002, Goodarzi et al. 2006). ATM and ataxia telangiectasia and Rad3-related (ATR) are serine/threonine protein kinases that signal DNA damage and activate the DNA damage checkpoint, leading to cell-cycle arrest during repair.

PNK also interacts with CK2-phosphorylated XRCC4 and it is believed to perform a similar end processing role in NHEJ as it does in SSBR (wherein it interacts with XRCC1) (Limoli et al. 1998, Chappell et al. 2002, Segal-Raz et al. 2011; Bernstein et al. 2005, Koch et al. 2004, Mani et al. 2010). Aprataxin has also been implicated in DSBR.

It interacts with CK2-phosphorylated and XRCC4 and has been shown to remove adenylate groups from the 5' termini of both SSBs and DSBs in vitro (Clements et al. 2004, Rass, Ahel, and West 2007).

Another end-processing factor that has been implicated in NHEJ is tyrosyl-DNA phosphodiesterase 2 (TDP2), a protein that resolves damage arising from abortive topoisomerase 2 (Top2) activity. Top2 induces DSBs as part of a reaction to relax DNA supercoils. This reaction mechanism involves formation of an intermediate in which the topoisomerase is covalently linked to the 5' terminus of the break via a phosphotyrosyl bond (Wang 2002, Nitiss 2009). Normally this is a very transient intermediate and the DSB is rapidly resealed in the final stage of the reaction, but under certain circumstances, such as in the presence of Top2 poisons like etoposide, a stable DSB with 5'-Top2 may persist. Tdp2 is a recently identified phosphodiesterase that cleaves 5'-phosphotyrosyl bonds and has been shown to repair Top2-DSBs (Zeng et al. 2011).

DSB processing can lead to deletions and gaps in the code, which require filling by a DNA polymerase. The X family of DNA polymerases have been implicated in carrying out gap-filling during NHEJ, including polymerases μ and λ, which interact with Ku and XRCC4/LigIV, and terminal deoxyribonucleotidyltransferase (TdT), which interacts with Ku, (Nick McElhinny et al. 2000, Mueller et al. 2008).

Once the DNA termini have been processed, and any gaps have been filled, the final step in NHEJ is to reseal the strands. Ligation of the DSB is carried out by DNA LigIV

in a complex with XRCC4 (Critchlow, Bowater, and Jackson 1997, Grawunder et al. 1997, Grawunder et al. 1998). The recruitment and stability of XRCC4-LigIV at the DSB is mediated by interactions with Ku70/80, DNA PK and the ADP-ribose binding protein, aprataxin and PNK- like factor (APLF) (Mehrotra et al. 2011; Rulten et al. 2011; Rulten et al. 2008; Macrae et al. 2008; Calsou et al. 2003; McElhinny et al. 2000). XRCC4 –like factor (XLF) is another factor recruited to DSBs via an interaction with Ku70/80 and functions to stimulate NHEJ (Ahnesorg, Smith, and Jackson 2006, Yano et al. 2008). XLF is similar in structure to XRCC4 and facilitates rapid end-joining by stimulating DNA ligation and promoting the re-adenylation of LigIV following ligation (Gu et al. 2007, Riballo et al. 2009, Hammel et al. 2011). An overview of classical NHEJ is shown in Figure 1.16.

Mutation or suppression of classical NHEJ proteins has serious consequences in mammals. Mutations in DNA-PKcs can cause defective V(D)J recombination and arrested B- and T- lymphocyte development in severe combined immune-deficient (SCID) mice (Finnie et al. 1996, Blunt et al. 1995). Interestingly, this defect can be partially rescued by radiation treatment or radiomimetic drugs, possible by activation of alternative double strand break repair mechanisms (Danska et al. 1994, Murphy et al. 1994). Deletion of PARP1 (one function of which is to suppress recombination) rescues lymphocyte development in the SCID mouse (Morrison et al. 1997). This suggests that elevated levels of recombination in the absence of PARP1 aid V(D)J recombination in the absence of DNA-PK activity (Morrison et al. 1997, Chatterjee, Berger, and Berger 1999).

Consistent with this, an alternative NHEJ pathway involving PARP1, XRCC1, and DNA ligase III-α has been proposed (Audebert, Salles, and Calsou 2004). Recombinant PARP1, XRCC1 and DNA ligase III-α are able to repair DNA double strand breaks with blunt or 5' or 3' recessed termini in vitro. Exclusion of any of these proteins abolished repair activity indicating that all three proteins are required (Audebert, Salles, and Calsou 2004).

1.3.4 Homology Directed Repair

Repair pathways that utilize a homologous sequence from an undamaged DNA template to repair a DSB are known collectively as homology-directed repair (HDR) (Figure 1.17) (Hartlerode and Scully 2010; Pâques and Haber 1999). These repair mechanisms are of prime importance during the late S and G2 phases of the cell cycle owing to the presence and proximity of sister chromatids (Delacôte and Lopez 2008; Sonoda et al. 2006).

The Mre11-Rad50-NBS1 (MRN) complex is critical in the early response to DSBs leading to HDR (Williams, Williams, and Tainer 2007). Amongst its many other roles, it is thought that two MRN complexes carry out a similar function during HDR to the DNA PKcs/Ku/DSB synaptic complex during NHEJ, by tethering the ends of a DSB together via homodimerisation of the Rad50 subunit (Hopfner et al. 2002, Williams et al. 2008, Lavin 2007) . Following detection of the break, the DNA ends are resected in a 5'-

3' direction to generate 3' ssDNA overhangs with a 3'-OH terminus. MRN, in concert with CtIP, has been shown to initiate DNA resection by trimming the DNA ends (Sartori et al. 2007; Huertas and Jackson 2009; Coleman and Greenberg 2011, Mimitou and Symington 2008). End resection is then mostly carried out by two nucleases, DNA2 and EXO1, in combination with the helicase BLM (Z. Zhu et al. 2008; Mimitou and Symington 2008). BRCA1 has also been implicated in the regulation of DNA resection (Coleman and Greenberg 2011).

The ssDNA generated by resection is rapidly bound by the ssDNA binding protein RPA which melts the DNA secondary structure (Sung and Klein 2006). RPA is then displaced from the ssDNA by the Rad51 recombinase via mediator proteins BRCA1/BARD1 and BRCA2/DSS1 to form a Rad51 nucleofilament, which carries out the strand invasion and homology search steps of HDR (Wong et al. 1997, Pellegrini et al. 2002, San Filippo et al. 2006). Strand invasion involves capture of the intact duplex by the Rad51 nucleofilament which forms a D-loop intermediate, where the 3' termini of the invading strand is primed for DNA synthesis. It is at this point that the various theoretical pathways of HDR diverge.

In the homologous recombination (HR) pathway, the resected second DNA end is captured by the migrating D-loop, forming a double Holliday Junction (HJ) (Pâques and Haber 1999, Hartlerode and Scully 2010). These double HJs are then resolved enzymatically by a number of structure-specific endonucleases (Wu and Hickson 2003, Chen et al. 2001, Rass et al. 2010). Depending on the orientation of resolution this can

lead to either a crossover or non-crossover event (Pâques and Haber 1999, Hartlerode and Scully 2010). In the synthesis-dependent strand-annealing pathway (SDSA), following DNA synthesis and D-loop migration, the newly synthesised invading strand is displaced and anneals back to the second resected end of the break (Pâques and Haber 1999, Hartlerode and Scully 2010).

Single-strand annealing (SSA) is an error prone HDR pathway that takes place when a DSB arises between two direct repeats (Pâques and Haber 1999, Hartlerode and Scully 2010). Resection exposes the repeats, generating two complementary single strands that anneal together. The resulting DNA flaps generated are excised and the DNA nicks are ligated by ligase IV (McElhinny et al. 2000).

Finally, break-induced recombination (BIR) proceeds when a one-ended DSB invades the intact duplex, forming a recombination induced replication fork (Paques and Haber 1999, Hartlerode and Scully 2009). This may be a particularly important repair pathway during DNA replication as a way of restarting a collapsed replication fork caused when an elongating fork collides with a SSB (Kuzminov 2001).

1.4 DNA Damage Response in Ageing and Disease

The processes of DNA repair are not perfect and over time unrepaired or misrepaired damage accumulates in the genome. In non-dividing cells, DNA damage accumulation may lead to cell death or loss of gene expression and impaired cell function. The

accumulation of unrepaired DNA damage is most pronounced in long-lived non-replicating or slowly replicating cells, such as neurons, skeletal and cardiac muscle (Barzilai 2007, Caldecott 2008). In dividing cells, accumulation of DNA damage may additionally lead to mutations; resulting in function impairment, cell death or cancer. The deleterious consequences of persisting DNA damage, have already been outlined, and will be discussed in more detail in terms of human pathology in Section 1.5. But it is worth noting that the inherent imperfections of the DDR are critical in driving two fundamental forces of biology; evolution (of the species) and ageing (of the individual).

Evolution

When DNA damage is left unrepaired, or is repaired erroneously, a mutation may result (e.g. Figure 1.8). In dividing cells, mutations may propagate into the genome of the cell's progeny. When mutations occur in a germ line cell, then the mutation may be passed on to gametes and the organism's offspring. Mutations may either:

a) have no effect

b) alter the gene product

c) prevent the gene from functioning

When mutations change the gene product, the outcome will most often be deleterious or neutral. But occasionally the change may be beneficial, conferring a survival/reproductive advantage to the host, and favouring the propagation of their genetic material over that of their competitors by the processes of natural selection (Darwin and Peckham 1959).

Mutations can involve large sections of a chromosome becoming duplicated (i.e. by a recombination event), which can introduce extra copies of a gene into a genome. Extra copies of genes are the raw material by which new genes evolve (Lynch and Conery 2000, Hughes 2002). Hence we can see evidence of gene families in which many divergent genes descend from a single ancestral gene (i.e. the histidine triad (HIT) family of nucleotide hydrolases and transferases, of which aprataxin is a member)(Date et al. 2001, Moreira et al. 2001).

The rate of evolution in a species, or a gene, is a function of the rate of mutation. Consequently, the rate and accuracy of DNA repair mechanisms have an influence over the process of evolutionary change (Maresca and Schwartz 2006). Evolution allows a species to adapt to environmental changes in order to survive and reproduce.

Ageing

Whilst ageing typically involves many deleterious effects it also has several benefits at the level of the individual and the population. Ageing is synonymous with senescence at both the cellular and the organismal level: i.e. the cell/organism broadly switches from a "growth" phase to a "maintenance" phase. At the expense of rapid cell turnover and growth, slower and more precise repair mechanisms are employed to preserve function (Hoeijmakers 2007). At the level of the whole organism, diminishing fertility with age in mammals means that reproduction generally takes place while the adult is able to support their young, and in modern humans the emergence of the late adulthood age group is accredited with the development of human culture as it permits the clear transmission of information from one generation to another, and the division of labour

such as childcare, and crop cultivation (Caspari and Lee 2004). Hence, the biological processes involved with ageing protect genomic integrity and benefit populations. Eventually though, these systems start to fail and age-related disease emerge.

The cellular compartment, part of the chromosome and nature of DNA lesion most associated with age-related disease will be briefly discussed in order to highlight their importance with respect to neurological disease.

1.4.1 Mitochondria

Mitochondrial DNA (mtDNA) seems to be more susceptible to DNA damage and consequently sustains higher mutation rates (an estimated ten times higher) than nuclear DNA (nDNA). Several factors may contribute for the heightened damage susceptibility including exposure to high levels of reactive oxygen species produced during oxidative phosphorylation, lack of protective histones, and a limited capacity for DNA repair (Beal 1996, Croteau and Bohr 1997, Lightowlers et al. 1997). The tissues most associated with age-related degeneration (neurons and skeletal/cardiac muscle) are those with the most mitochondria. Both inherited and somatic mitochondrial mutations are associated with a wide variety of degenerative disorders and cancers (Wallace, 1994, Wallace, 2001).

In mice, when catalase expression is increased in mitochondria, oxidative damage in skeletal muscle is decreased and lifespan is extended by around 20% (Schriner et al.

2005, Linford, Schriner, and Rabinovitch 2006), suggesting that mitochondria are a significant source of the oxidative damages contributing to ageing.

1.4.2 Telomeres

The ends of eukaryotic linear chromosomes are double stranded discontinuities that must be protected from the processes of DSBR. Telomeres are specialized DNA-protein structures that cap the ends of chromosomes (McEachern, Krauskopf, and Blackburn 2000), thereby protecting them from degradation by nucleases and replicative stress, and fusion by cellular DNA repair processes (Figure 1.18) (Rodier et al. 2005). Functional telomeres are essential for maintaining the integrity and stability of genomes (Blackburn 1990). In vertebrate cells, telomeres consist of several kilobase pairs of non-coding DNA tandem repeats of the sequence TTAGGG, a few hundred base pairs of single-stranded DNA at the 3' end of the telomeric DNA tract, and a host of proteins that organize the telomeric double and single-stranded DNA into a protective three dimensional structure (Rodier et al. 2005).

The terminal non-coding telomeric DNA whose presence stabilizes chromosomes was first reported the best part of a century ago (Muller 1938, McClintock 1941). Over the last four decades, much work has been undertaken to understand the structure, function and biological impact of telomeres. In 2009 Drs Elizabeth Blackburn, Jack Szostak and Carol Greider won a Nobel Prize for their work on how chromosomes are protected by

telomeres and the enzyme telomerase (Nobel Prize, 2009).

DNA polymerases replicate DNA in the 5'→ 3' direction, and are unable to start DNA synthesis de novo, so with each round of replication, the lagging strand contains a 3' single stranded DNA overhang. Thus DNA-dependent RNA polymerase is used to synthesize an 8 to 12 bp stretch of RNA primer annealed to the 3'single stranded DNA that is able to prime DNA synthesis of 'Okazaki fragments' from its 3' hydroxyl end (Okazaki et al. 1968). The RNA primer is later removed and filled by a DNA polymerase (Rossi and Bambara 2006). However, there remains a small overhang at extreme 3' ends because the placement of the RNA template leaves at least a 8-12 bp gap from the end of the strand (Figure 1.19). Without replenishment of the non-coding telomeric 'buffer' DNA, over continuous rounds of replication the ends of chromosomes would progressively shorten and genomic information would be lost (Saldanha, Andrews, and Tollefsbol 2003). This is known as the 'End Replication Problem' and is solved by telomerase - a reverse transcriptase that performs this telomere replenishment role (Greider and Blackburn 1985; Blackburn 1990).

Telomerase is a ribonucleoprotein complex that extends the 3' single strand overhang with TTAGGG repeats using an RNA template (Greider and Blackburn 1985). The lagging strand is then filled in by DNA polymerase-α, which contains a DNA primase (which synthesized the RNA primer complementary to the new 3'single strand overhang) as one of its subunits (Lee et al. 2006) (Figure 1.19). With each cell cycle about 50-150 base pairs of terminal DNA is still necessarily lost, leading to

progressively shortened 5' termini in the daughter strand (Sozou and Kirkwood 2001). Without telomeres, the progressive shortening of the chromosome would lead to rapid loss of DNA sequence, and genomic instability - a common cause and hallmark of cancer (Gray and Collins 2000). Progressive shortening of the non-coding telomeres acts as a cellular clock and is associated with ageing (Vijg and Dollé 2002). As such, appropriate telomere maintenance represents a balance between ageing and cancerous growth.

Defective telomere maintenance and stability is associated with numerous diseases including pulmonary fibrosis, liver disease and progerias (Armanios 2009). Persisting oxidative DNA damage has been proposed as one cause of telomere instability (Satoh et al. 2008, von Zglinicki 2002).

1.4.3 Oxidative DNA Damage, Prevention and Repair

In addition to the mechanisms of the DNA damage response, elegant physical and enzymatic methods exist to protect the genomic information from corruption. Oxidative DNA damage is a focus of this thesis and provides an excellent example of these DDR-independent protection mechanisms. I will discuss the main aspects of oxidative DNA damage prevention and repair here. A detailed review of the subject is provided by (Slupphaug 2003).

Dysruption to the normal redox balance in cells leads to toxic effects. Peroxides and free radical intermediates of oxidative metabolism cause damage to proteins, lipids and DNA. Oxidative stress reflects an imbalance in favour of the accumulation of reactive oxygen species and damages sustained by them, over a biological system's capacity to neutralise them and/or repair the damage they cause.

Reactive oxygen species (ROS) such as superoxide anions, OH radicals and hydrogen peroxide can induce a large variety of oxidative DNA lesions (Figure 1.20) (Cadet 2003, Sander et al. 2005, Beckman and Ames 1997). Endogenous ROS are generated during a number of cellular processes. For example during the electron transfer chain, when "leaked" electrons encounter oxygen, during the immune response, when phagocytic cells produce an oxidative "respiratory burst" to kill virally or bacterially infected cells, and during lipid peroxidation in peroxisomes (Beckman and Ames 1997, Cooke et al. 2003).

Superoxide radical ($O_2^{\cdot -}$), hydroxyl radical ($OH^{\cdot}$) and hydrogen peroxide (H_2O_2) are all products of redox cycling in cells that may damage DNA (Figure 1.21). The large amount of ROS generated by the cell means that a high level of oxidative DNA damage can be measured in normal tissues at any time. The most common damaged purine produced is 7,8-dihydro-8-oxoguanine (8-oxo-G), while the most common damaged pyrimidine produced is thymine glycol (Tg) (Figure 1.7). More than 20 different types of base damage have been identified following exposure to oxidative stress (Slupphaug 2003). The most prevalent of these are shown in Fig. 1.20.

Most indirect SSBs arising as intermediates of the base excision repair pathway (BER) are caused by ROS-induced base damage (ie 8-oxo-G) and are generally a single nucleotide gap with "damaged" DNA termini. These are termini with chemistries that differ from the conventional 3'OH and 5'P moieties that are required for DNA ligation. An estimated 70% of 3' termini at ROS-induced SSBs feature a 3'-phosphate and an estimated 30% feature a 3'PG. The 5' termini of these SSBs is generally an undamaged 5' – phosphate although a small percentage feature a 5'-hydroxyl (Limoli et al. 1998, Caldecott 2001).

The first line of defence against ROS is enzymatic inactivation of superoxide by superoxide dismutase (SOD), in which two superoxide radicals and two protons generate the less toxic hydrogen peroxide and oxygen. Hydrogen peroxide is then converted to water and oxygen by catalase (Figure 1.21 a). SOD activities are present in the mitochondria, nuclei, and extracellular matrix. Three species, SOD1 (also known as CuZn-SOD), SOD2 (also known as Mn-SOD) and SOD3 (also known as EC-SOD) have been identified in humans. SOD1 and SOD3 are clearly related and thought to have a common ancestor, while SOD2 is structurally very different and may have a different origin. SOD1 is a cytoplasmic enzyme, SOD2 is mitochondrial and SOD3 is extracellular. Mutations in SOD1 are associated with familial amyotropic lateral sclerosis. The $SOD1^{G93A}$ mutant causes toxic elevation of ROS levels in cells. The $SOD1^{G93A}$ mutant is understood to exert its oxidative damage to DNA by the conversion of hydrogen peroxide to highly toxic hydroxyl radicals by way of these Fenton-type

reactions (Mao et al. 1993) (Figure 1.21 b), and is used to model ALS in mice (Gurney et al. 1994, Gurney 1997, Howland et al. 2002, Barbosa et al. 2010). Mice with targeted disruption of the SOD2 gene develop lethal cardiomyopathia, demonstrating the importance of these enzymes in vertebrates (Zelko, Mariani, and Folz 2002, Fang, Yang, and Wu 2002).

Many other factors contribute to the defence against ROS and cellular consequences of ROS, including antioxidant amino acids (e.g. arginine) and vitamins (e.g. Vitamins A,C and E), thiols (especially glutathione), tea polyphenols, enzyme-bound minerals (e.g. selenium and zinc) and antioxidant enzymes (e.g. glutathione reductase, glutathione peroxidases) (Fang, Yang, and Wu 2002, Slupphaug 2003). Secondly, enzymes such as 8-oxo-dGTP, hydrolyse oxidised dNTPs to the corresponding dNMP, preventing the potentially mutagenic incorporation of a damaged base into nascent DNA (Slupphaug 2003). Finally, several DNA repair mechanism resolve oxidative damage. BER is the primary oxidative damage repair pathway, while TCR and MMR provide important backup pathways for repair of transcribed and newly replicated strands, respectively (Slupphaug 2003).

1.5 DNA Damage Response Defects and Human Genetic Disease

As described above, the wide array of DNA lesions that arise in cells are repaired by numerous overlapping DNA repair pathways in order to maintain genome integrity. The

importance of each repair pathway to human health is highlighted by the existence of human genetic disease which are caused by defects in these pathways. Three main classes of symptoms are associated with defective DNA damage response mechanisms are i) predisposition to cancer ii) deficiencies in the immune system, and iii) deficiencies in the nervous system (Hoeijmakers 2001, Hoeijmakers 2007, Jackson and Bartek 2009, McKinnon and Caldecott 2007, McKinnon 2009).

Cancer is a family of diseases arising from genomic instability (Negrini and Calin 2010). DNA damage leading to mutation can cause the loss of tumour-suppressor genes or the improper activation of oncogenes, triggering malignancy and uncontrolled cellular proliferation (Hoeijmakers 2001). Several lymphoid tumours are associated with specific chromosomal translocations involving proto-oncogenes (Schlissel, Kaffer, and Curry 2006). Defective DNA damage response results in an elevated mutation rate, known as a 'mutator phenotype', such as that resulting from inherited defects in MMR and leading to a predisposition to colorectal and endometrial carcinomas (Hoeijmakers 2001, Jiricny 2006). Moreover, the fact that most carcinogens are DNA damaging agents, or otherwise affect the DDR, further highlights the link between DNA damage and cancer.

Defects in countless other DDR pathways have been implicated in the aetiology of cancer. Defects in the global genome NER pathway leads to a pronounced UV-sensitivity and a high incidence of skin cancer (Lehmann et al. 1975). Mutations in numerous proteins in the DSB signalling cascade, such as ATM and Nbs1, also impart susceptibility to cancer.

The link between DNA repair defects and immunodeficiency is due to essential roles specialised DNA repair pathways have in the development of the vertebrate immune system (Dudley et al. 2005). Multiple DNA repair pathways are involved in class switch recombination, a specialised DNA repair pathway involved in the production of antibodies (Dudley et al. 2005).

In addition, members of the NHEJ pathway play crucial roles in the production and diversification of the antigen receptors expressed on B- and T- lymphocytes in a pathway called V(D)J recombination (Hartlerode and Scully 2010) and various immunodeficient human disorders are caused by mutations in proteins involved in this pathway. Deficiencies in ATM, Mre11, XLF, RNF168, Ku70/80, LigIV and Artemis are all associated with severe immunodeficiency disorders (Chun and Gatti 2004, Stewart et al. 2007; Zhu et al. 1996, Bohgaki et al. 2011, Uziel et al. 2003, Goodarzi et al. 2006).

Finally, defective DNA response can also result in disorders of the nervous system. There are two main classes of neuropathology that are linked to defective DNA repair; primary microcephaly and progressive neurodegeneration (McKinnon 2009, O'Driscoll and Jeggo 2008). Primary microcephaly is a clinical term, which is used to describe an abnormally small head size - defined as head circumference 3 standard deviations below the mean, apparent from birth (O'Driscoll and Jeggo 2008). The underlying cause of the reduced head circumference is a reduction in total brain volume, as the outward pressure of the developing brain is the driving force for the growth of the head and skull. An early period of rapid proliferation of neuronal progenitor cells in the ventricular (VZ)

and subventricular zones (SVZ) that line the ventricles of the developing brain is critical for the development of the myriad neurons that comprise the mature nervous system (Bayer et al. 1991, Chan et al. 2002). Once these neuronal progenitors have replicated, cells destined to become neurons exit the cell cycle, differentiate and migrate away from the VZ and SVZ, towards the cortical plate (Bayer et al. 1991, Chan et al. 2002, Carmichael and Woods 2006). Due to the rapid proliferation that the neuronal progenitors undergo, they are heavily reliant on efficient DNA repair pathways to resolve replication-associated DNA damage (Barnes et al. 1998, Gao et al. 2011).

Additionally, these neuronal progenitors also have a relatively low threshold of DNA damage that is required to induce apoptosis (Hoshino and Kameyama 1988, Hoshino, Kameyama, and Inouye 1991). Therefore defects in DNA repair are believed to lead to an elevated rate of apoptosis in the proliferating progenitors due to persisting replication stress-induced damage, and a diminished total number of neurons in the developing brain and consequential microcephaly (Gatz et al. 2011).

Microcephaly is a common feature amongst defective DNA repair disorders, with defects in NHEJ, NER, SSBR, and MRN-dependent DSB signalling all leading to microcephalic disorders (Lehmann 2003, Shen et al. 2010, O'Driscoll et al. 2001). The other type of neuropathology that can arise from defective DNA repair is the progressive neurodegeneration of the brain. Neurodegenerative disorders usually present sometime after birth and are typically associated with the progressive degeneration of specific regions of the brain such as the cerebellum (Date et al. 2001, Moreira et al. 2001). The

progressive degeneration of the adult brain is thought to be due to the accumulation of DNA lesions in post mitotic cells. Neurons are highly active cells and generally exhibit high levels of mitochondrial respiration, and also have a reduced capacity to neutralise reactive oxygen species, resulting in elevated levels of oxidative DNA damage in neurons (Barzilai 2007, Weissman et al. 2007).

Furthermore, the adult brain has a limited capacity for cellular regeneration and since post mitotic neurons remain in the G0 phase of the cell cycle, they lack the DNA repair pathways that operate during S-phase and G2, such as HR (Rass, Ahel, and West 2007a). Hence the brain is exquisitely sensitive to repair defects as the usual backup mechanisms are not present. Accumulated DNA lesions may result in disruption to transcription, loss of cell functionality and/or apoptosis (Lagerwerf et al., 2011). Defects in NER, SSBR, and ATM- and Mre11-dependent DSB signalling, and can all result in disorders characterised by progressive neurodegeneration of the cerebellum (Barbot et al., 2001, Chun & Gatti, 2004, Date et al., 2001, Lavin, 2008, Stewart et al., 1999).

1.5.1 DNA Damage Response Defects and Neurological Dysfunction

As the brain is largely protected from exogenous DNA damage sources by the cranium and the blood-brain barrier, DNA lesions in the brain result predominantly from endogenous sources. The high rate of oxidative metabolism in the brain and the resulting high concentrations of reactive oxygen species produces high levels of DNA damage, especially single-strand breaks and oxidative damage (De Bont 2004, Lindahl 1993). Robust DNA repair processes are generally associated with replication in proliferating

cells (Barnes and Lindahl 2004). The absence thereof in the post-mitotic neurons makes them more reliant on the functioning repair mechanisms at their disposal - and exquisitely sensitive to loss of functionality therein.

1.5.2 Autosomal Recessive Cerebellar Ataxias

Autosomal recessive cerebellar ataxias (ARCAs) are a group of rare neurological disorders, which present with ataxia (lack of muscle coordination) and a range of opthalmological and neurological symptoms due to cerebellar dysfunction. Amongst the many different types of ARCA, a subset are caused by defective DNA damage response. These include Ataxia Telangiectasia (A-T), Ataxia Telangiectasia-Like Disorder (A-TLD), Xeroderma Pigmentosum (XP), Spinocerebellar Ataxia with Axonal Neuropathy Type 1 (SCAN) and Ataxia with Oculomotor Apraxia Type 1 and 2 (AOA1 and AOA2).

Ataxia Telangiectasia

Ataxia Telangiectasia (A-T) is the best characterised DNA repair-defective ARCA (1,2) and is caused by mutation of the Ataxia Telangiectasia Mutated gene (*ATM*). Symptoms of progressive cerecellar ataxia present an early age of onset (between 2 and 4 years) and patients are normally wheelchair-bound by their teens (Sedgwick, Robins, and Lindahl 2006). Oculomotor abnormalities (loss of eye movement control) affects most patients (Lewis 1999), and oculocutaneous telangiectasia (blood-shot eyes) generally

present between 2 and 8 years. The extraneurological features of AT include a predisposition to malignancy – especially leukaemia and lymphoma extreme sensitivity to many anti-cancer treatments including radiation and mutagenic chemicals, and immunodeficiency. A-T is caused by mutations in the Ataxia-Telangiectasia Mutated (ATM) gene, resulting in reduced kinase activity of ATM, or reduced protein stability (Lakin et al. 1996).

Ataxia with Oculomotor Apraxia Type 2

Ataxia with Oculomotor Apraxia Type 2 (AOA2) (also referred to as non-Friedrich spinocerebellar ataxia type 1 (SCA1)), has a clinical presentation similar to that of AOA1 patients. Patients develop a late-onset (11-22 years) progressive cerebellar ataxia (Le Ber, Brice, & Dürr, 2006, Moreira et al., 2001) featuring gait ataxia, progressive peripheral sensory and motor neuropathy, dysarthria and oculomotor apraxia (Le Ber, Brice, and Dürr 2006). AOA2 is not associated with mental impairment or predisposition to malignant or infectious disease. AOA2 patients display elevated levels of γ-globulin, α-fetoprotein and creatin kinase (Le Ber, Brice, and Dürr 2006). AOA2 is caused by mutations in the SETX gene (Moreira et al. 2001), which encodes the putative DNA/RNA helicase senataxin. The function of senataxin is not yet clear, but cells from AOA2 patients display hypersensitivity to single strand break inducing agents, especially hydrogen peroxide (Suraweera et al. 2009) - suggesting a role in DNA repair. Recent reports also suggest a role in mRNA processing and transcriptional regulation (Suraweera et al., 2009, Yüce-Petronczki & West, 2012).

Spinocerebellar Ataxia with Axonal Neuropathy Type 1

Spinocerebellar Ataxia with Axonal Neuropathy Type 1 (SCAN1) is another autosomal recessive spinocerebellar ataxia of onset between 12 and 15 years of age. Peripheral neuropathy results in the progressive loss of touch and pain sensations in the limbs (Takashima et al. 2002). Progressive ataxia results in patients becoming wheelchair-dependent but unlike A-T, AOA1 and AOA2, oculomotor abnormalities have not been reported (Takashima et al. 2002). SCAN1 is caused by mutations in the TDP1 gene, which encodes the DNA end-processing factor Tyrosyl-DNA phosphodiesterase, Tdp1. This enzyme resolves phospho-tyrosine residues resulting from abortive Topo1 activity (Figure 1.6).

Ataxia with Oculomotor Apraxia Type 1

Ataxia with Oculomotor Apraxia Type I (AOA1) is an autosomal recessive spinocerebellar ataxia (ARCA) (Aicardi et al. 1988). It was initially described as a variant form of Friedreich's ataxia (FRDA) and is also referred to as Early Onset Ataxia with Hypoalbuminemia (EAOH) (Shimazaki et al. 2002). In contrast to FRDA, patients with AOA1 never develop cardiomyopathy, but do develop severe sensory and motor neuronopathy, hypoalbuminemia and moderate cognitive impairment. In 2001, the gene mutated in AOA1 was identified as APTX, the gene for aprataxin. Incidence and prevalence vary markedly among different ethnic groups and geographic areas.

Prevalence is highest in Japan, where it is the most common form of ARCA, and second highest in Portugal, where it accounts for ~21% of ARCA cases (Barbot et al. 2001).

AOA1 is characterized by three clinical features: i) cerebellar and sensory ataxia and involuntary movement ii) ocular motor apraxia (OMA), defined as the impaired initiation of saccadic eye movement, accompanied by head thrusts, and iii) sensory and motor neuronopathy. These clinical features are accompanied by two biochemical markers, hypoalbuminemia and hypercholesterolemia (Le Ber et al. 2003). Gait ataxia generally develops in AOA1 patients in the first decade of life. Progressive loss of muscle coordination affects balance, movement and speech. Loss of limb control (called limb dysmetria) results in patients becoming wheelchair-bound within 5-20 years after disease onset (Aicardi et al., 1988, Barbot et al., 2001). AOA1 patients can also display a range of visual control defects, including and impaired ability to perform both horizontal and vertical eye movements (Aicardi et al., 1988, Le Page et al., 2003). They take longer to focus on an object and have difficulty coordinating the movements of the eyes and head to track a moving object (Le Ber, Brice, and Dürr 2006). Some patients also display dysarthria and/or masked facies (a reduced capactiy to display facial expression (Aicardi et al., 1988, Le Ber et al., 2006). Reports of the mental capacity of AOA1 patients have produced conflicting results: Le Ber et al. reported mental impairment (either retardation or dysexecutive syndrome) in all patients examined, while Aicardi et al. reported that their patients had normal intelligence (Aicardi et al. 1988). Atrophy of the cerebellum is obvious upon MRI imaging, even early in the course of the disease (Le Ber, Brice, and Dürr 2006).

Although hypoalbuminemia and hypercholesterolemia are characteristic biochemical markers of AOA1, they only become obvious after ~ 20 years of age (Le Ber, Brice, and Dürr 2006). The observed hypercholesterolemia is corrected by infusion of albumin, while the hypoalbuminemia is not corrected by reducing serum cholesterol levels, indicating that the hypoalbuminemia causes hypercholesterolemia (Fukuhara 1995). The rate of degradation of serum albumin is normal (Le Ber et al., 2006, Tranchant et al., 2003), suggesting that albumin synthesis in the liver is impaired. Interestingly, although it shares many neurological symptoms with other DNA repair defective disorders, such as ataxia-telangiectasia, it lacks any of the other extraneurological features such as immunodeficiency or cancer predisposition.

Cell lines derived from AOA1 patients have been reported to be hypersensitive to a range of DNA damaging agents that generate single-strand breaks such as camptothecin, hydrogen peroxide, dl-buthionine-(S,R)-sulfoximine (BSO) (Clements et al., 2004, Gueven et al., 2004), and aprataxin has shown SSB end-processing function *in vitro* (Ahel et al. 2006). Data relating to the sensitivity of AOA1 patient cells and cultured $APTX^{-/-}$ cells have been somewhat contradictory and one main aim of this thesis is to clarify these points.

1.5.3 Aprataxin

APTX is widely expressed in most tissues and across the nervous system. In situ

hybridization analysis of mouse brains reveals that APTX mRNA is expressed at high levels in Purkinje cells and cerebellar granular cells (Brenner 2002). In 2006, aprataxin was shown to demonstrate SSB end-processing function in vitro - in which a 5'AMP modification is deadenylated and the correct, ligatable 5'P terminus is restored (Figure 1.14) (Ahel et al. 2006).

The efficiency of deadenylation by aprataxin is equivalent at double-strand breaks and single-strand breaks but binds double stranded DNA with much higher affinity than single stranded DNA (Rass, Ahel, and West 2007a). Further to its SSB end-processing function, and through its interaction with various repair proteins, such as XRCC1, XRCC4 and MDC1, aprataxin is believed to have wider roles in the DNA damage response, although little is presently known about the function of these interactions.

The forkhead associated (FHA) domain at the N-terminus of aprataxin is homologous to that of PNKP, and mediates interactions with CK2-phosphorylated XRCC1 in the formation of a single strand break repair (SSBR) complex (Clements 2004), following DNA damage (Gueven et al. 2004). Both PNKP and aprataxin are also sequestered to a double strand break repair (DSBR) complex through FHA domain-mediated interaction with CK2-phosphorylated XRCC4 (Clements et al. 2004).

XRCC1, is a molecular scaffold protein that plays a central role in the recruitment of PARP-1, PNK, DNA polymerase β, and DNA ligase III to a SSBR complex, and there is evidence that these proteins may work synergistically in the DNA damage response

(Harris et al. 2009) (Figure 1.5). Recently, aprataxin was shown to interact with MDC1 at sites of DNA damage (Figure 1.11). MDC1 is required for efficient phosphorylation of H2AX, for recruitment and retention of ATM and MRN at DNA breaks and for the recruitment of the ubiquitin ligase RNF8 to ubiquitinate H2AX at sites of damage (Becherel et al. 2010).

Since the seminal paper by Ahel et al in 2006 identified the DNA repair function of aprataxin – resolution of abortive ligation intermediates – evidence has been building of further reaching roles for aprataxin in DNA repair, ranging from other direct repair functions (3' phosphatase activity and phosphoglycolate removal (Takahashi et al. 2007) to involvement in repair protein complexes (Becherel et al., 2010, Clements et al., 2004, Harris et al., 2009, Rass et al., 2007) to modulating the transcription of key repair proteins (Harris et al. 2009)). This thesis aims to extend understanding of aprataxin function, using *in vitro* DNA repair assays, cell-based assays and tissues from animal models.

Chapter Two

Materials and Methods

2.1 Generation of mutant mice

The $Aptx^{-/-}$ mice were generated as described previously in C57/6J/129 background (Ahel et al. 2006; El-Khamisy et al. 2009). To generate the Aptx/SOD1 double mutants, $Aptx^{+/-}$ females were crossed with male $SOD1^{G93A}$ transgenic mice kindly supplied by the Jackson laboratory (Gurney et al. 1994) (female $SOD1^{G93A}$ mice are infertile expressing human $SOD1^{G93A}$), for two generations . This breeding plan was used to generate $Aptx^{+/+}$, $Aptx^{-/-}$, $Aptx^{+/+}SOD1^{G93A}$ and $Aptx^{-/-}SOD1^{G93A}$ mice (and embryos for generating MEFs). See Table 2.i and 2.ii for details on animals and tissues used in the study.

2.2 Isolation, genotyping and maintenance of MEFs

All cells used in the study were MEFs isolated from embryos on embryonic day 13 by separation from head and limbs and quick homogenisation by pipette in trypsin, and then cultured in complete medium (DMEM supplemented with 15% FCS, 100 units/ml penicillin, 100 mg/ml streptomycin, 2 mM L-glutamine) in 3% O_2 and 5% CO_2, at 37^{o}C. Genotyping of adult mice was done using tail biopsies and genotyping of embryos was done using the embryo heads. Genotypes of MEFs were further confirmed by repeating the PCR on cellular lysate. Tissues were digested in lysis buffer: 20 mM tris-hydrochloric acid (Tris- HCl) (pH 7.5), 10 mM EDTA, 1 mM EGTA, 100 mM NaCl, 1% Triton X-100, containing proteinase K (10 mg/ml, Invitrogen), 2 µl in 200 µl lysis buffer, 55^{o}C overnight. The soluble DNA produced was diluted 1:50 and used as a template in PCR reactions containing three primers for the aprataxin gene, as described previously (Ahel et al. 2006). PCR products were run on a 1% agarose DNA gel. Genotyping tissues for SOD-1 was performed by digestion of biopsies (as above) and amplification by PCR using the method of the Jackson laboratory, with a set of primers to amplify both the endogenous SOD-1, and the mutant human SOD-1. PCR products were run on a 1% agarose DNA gel (0.0001% EtBr) and visualised with UV. Details of the primers used may be found in Table 2.iii.

2.3 Preparation of cell-free protein extracts

Approximately 5 x 10^5 cells were harvested by centrifugation at 1,500 rpm and washed three times in PBS. Cell pellets were lysed by incubation with 0.2 ml cell lysis buffer on ice and cell free extracts were prepared by centrifuging at 13,000 rpm for 20 min at 4°C. The supernatant was retained and the protein concentration quantified by the Lowry method using the DC Protein Assay (BioRad) with BSA used as a protein standard.

2.4 SDS - Polyacrylamide Gel Electrophoresis (SDS-PAGE)

SDS-PAGE gels consisting of 10% resolving gel (10 ml final volume: 4 ml ddH_2O, 3.3 ml 30% acrylamide/bisacrylamide (37.5:1) mix (Flowgen), 2.5 ml 1.5 M Tris pH 8.8, 0.1 ml 10% SDS, 0.1 ml 10% APS, 4 µl TEMED) and 5% stacking gel (4 ml final volume: 2.7 ml ddH2O, 0.67 ml 30% acrylamide/bisacrylamide (37.5:1) (Flowgen) 0.5 ml, 0.5 ml 1M Tris pH6.7, 40 µl 10% SDS, 40 µl 10% APS, 4 µl TEMED), were prepared according to Sambrook and Russell (Sambrook and Russell, 2001). Protein samples (purified recombinant protein, bacterial and mammalian cell extract) were denatured by incubation in SDS loading buffer (50 mM Tris pH8.0, 2% w/v SDS, 10% w/v glycerol, 0.1% w/v bromophenol blue 200 mM DTT) at 94°C for 5 min. The denatured samples were briefly centrifuged at full speed and aliquots were separated on SDS-PAGE using Precision Plus Protein Prestained Dual Colour Standards (BioRad) as markers. Electrophoresis was carried out using Mini Protean 3 apparatus (BioRad) in 1x running buffer (25 mM Tris, 250 mM glycine, 0.01 % w/v SDS) at 150 V for 60 min. Total protein was visualised by staining in Coomassie brilliant blue solution (0.25% w/v Coomassie brilliant blue G-250 (BioRad, 50% v/v methanol, 10% v/v acetic acid) for 30 min and destaining (10% v/v methanol, 10% v/v acetic acid) for 30 min and dried.

2.5 Immunoblotting of proteins

Cell free extracts were aliquoted and stored at -80°C. Samples were run on a 12.5% SDS-PAGE gel. Proteins were transferred to a Hybond C extra nitrocellulose membrane at 25 V for 2 h (wet transfer method). Following transfer, the membrane was blocked (5% milk in PBS for 1 h at RT), and incubated overnight at 4^{o}C with primary antibody: Aprataxin (Anti-APTX rabbit polyclonal, Taylor lab, 1:1000, 5% milk), or SOD1 (Anti-SOD1 rabbit polyclonal, Santa Cruz Biotechnology, 1:2000, 5% milk). β-actin was used as a control (Anti-β-actin mouse monoclonal, Sigma, 1:2000, 5% milk). The membrane was then washed in Tris-Buffered Saline/Tween 20 (50 mM Tris, 150 mM NaCl, 0.05% Tween, adjust pH with HCl to pH7.6) and then incubated at room temperature for one hour in goat anti-rabbit HRP-conjugated secondary antibody (Dako, 1:4000) or anti-mouse HRP-conjugated secondary antibody (Dako, 1:5000) in 1 x TBST. Membranes were washed again and incubated in enhanced chemiluminescence (ECL) western blotting detection reagent (GE Healthcare) for 1 minute and developed on autoradiography blue sensitive film (GRI) using a Xograph Compact 4 automatic X-ray film processor.

2.6 Overexpression of recombinant aprataxin in *E.Coli*

The pB352-hAPTX bacterial expression vector (Clements et al., 2004) was transformed into chemically competent BL21 (DE3) *E.coli* cells: 0.2 – 2 μg plasmid DNA was incubated with 50 μl of chemically competent BL21 (DE3) cells on ice for 30 min before heat shocking at 42°C for 45 sec, and then cooling on ice for 5 min. 1 ml of LB was added, then the transformation mixture was incubated at 37°C for 1 h while shaking at 220 rpm. The transformation mixture was plated onto LB agar plates containing 50 μg/ml ampicillin and incubated overnight at 37°C. Single colonies were picked and used to inoculate 10 ml starter culture consisting of LB containing 50 μg/ml of the appropriate antibiotic and the culture was incubated overnight at 37°C, shaking at 220 rpm.

The starter culture was centrifuged at 4,800 rpm for 20 min, resuspended in fresh LB media and diluted into a large scale 500 ml culture and incubated at 30°C to a final OD_{600} = 0.01. The large scale aprataxin culture reached OD_{600} = 0.01 after 3 hours and was used for further purification steps. The culture was incubated at 30°C until OD_{600} = 0.6 and a 1 ml pre-induction sample was taken for analysis, 0.5ml of 1M IPTG was added to make a final concentration 1mM and the culture was incubated at 30°C until OD_{600} = 1.2. A 1 ml post induction sample was taken for analysis and the rest of the culture was harvested by centrifugation at 5,000 rpm for 20 min. The pellet was washed once in PBS and stored at -20°C. Aliquots of the 1 ml pre- and post-induction samples were analysed by SDS-PAGE.

2.7 Preparation of clarified cell extract from *E. Coli*

Bacterial cell pellets containing overexpressed recombinant aprataxin were resuspended in 20ml sonication buffer (25 mM Tris-HCl (pH7.0), 0.5 M NaCl, 10% glycerol, 1 mM DTT, 1 mM imidazole (pH8.0) and 1 mM PMSF). Crude cell extract was prepared by sonicating the resuspended cell pellet at 30% power for 10 X 30 sec bursts, each followed by a 30 sec cooling period. The soluble was separated from the insoluble material by spinning at 14,000 rpm for 20 min at 4°C. The supernatant was retained, snap frozen in liquid nitrogen and stored at -80°C. 100 µl samples of the soluble and insoluble material were retained for anaylsis by SDS-PAGE.

2.8 Purification of His-tagged aprataxin by immobilized affinity chromatography

Human recombinant His-tagged APTX was overexpressed in BL21 (DE3) *E.coli* cells as previously described. The first purification step was immobilised metal affinity chromatography (IMAC) on Ni-NTA agarose beads (first described in Porath et al.1975). In IMAC, metal ions (Ni^{2+}) are bound to a metal chelating group (NTA) immobilised on agarose beads. The Ni^{2+} ions form interactions with imidazole side-chains present within histidine residues, retaining any histidine containing proteins on

the beads. To take advantage of this proteins are fused to tags consisting of six or ten histidine residues, allowing the recombinant protein to bind to the Ni^{2+} on the column with high affinity. Proteins are eluted from the beads with a buffer containing an excess of free imidazole, which competes with the histidine side chains for interaction with the column. A Ni-agarose column with a 5.0 ml bed volume was prepared by loading 1 ml Ni-NTA Agarose resin (Qiagen) onto a Bio-Rad PolyPrep column and washing with 10 column volumes of sonication buffer (25 mM Tris-HCl, 0.5 M NaCl, 10% glycerol, 1 mM DTT, 1 mM imidazole (pH8.0)). 20 ml clarified E.coli extract containing His-tagged recombinant protein was loaded onto the Ni-NTA agarose column at 4°C. All subsequent steps were also carried out at 4°C. The column was washed three separate times with 10 column volumes of sonication buffer containing 20 mM, 40 mM and 80 mM imidazole respectively. His-tagged protein was then eluted with 5 column volumes of sonication buffer containing 250 mM imidazole and 0.5 ml elution fractions were collected. Aliquots of the column load, flow through, washes and elution fractions were analysed by SDS-PAGE. Samples were snap frozen and stored at -80^{o}C.

2.9 Purification of recombinant aprataxin by cation exchange chromatography

IMAC elution fractions containing His-APTX were subsequently purified by cation exchange chromatography using a 1.6 ml POROS column on a BioCAD ® Sprint Perfusion Chromatography System (Applied Biosystems, United Kingdom). The column was washed with 20 column volumes of ice cold high salt buffer (25 mM Tris-HCl, 1 M NaCl, 10% glycerol, 1 mM DTT) and then 20 column volumes of ice cold low salt buffer (25 mM Tris-HCl, 0.1 M NaCl, 10% glycerol, 1 mM DTT). Prior to washing, the high and low salt buffers were filtered through a 0.22 μm filter unit. pH strongly affects the charge characteristics of a protein and the affinity of the target protein for the column. The isoelectric point (pI) of a protein describes the pH at which a molecule has a net charge of zero. Accordingly, the purification of proteins must be carried out at pH specific to the pI of that protein to optimise the yield. Accordingly, recombinant aprataxin was purified using buffers of pH 8 (Table 2.iv). Buffers were made as described above and pH-adjusted with NaOH. All buffers and protein solutions

were kept on ice. Peak elution fractions from IMAC were pooled, loaded onto the cation exchange column and washed with 10 column volumes low salt buffer. His-APTX was eluted with a salt gradient from 0.1 M NaCl to 1 M NaCl over 15 column volumes. 1 ml elution fractions were collected. Aliquots of the column load, flow through and elution fractions were analysed by 10% SDS PAGE and peak fractions were dialysed into storage buffer (25 mM Tris-HCl, 150 mM NaCl, 10% glycerol, 1 mM DTT) using a D-Tube Dialyzer (Novagen). The protein concentration of the final dialysed fractions was quantified by the Lowry method using the DC Protein Assay (BioRad) with BSA used as a protein standard. The dialysed fractions were aliquoted, snap frozen in liquid nitrogen, and stored at -80°C.

2.10 Urea Polyacrylamide Gel Electrophoresis (Urea PAGE)

Urea polyacrylamide gels were prepared using the SequaFLOWGel Sequencing Kit (Flowgen Bioscience) using a 21 cm x 40 cm Sequi-Gen GT Sequencing Cell (Bio-Rad). Radiolabelled DNA was denatured by heating to 90°C in formamide loading buffer (30% formamide, 0.04% w/v bromophenol blue) and was separated on 15% urea polyacrylamide gels (50ml total volume: 30 ml SequaGel Concentrate, 15 ml SequaGel Diluent, 5 ml SequaGel Buffer, 40 µl TEMED. Prior to loading of the DNA samples, the polyacrylamide gel was pre-run by carrying out electrophoresis at 45 W for 45 min. Denatured DNA samples were then loaded and electrophoresis was carried out in 1 x TBE (90 mM tris, 90 mM boric acid, 2 mM EDTA) at 45 W for 90 – 180 min. After electrophoresis the polyacrylamide gel was incubated in 10% acetic acid 10% methanol for at least 20 min, dried and exposed to a Phosphor Screen (GE Healthcare). Radiolabelled DNA was detected by phosphorimaging using a Storm™ phosphoimager (GE Healthcare) and visualised by ImageQuant TL software (GE Healthcare).

2.11 Native Polyacrylamide Gel Electrophoresis (Native PAGE)

15% native polyacrylamide gels were prepared using 40% acrylamide/bis-acrylamide (19:1) solution and 1 x TBE. DNA samples were loaded onto the native acrylamide gel in type II loading buffer (0.04% w/v bromophenol blue, 0.04% w/v xylene cyanol FF, 2.5% w/v ficoll (Type 400 from Pharmacia)) in distilled water. Electrophoresis was carried out using Mini Protean II apparatus (Bio-Rad) in 1 x TBE at 80 V for 2 h. After electrophoresis the polyacrylamide gels were incubated in 10% acetic acid 10% methanol, dried and exposed to Phosphor Screens (GE Healthcare). Radiolabelled DNA was detected by phosphorimaging using a Storm™ phosphoimager (GE Healthcare) and visualised by ImageQuant TL software (GE Healthcare).

2.12 Preparation of radiolabelled oligonucleotides

To prepare a radiolabelled oligomer for preparation of substrates to visualise DNA damage repair by cell extract and recombinant protein, 1 nmole of appropriate oligo was incubated with 2 µl T4 PNK (Roche Applied Science) and 2µl (5mCi/ml) [γ-^{32}P]-ATP in 1 x PNK buffer to a total volume of 40 µl and incubated at 37^{o}C for 1 h and then at 70°C for 10 min to de-activate the enzyme. Unincorporated radionucleotides were then removed by applying the reaction to an illustra MicroSpin™ G-25 Columns (GE Healthcare) and centrifuging according to manufacturer's specifications.

To prepare a SSB substrate in which repair of the 5' termini could be visualised, the oligomer upstream of the break (a 25mer or a 14mer in all experiments contained within this thesis) was 5'-radiolabelled.

To prepare a SSB substrate in which repair of the 3' termini could be visualised, the oligomer downstream of the break (an 18mer in all experiments contained within this thesis) was 5'-radiolabelled. To radiolabel an 18mer harbouring a 3' phosphate modification, T4 PNK 3' phosphatase free mutant (Roche) was used to prevent processing of the 3' termini.

The success of the radiolabelling was determined by analysing a sample of the reaction products by 15% urea PAGE. The radiolabelled oligonucleotides were annealed to a two-fold molar excess of appropriate unlabelled oligonucleotides by incubating 95°C for 5 min and then at RT for 30 min each before placing on ice. A control sample lacking either the oligomer upstream or downstream of the break was annealed in parallel to use as a size reference. The annealed products were fractionated by 15% native PAGE to check annealing efficiency.

All oligonucleotides used are detailed in Table 2.v and were obtained from Eurofins MWG Operon.

2.13 Preparation of model DNA single strand break substrates

Annealing reaction: Radiolabelled oligomer was annealed to a two-fold molar excess of unlabelled counterparts by incubating together at 95^{o}C for 5 min and then at RT for 30 min, then on ice for 10min.

To prepare double stranded oligonucleotide duplex harbouring a SSB but no missing nucleotides (referred to henceforth as a nick substrate) in which repair of the 5' termini could be visualised, the radiolabelled 25mer was annealed with an 18mer and complimentary 43mer oligonucleotide backbone.

Model abortive ligation intermediates (nick substrates with 5'-AMP modification at the break, were prepared by adenylating a nick substrate using a T4 DNA Ligase. 7.5 μM of the nick substrate was incubated with 1 U of T4 DNA Ligase (Roche) at 30°C for 1 h in 25 mM Tris-HCl (pH7.5), 130 mM KCl, 1 mM DTT, 10 mM MgCl2, and 1 mM ATP. A mock adenylated control lacking T4 DNA ligase was prepared by incubated 7.5 μM of the oxidative SSB with ligase storage buffer (20 mM Tris-HCl (pH 7), 60 mM KCl, 1 mM EDTA, 5 mM DTT, 50% glycerol (v/v)). The adenylation reaction is not expected to run to completion and the reaction product will contain some unadenylated ^{32}P-25mer, necessitating purification of the AMP-32P-25mer by denaturing gel extraction using the Crush and Soak method.

Crush and Soak method: The reaction products were fractionated by 15% urea PAGE and the position of the adenylated and mock adenylated 25mer oligonucleotides was determined by autoradiography using blue sensitive film. The AMP-^{32}P-25mer and ^{32}P-25mer were excised from the gel. The DNA was eluted from the acrylamide by crushing the gel slice and incubating overnight at RT in 2 x volume Crush and Soak buffer (300 mM sodium acetate, 1 mM EDTA (pH8.0)). The resulting slurry was centrifuged at high speed and the supernatant retained. 1µl of Pellet Paint® NF Co-precipitant (Merck Biosciences) was added to the supernatant followed by 2 x volume of ice cold absolute ethanol. The solution was incubated at -80°C overnight and the DNA pelleted by centrifugation at 14,000 rpm for 20 min at 4°C. The pellet was washed twice with ice cold 70% ethanol, air dried and the purified DNA resuspended in 30 µl Buffer EB (Qiagen).

Image-Quant software was used to determine the concentration of gel-extracted adenylated 25mer by comparing the signal produced of a known volume on a 15% urea PAGE gel to the signal produced by the same volume of pre-extraction ^{32}P-labelled 25mer of known concentration. Finally the adenylated 25mer was annealed to the 18mer and 43mer oligonucleotide backbone in a 1:2:2 ratio.

The double stranded oligonucleotide duplex substrate harbouring a three nucleotide gap (referred to henceforth as gap substrates) in which gap-filling from the 3'terminus may be visualised, was prepared by annealing 5'-radiolabelled 18mer with 14mer and complimentary 36mer oligonucleotide backbone.

Fully annealed duplexes were purified by fractionation of the annealing reaction products by 15% native PAGE and gel extraction using the crush and soak method as described previously, and quantified by comparison of signal produced on a native gel to that produced by oligo of known concentration, as described previously.

2.14 In vitro repair of adenylated nick substrates by cell-free protein extracts

For reactions involving cell-free protein extracts, 25 nmol of adenylated SSB substrate was incubated with the indicated concentrations of protein extract for 60 min at 30°C in 1 x reaction buffer (660 mM Tris- HCl, 50 mM $MgCl_2$, 50 mM DTT, pH 7.5 at 20^{o}C),10 μM deoxynucleoside triphosphates (dNTPs), 1 mM ATP). 1000 x fold molar excess of competitor oligonucleotide (Table 2.v) was added to the reactions to suppress non-specific nuclease activity. Reactions were stopped by addition of 1/3 volume of formamide gel loading buffer (90% formamide, 0.12% w/v bromophenol blue) and denaturing by incubation at 90°C for 5 min. Reaction products were separated by 15% urea PAGE gels and visualised by phosphorimaging as described previously. Image-Quant software was used to quantify spread of oligonucleotide product sizes by quantifying the signal of each product as a proportion of the sum of all products.

2.15 In vitro repair of gap substrates by cell-free protein extracts

For reactions involving cell-free protein extracts, 25 nmol of gap substrate was incubated with cell-free protein extract for 30 min unless otherwise stated at 37°C in 1 x reaction buffer (660 mM Tris- HCl, 50 mM $MgCl_2$, 50 mM DTT, pH 7.5 at 20^{o}C),10 μM deoxynucleoside triphosphates (dNTPs), 1 mM ATP. 1000-fold molar excess of competitor oligonucleotide (Table 2.v) was added to the reactions to suppress non-specific nuclease activity. Reactions were stopped by addition of 1/3 volume of formamide ‘stop buffer’ (90% formamide, 0.12% w/v bromophenol blue, 10% glycerol) and denaturing by incubation at 90°C for 5 min. Reaction products were separated by 15% urea PAGE gels and visualised by phosphorimaging as described previously.

2.16 In vitro repair of gap substrates by recombinant proteins

Recombinant aprataxin was prepared as previously described. Recombinant Pol β, PNK and LigIIIα were kind gift from John Reynolds and were prepared as described in (Reynolds 2011). For in vitro repair reactions involving recombinant proteins, 100 nmol of gap substrate was incubated with the indicated concentrations of recombinant proteins for 30 min at 37°C unless otherwise stated in 1 x reaction buffer (660 mM Tris-HCl), 50 mM $MgCl_2$, 50 mM DTT, pH 7.5 at 20^{o}C), 10 μM dNTPs, 1mM ATP. Reactions were stopped by addition of 1/3 volume of formamide gel loading buffer (90% formamide, 0.12% w/v bromophenol blue) and denaturing by incubation at 90°C for 5 min. Reaction products were separated by 15% urea PAGE gels and visualised by phosphorimaging as described previously.

2.17 Cell growth and survival assays

Primary MEFs were used at passage 4-6 for survival assays. 100-600 cells per ml (the higher the dose of damaging agent, the higher the number of cells plated to produce a countable number of survival colonies according to test experiments) were grown in 10cm^2 plates (triplicates) and then treated with the appropriate DNA damaging agent: X-rays 250 kV at 12 mA, dose rate 0.5 Gy/min) using the AGO 320/250 X-ray cabinet, or H_2O_2 in PBS at the indicated doses, for 10min in the dark. Cells treated with X- rays were returned immediately to the incubator, and cells treated with H_2O_2 were washed three times in PBS and then returned to the incubator. In each experiment, all cells were allowed to grow for the same amount of time, between 5 and 7 days, until colonies had formed. Media was removed and cells were fixed with 80% ethanol for two minutes, then ethanol was removed. A minute later, enough 1% methylene blue stain was added to cover the bottom of the plate, and left for 30-40 mins. Stain was removed and plates left upside down to dry before colonies were counted.

The surviving fraction of cells of each genotype at each dose was calculated according to the number of colonies formed and the plating efficiency, using the equations:

Plating Efficiency = colonies observed/number of cells plated

Surviving Fraction = colonies observed/cells seeded x plating efficiency

The average surviving fraction across triplicates was calculated and the logarithm of the average across all experiments (three X-ray experiments and four H_2O_2 experiments) was plotted against dose. Appropriate statistical tests for the clonogenic survival assays performed (two-tailed Student's T-tests) were performed to calculate the standard error of the mean, using the equation:

Results were replicated in two separate MEF lines and all assays were performed at early passage number – between passage 1 and 5.

2.18 Senescence assays

The senescence of primary MEFs was assayed at alternate passages up to passage 10, using the Senescence β-Galactosidase Staining Kit (Cell Signalling Technology), which exploits pH-dependent β-Galactosidase activity as a readout for senescence. MEFs were fixed with 80% ethanol for 10 min, then stained with X-Gal solution (20 mg/ml) and incubated at 37^{o}C overnight (or as long as necessary to produce comparable staining between samples – between 24 and 72 h). Cells were observed under a microscope (200 x total magnification) for development of blue stain. From each population, three representative samples of 100 cells each were counted to find the average percentage of cells stained blue (senescent).

2.19 RNA synthesis recovery assays

MEFs were plated onto 3.5 cm dishes of each cell line at approximately 2 x 10^4 cells in 2 ml 15% FCS-medium containing 0.02 µCi/ml thymidine [2-^{14}C] and incubated at 37^{o}C for 48 h (approximately 2 cycles) to label DNA . Medium was removed, cells washed with PBS, and incubated with either PBS or 50 µM H_2O_2 for 10 min at room temperature in the dark. Cells were washed three times in PBS, and then 1 ml 15% FCS-medium containing 5 µCi/ml ^{3}H-uridine was applied and cells were incubated for 15 mins. Medium was removed, and cells were washed three times in PBS. 0.25 ml 2% SDS was applied and the cells were scraped off the dish with a silicone rubber to collect DNA and RNA. Dishes were left tilted in rows. Strips of Grad 17 Whatman chromatography paper was marked into 16 x 1-inch labelled (in pencil) sections. 100 µl samples were pipetted onto paper strips, in duplicate. Strips were incubated with 5% trichloroacetic acid (TCA) for 5 mins followed by 2 x 5 min incubation with IMS. Finally, samples were left to dry thoroughly and radioactivity was quantified using the Beckman Coulter LS6500 Multi-Purpose Scintillation Counter. Results were plotted as RNA synthesis (% of unirradiated) against dose.

2.20 Alkaline single-cell agarose gel electrophoresis (comet assay)

Approximately 2 x 10^5 MEFs at passage 5 were plated in 3.5 cm culture dishes in complete media and incubated for 16 h at 37^{o}C prior to mock-treatment (control) or treatment. For H_2O_2 treatment, cells were incubated with 90 µM H_2O_2 in PBS on ice for 10 mins. Control cells were incubated with PBS on ice for 10mins. For exposure with 20 Gy γ-rays, 4 x 10^5 cells/ml were irradiated in suspension in complete medium using a ^{137}Cs gamma source (dose rate 7.5 Gy/min), controls were incubated at the same temperature for the same amount of time, but unirradiated. After treatment with H_2O_2 or γ-rays cells were washed in ice-cold PBS and incubated for the desired repair periods. Adherent cells were trypsinised and harvested in ice-cold PBS (1 ml/3.5 cm plate) and 0.2ml of the cell suspension analysed by alkaline comet assay as described previously (Chiang, Carroll, & El-Khamisy, 2010). Briefly, cells were immobilized in agarose on slides, lysed and eletrophoresed. DNA was neutralised, stained with SYBR green (1:10000 dilution) and visualised by fluorescent microscopy (Nikon Eclipse E400) at 20

x magnification. Comet tail moment for 100 cells per sample was determined using Comet Assay IV software (Perceptive Instruments). The average tail moment and scatter graphs of tail moments were plotted for each repair time point. Each sample was tested in triplicate in each experiment. The average surviving fraction from five independent experiments was plotted (+/- standard error of the mean - SEM). Statistically significant differences were determined using SPSS software: ANOVA (two-factor with replication).

2.21 Telomere length assays

This assay (described in Chang and Harley, 1995, and Landsorp et al., 1996) was performed for the most part as described in the TeloTAGGG Telomere Length Assay® specification manual (Roche cat. # 2209136), with a few modifications.

DNA digestion and separation

Genomic DNA was digested by a Hinf I/Rsa I enzyme mixture – 20 U/µl of each, and incubated for 2 h at 37^{o}C. The reaction was stopped by adding gel electrophoresis buffer and quick-spinning of the reaction vials. Separation of digested DNA was done by agarose gel electrophoresis following standard protocols on a 0.8% agarose gel in 1 x TAE buffer (0.04M Tris-acetate, 0.001 M EDTA, pH 8.0). 1-2 µg of each digested DNA sample is loaded into each lane, with one lane on either side of the gel set aside for a molecular weight marker. The gel was run at 5 V/cm in 1 x TAE buffer for 3-4 h.

S**outhern transfer**

Southern transfer was performed by capillary transfer using 1 x SSC transfer buffer (20 x SSC: 3M NaCl, 0.3M Sodium Citrate, pH7.0) to a positively charged nylon membrane. After the transfer, the DNA was fixed on the wet blotting membrane by UV-crosslinking (120 mJ). The blotting membrane was washed twice with 2 x SSC buffer for 10 min.

Prehybridization

The blot was incubated in pre-warmed digoxigenin-labeled probe (DIG) at 42^{o}C with gentle agitation.

Hybridization

The hybridization and chemiluminescence detection steps were performed according to the TeloTAGGG telomere length ass protocol (Roche cat. # 2209136). 1 µl telomere probe (digoxigenin-labelled telomere specific hybridization probe, Roche cat. # 2209136) was added per 5ml prewarmed DIG solution and the membrane was incubated in the new solution for 3 h at 42^{o}C with gentle agitation. The membrane was washed twice with stringent wash buffer I (2 x SSC, 0.1% SDS) at RT with gentle agitation, then washed twice with stringent wash buffer II (0.2 x SSC, 0.2% SDS) at 50^{o}C (each wash for 15-20 min with gentle agitation).

Detection of Telomeric DNA

The membrane was washed in at least 100 ml 1 x washing buffer (1 x maleic acid buffer (100mM maleic acid, 150mM NaCl, 0.1% Tween-20), 3-5% Tween-20) for 1 – 5 min at RT with gentle agitation. The membrane was incubated in 100 ml 1 x blocking solution for 1 hr at RT with gentle agitation. Next the membrane was incubated in 50 ml Anti-DIG-AP working solution (0.75 µg/µl, Fab fragments of polyclonal antibody from sheep, conjugated to alkaline phosphatase (AP), Roche, #2209136) for 30 min at RT with gentle agitation, washed twice, then incubated in 100 ml 1 x detection buffer (Roche, #2209136, undisclosed ingredients) for 2-5 min at RT with gentle agitation. The detection buffer was discarded and excess liquid removed from the membrane by placing the membrane, DNA side up, on a sheet of absorbent paper. The membrane must not dry out. The wet membrane was placed immediately, DNA side up, on a page of acetate and approx. 20 drops substrate solution (Roche, #2209136 formulation undisclosed but containing CDP-Star, a highly sensitive chemiliminescence substrate) were immediately applied to the membrane. Another piece of acetate was immediately placed on top and all bubbles squeezed out to ensure an even application. The membrane was incubated in substrate solution in the dark for 5 min at RT. Then excess substrate solution was squeezed out and the membrane and acetates were wrapped in cling-film and exposed to X-ray film for 20 min at RT. Signals produced by various cell samples were compared by eye. The positive control DNA supplied with the kit is purified genomic DNA from immortal cell lines.

2.22 Cell cycle analysis

Cell cycle analysis experiments were performed using primary MEF cultures. 1 x 10^5 - 1 x 10^6 cells were harvested, centrifuged and medium removed. Cells were resuspended in 200 µl cold PBS and 700 µl ice cold ethanol was added drop by drop whilst vortexing to avoid clumping and left at -20^{o}C for 2 h.

Cells were washed twice with PBS and 500 µl of propidium iodide solution was added per sample (25 µl RnaseA 1 x, 25 µl propidium iodide (Sigma) 50 ug/ml, 450 µl PBS). Tubes were wrapped in foil and left at room temperature for 15 mins. Samples were analysed on FACSCanto which sorts cells according to nuclear material and cell size. The spread of cells were arranged into 'gates' and these were used as approximations of stages of the cell cycle. Results were plotted on bar charts for comparison.

2.23 Quantitative Polymerase Chain Reaction (Q-PCR)

For analysis of IGF-1 expression by qPCR, RNA was extracted from adult mouse liver (aged 3 months) using the RNeasy Plus Mini Kit (Qiagen), checked for DNA contamination by running a sample on a DNA gel, and then cDNA was generated using the Promega reverse transcription system, in which 2 µg RNA and 0.5 µg oligo dT are incubated at 70^{o}C for 5 min and then added to a master mix of M-MLV 5X Reaction Buffer (5 µl), 10 mM dNTPs (1.25 µl) Recombinant Rnasin® Ribonuclease Inhibitor (25 units), and M-MLV Reverse Transcriptase (200 units), and incubated at 42^{o}C for 1 h. Then 1 µl RNase A (Promega) was added and the mixture was incubated at 37^{o}C for 30 mins. cDNA was purified with the QIAquick Spin PCR purification kit and 2.5 µl of the product used in Q-PCR reactions with Quantitect SYBR® Green PCR Master Mix (Qiagen), 100 nM each of the appropriate forward and reverse primers, (see Table 2.vi for primer details), and water to make solutions up to 25 µl. The reactions were run in a Stratagene MX4000 Q-PCR machine.

All data sets were collected from three samples from at least two animals for each genotype. Each qRT-PCR reaction was carried out in triplicate with at least three reactions for each gene. For analysis the mean CT of the β-actin (control) triplicates

were calculated for each genotype and then subtracted from each genotype's individual triplicate CT for the IGF-1 (gene of interest) to give a calibrated ΔCT. The mean ΔCT of the comparator genotype was then subtracted from the ΔCT of each genotype of interest's gene of interest ΔCT to give a comparative ΔΔCT. To calculate a fold change, the ΔCT of the comparator's IGF-1 triplicates was divided by the mean ΔCT of the comparator resulting in a mean value of 1. A fold change for the other genotypes was calculated by $2^{-\Delta\Delta CT}$ for each triplicate. Fold change significance was analysed across the experiments using a Student's T-Test.

Chapter 3 : Results (1)

Aprataxin facilitates gap filling at single-stranded DNA breaks *in vitro*

3.1 Introduction

Resolution of SSBs is a multi-step chemical process involving the formation of reaction intermediates. One such intermediate results from the adenylation of the 5'-terminus of the SSB, to form a 5'-adenosine monophosphate (5'AMP). The formation of a 5'AMP is catalysed by a ligase during the process of ligation - the final stage of repair. Adenylation of the 5'-phosphoryl (5'P) group activates it for formation of a phosphodiester bond by attack from a 3'hydroxyl (3'OH), covalently resealing the sugar-phosphate backbone of the DNA, restoring the duplex (Figure 1.14).

If the 3'OH is not present, then the ligase may detach leaving the 5'AMP in a process called 'abortive ligation' (Figure 1.15). Aprataxin can remove the 5'AMP with high efficiency *in vitro* (Figure 1.13). Despite the existence of other mechanisms to remove this blocked terminus, mutations in aprataxin leading to loss of function (Date et al. 2001; Moreira et al. 2001) or nuclear transport (Crimella et al. 2011) result in the neurodegenerative disease Ataxia Oculomotor Apraxia (AOA1), characterised by cerebellar atrophy (Date et al. 2004; Moreira et al. 2001). Thus far the reasons for acute dependency upon aprataxin in the cerebellum remain elusive. The neural tissues of the cerebellum are adept at short-patch SSBR (Reynolds, El-Khamisy, Katyal, et al. 2009; El-Khamisy et al. 2009) but the expression of proteins that have hitherto been associated with long-patch SSBR (such as the clamp PCNA and flap cleavage enzyme FEN1) is limited (Englander 2008). This chapter provides evidence that aprataxin promotes 3' extension to fill the gap at a single-strand break. Conversely, in the absence of aprataxin, 3' extension is attenuated.

3.1.2 Aims of this chapter

Since the discovery that aprataxin cleaves 5'AMP *in vitro*, efforts have been focused on confirming this activity in cells, and correlating it with the pathogenesis of AOA1, the cerebellar ataxia resulting from a loss of aprataxin function. Aprataxin-deleted chicken DT40 cells, $Aptx^{-/-}$ mouse fibroblasts, AOA1 human fibroblasts, and AOA1 lymphoblastoid cells have all failed to demonstrate a measurable defect in global SSBR rates (Reynolds, El-Khamisy & Caldecott 2009). However, a global SSBR defect was observed in $TDP^{-/-}Aptx^{-/-}$ cortical astrocytes (El-Khamisy et al. 2009).

Questions in mind while designing and undertaking the experiments discussed here were:

- What is the relevant toxic lesion in the pathogenesis of AOA1?
- What is the order of events during repair of a SSB?
- Does the adenylation of a 5' terminus by a ligase take place before the filling of the gap?
- If so would this have an effect on the gap-filling reaction?
- Would an aprataxin-deleted cell lysate be able to repair single-strand breaks missing more than one base as efficiently as a wild-type counterpart?

3.2 Results

Recombinant aprataxin was overexpressed in *E. Coli* (Figure 3.1 A) and purified by IMAC (Figure 3.1 B) and cation exchange chromatography. The eluted aliquot with the best yield/purity was selected and quantified by comparison to a BSA standard titration (Figure 3.1 C).

To test the enzymatic activity of the lysates, DNA substrates were prepared to assess the activity of Tdp1: an 18mer with a radiolabel (^{32}P) at the 5' terminus and either a phosphotyrosine or a phosphate at the 3' terminus (Figure 3.2 A). To test the enzymatic activity of the recombinant aprataxin and confirm the presence of aprataxin activity in Wt lysates, and the lack of aprataxin activity in Aptx$^{-/-}$ lysates, two DNA substrates were prepared: a 25mer with a radiolabel (^{32}P) within the phosphate group at the 5' terminus (25P), and a similar radiolabelled 25P, with an AMP group bound to the radioactive 5’ phosphorus (25A) (Figure 3.2 B).

Wild-type and Aptx$^{-/-}$ MEFs were isolated, genotyped and cultured, and cell-free lysates were prepared. Activity of Tdp1 in both lysates was confirmed by in vitro repair experiments in which both lysates demonstrated ability to cleave tyrosine from the 18Y DNA substrate (Figure 3.2 C). Absence of expression in the Aptx$^{-/-}$ cells was confirmed by Western blot, with β-actin used as the control protein (Figure 3.2 D).

In vitro repair experiments using the 25A DNA substrate confirmed the ability of recombinant aprataxin and Wt lysate to cleave 5’AMP. Similar concentrations of Aptx$^{-/-}$ lysate demonstrated no 5’adenylate cleavage activity (Figure 3.2 E).

In order to test the ability of the lysates to repair a single-strand break a "gap substrate" was prepared, in which a 5' ^{32}P radiolabelled 18mer, and a 14mer were annealed to a complementary 36mer in order to make a double stranded oligonucleotide duplex harbouring a SSB with a 3'OH and 3 nucleotide gap (Figure 3.3 A). The 3'OH group present is the substrate for a DNA polymerase, which can extend from the 3'OH to fill the gap (Figure 3.3 B).

Reactions to test the activities of Wt and Aptx$^{-/-}$ lysates on the gap substrate showed less extension by the Aptx$^{-/-}$ lysate reaction than by the Wt lysate. As well as a reduction in the amount of fully repaired product, the size of products formed overall were smaller in the Aptx$^{-/-}$ reaction (Figure 3.3 C). Two repeats of the reactions presented in Figure 3.3 were carried out, using the same lysate aliquots, the same conditions and were run simultaneously (Figure 3.3 A and B). The relative abundance of each size of product formed was calculated using ImageQuant and the data were combined to quantify the variation in spread of product size and the variation between similar experiments (Figure 3.4 E).

Next, repair reactions were set up containing either Wt, or Aptx$^{-/-}$ lysate, and combinations of the recombinant proteins PNK, Pol β, ligase III α (Figure 3.5 A). The reaction time was 1.5 hrs and most of the reactions proceeded to 36mer (or even one nucleotide further in some cases). But the products of the reaction containing Aptx$^{-/-}$ lysate and no ligase (Figure 3.5 A, lane 6) were significantly smaller – i.e. the reaction had not continued as far as the other reactions. In the absence of the recombinant ligase, Wt lysate was able to complete repair to make the complete 36mer, but the Aptx$^{-/-}$ lysate was not.

The results suggest that the lack of aprataxin activity in Aptx$^{-/-}$ lysate result in a blocked 5' terminus that is unavailable for ligation, thereby forcing the polymerase activity (most likely Pol β as it is in excess in these reactions) to displacement synthesis which takes longer to extend to the full length of the oligonucleotide than simply filling the gap (non-displacement synthesis) and ligation. Quantifications of the products produced by reactions run in lanes 3 and 6 were plotted on a bar chart as an alternative illustration of the spread of product sizes produced (Figure 3.5 B). The difference between the size of products formed in reactions presented in lanes 3 and 6, that were similar other than containing either Wt, or Aptx$^{-/-}$ lysate respectively, was so striking that further experiments involving recombinant Pol β and the cell lysates were carried out to investigate this observation.

Further experiments with the cell lysates and titrations of Pol β in which reactions were run for 30 mins, in order to understand the early time-points of the reaction, showed that gap filling was impaired in the presence of Aptx$^{-/-}$ lysate, relative to Wt lysate (Figure 3.6). The observed stalling at product size 21 appears to support the notion that repair of gap substrate by Wt lysate involves predominantly a non-displacement synthesis model. In this model, the gap is filled, and there is a brief pause while the ligation reaction takes place to complete repair. The Aptx$^{-/-}$ lysate reaction shows DNA synthesis taking place at a slower rate than in the Wt reactions, at each concentration of Pol β used, and less evidence of stalling at product size 21 before proceeding to displacement synthesis (Figure 3.6).

The shorter reaction time of 30 mins was used for the rest of the in vitro experiments in order focus on the gap filling stage of the reaction. Further experiments showed that the difference in extension by Aptx$^{-/-}$ lysate compared to Wt lysate changed with the amount of Pol β added (Figure 3.7). The greatest difference in 3' extension observed was with Pol β at a concentration of 62nM. Presumably at higher concentrations of Pol β a displacement synthesis is favoured, regardless of the presence of aprataxin or not. Extension in the presence of Wt or Aptx$^{-/-}$ lysate showed similar patterns of stalling but progressed at a slower rate in the reaction containing Aptx$^{-/-}$ lysate, at all concentrations of Pol β (Figure 3.7).

To test whether the effect was due to a direct interaction between aprataxin and polymerase, or dependent on components within the lysate, repair reactions were set up in which no lysate but a titration of recombinant Pol β and either recombinant aprataxin, or the same concentration of BSA, was present. Recombinant aprataxin was found to markedly increase the extension by recombinant Pol β, independent of lysate components (Figure 3.8), suggesting that the interaction is direct.

3.3 Discussion

The data presented in this chapter reveal that aprataxin promotes gap filling by the extension of a 3'OH at a DNA gap substrate. The repair of a "short-patch" (one-nucleotide gap) SSB in the absence of aprataxin was shown to be defective in vitro (Reynolds, El-Khamisy, Katyal, et al. 2009) when the 5' terminus is adenylated. In the experiments presented here, the DNA substrate has a three-nucleotide gap and the 5'

terminus has not been pre-adenylated but the abortive action of a ligase at the 5'-P terminus could produce a 5'AMP.

Aprataxin (which has DNA end processing activity) and polymerases (which can synthesize DNA to fill the gap at SSBs and anneal chromosome ends at double strand breaks) interact in the same multi-protein repair complexes (see Figure 3.9 and 3.10) (Caldecott 2001; Clements et al. 2004). These consist of X-ray cross-complementing proteins (XRCC1 and XRCC4, which serve as scaffolds to recruit and stabilize various repair proteins at the sites of SSBs and DSBs respectively). XRCC1-DNA Ligase III form the core of the protein complex coordinating SSB repair (SSBR) (Caldecott et al. 1995; Caldecott et al. 1996) and XRCC4-LigIV form the core of the protein complex coordinating DSB repair (DSBR) (Grawunder et al. 1998).

Such multi-protein complexes are responsible for detecting lesions, and coordinating correct repair. It is not currently known to what extent the complex is responsible for actively selecting the correct sequence of activities for the lesion but cross-talk between proteins in the complex is likely important, in order to spatially and temporally arrange the lesion-specific sequence of repair activities correctly.

Reynolds et al. showed that in the absence of aprataxin, then short-patch repair of a 5'AMP SSB is blocked in the presence of elevated levels of ATP due to low levels of non-adenylated ligase (Reynolds, El-Khamisy, Katyal, et al. 2009). The ATP concentrations used in the repair experiments presented here were moderate (1 mM) but may have been high enough to limit the availability of non-adenylated ligase available for ligation of a 5'AMP and 3'P.

The enhancement in recombinant Pol β activity in the presence of recombinant aprataxin alone - in the absence of cell lysate - (Figure 3.8) is surprising and intriguing, as it suggests that the activity enhancement occurs independent of any other SSBR machinery.

Following an abortive ligation and in the absence of aprataxin to remove the resulting 5'AMP, the attenuation of long-patch repair seems counter-productive. What would the effect be in cells? It may prevent the polymerase from unnecessarily proceeding to displace undamaged DNA (as is the case in the long-patch repair model), allowing more time for the 5' terminus to be processed in order for ligation to take place.

It may also reflect an *in vitro* – specific effect. One disadvantage of this *in vitro* repair assay is that it uses short stretches of linear DNA – quite unlike the DNA in cells. Furthermore, the process of lysis, snap freezing, thawing and the artificial conditions of the assay are unlikely to truly reflect the function of enzymes *in situ*. Therefore, whilst informative, it is difficult to extrapolate *in vitro* results to the situation at SSBs in cells or organisms, so the rest of the study into aprataxin function was carried out in cells and tissues from aged mice.

To test the hypothesis arising from the data presented in this chapter, further experiments could be performed to address the following questions:

- Do aprataxin and Pol β interact directly?
- Could raising the level of Pol β present compensate for aprataxin deficiency in

post-mitotic tissue?

- What would be the effect of losing both aprataxin and Pol β?
- Questions regarding the order of events taking place at a gap substrate. For example:
  - At what stage does a ligase bind - and dissociate?
  - Can a 5’ moiety itself affect 3’ processing and gap filling steps?
  - Is co-ordination of SSBR influenced by intermediary proteins and if so, how?

Chapter 4

Results (2)

How does loss of aprataxin affect growth, survival, senescence, and DNA repair in cells?

4.1 Introduction

Aprataxin has been shown to protect both nuclear and mitochondrial DNA against genotoxic stress, but so far the data on aprataxin function has fallen short of providing a comprehensive disease mechanism. Firstly, inaccessibility of the affected tissues and the inability to culture post-mitotic neurons (the cells that appear to be primarily affected in the disease) for use in functional assays have proved an obstacle. Whole animal models are apparently asymptomatic, and aprataxin-deleted mammalian cells in culture have so far revealed little or no defect in viability or DNA repair capacity (Becherel et al. 2006; Clements et al. 2004; Gueven et al. 2004; Harris et al. 2009; Mosesso et al. 2005). This probably suggests that only a small subset of breaks undergo abortive ligation to form the 5'AMP modification that is the substrate for aprataxin and that in most cellular circumstances, there are back-up repair pathways to compensate for a lack of aprataxin.

In this study I aim to evaluate the role of aprataxin in response to oxidative DNA damage. In devising a new cellular model, the success of strategies used in previous studies were drawn upon, in which single-strand breaks are stabilised (i.e. repair is delayed) in order to increase the proportion of breaks that undergo abortive ligation to form 5'AMP, thereby providing a suitable cellular model to elucidate the relevant lesions and cellular effects. One such study used aprataxin deletion alongside TDP1 deletion to reveal a measurable DNA repair defect in mouse astrocytes, following treatment with the oxidising agent, H_2O_2. The same effect was observed to a lesser extent following treatment with the alkylating agent, MMS (El-Khamisy et al. 2009). Another study, this time in yeast, used a mutant RAD27 (homologous to FEN1 in humans) alongside loss of functional HNT3 (homologous to the APTX protein in humans) in order to show a measurable survival defect following damage by H_2O_2 and - to a lesser extent the alkylating agent (Daley et al. 2010).

Data suggesting that unrepaired oxidative DNA damages are the most prominent relevant toxic lesion (El-Khamisy et al. 2009; Daley et al. 2010), led to the hypothesis that increasing the oxidative stress in a cell model would increase the cell's dependence on aprataxin and reveal a significant repair and survival defect in aprataxin-deleted cells. Here I used a mutant form of superoxide dismutase 1 ($SOD1^{G93A}$), which induces oxidative base damage and single strand breaks in DNA, in line with an enhanced hydrogen peroxide production (Barbosa et al. 2010) and is widely used in models of neurotoxicity, especially in the study of amyotrophic lateral sclerosis (ALS) (Gurney et al. 1994; Howland et al. 2002).

4.2 Aims of this chapter

The first aims of this chapter were to isolate and culture Aptx$^{-/-}$ and Wt MEFs counterparts and to verify (or otherwise) the findings of others with respect to DNA repair assays. The hypothesis arising from the literature on aprataxin function is that the primary critical lesions for which aprataxin is required for repair in the tissues of the cerebellum result from endogenous oxidative species. This hypothesis presents the testable prediction that if the oxidative load of a cell is raised, then the sensitivity of aprataxin-deleted cells may be increased to detectable levels. An important aim of this chapter was to test this prediction and assess the validity of raising the endogenous cellular oxidative load as a new model for examining aprataxin function in cells - more specifically, by use of transgenic expression of the human SOD1^{G93A} mutant.

4.3 Results

Aprataxin-deleted primary murine fibroblasts exhibit slow population doubling, correlating with an accelerated senescence phenotype

To investigate the effect of loss of aprataxin in cultured cells, $Aptx^{+/-}$ mice were mated to generate Wt and $Aptx^{-/-}$ MEFs were isolated and cultured for use in functional assays. Absence of aprataxin in $Aptx^{-/-}$ cell lysate was confirmed by western blotting (Fig. 4.1A). To characterise $Aptx^{-/-}$ MEFs we first monitored cellular growth of cells over a period of 50 days. Growth curves showed that $Aptx^{-/-}$ MEF populations doubled slower than their Wt counterparts (Fig. 4.1B and Supp. Fig. S1 in Appendix II). I reasoned that the difference in growth rate may reflect the reduced ability of $Aptx^{-/-}$ cells to repair endogenous levels of DNA damage at optimal rate, as evidenced by my own previous findings that gap filling was impaired in $Aptx^{-/-}$ lysates (Chapter 3 Results (1)) and those of others (Becherel et al. 2006; Clements et al. 2004; Gueven et al. 2004; Harris et al. 2009; Mosesso et al. 2005; Reynolds et al. 2009). However survival assays showed no significant survival defect in $Aptx^{-/-}$ cells following damage with X-rays or H_2O_2 (Fig 4.1 C,D), in agreement with previous reports (Clements et al. 2004)). The early plateau in the growth curve of $Aptx^{-/-}$ cells relative to Wt cells (Figure 4.1B) suggested that $Aptx^{-/-}$ cells may be starting to senesce early in response to persisting DNA damage. To test this, serum-arrested wild-type and $Aptx^{-/-}$ cells were tested for levels of acidic β-galactosidase staining; a widely used hallmark of senescence (Dimri et al. 1995). These analyses revealed a marked passage-dependent acceleration of senescence in $Aptx^{-/-}$ MEFs compared to wild-type counterparts (Fig. 4.2 A and B). Since the transcript profile of cells changes with ageing (Brink et al. 2009), this observation prompted an investigation into the cells' capacity for transcription.

Transcription recovery following oxidative damage is delayed in aprataxin-deleted primary fibroblasts

Reactive oxygen species are the predominant source of endogenous oxidative DNA breaks in cells (Lindahl 1993; De Bont 2004). Since unrepaired DNA breaks can block transcription we compared Wt and Aptx$^{-/-}$ cells for their ability to resume transcription following oxidative DNA damage. Whilst incubation of cells with hydrogen peroxide resulted in a comparable reduction of total RNA levels in Wt and Aptx$^{-/-}$ cells, subsequent incubation in H_2O_2-free media revealed a significant ($p < 0.01$, Students T-test) deficit in RNA synthesis in Aptx$^{-/-}$ MEFs (Fig. 4.2C). These observations suggest that Aptx$^{-/-}$ cells have more unrepaired oxidative DNA breaks after damage, which require repair before transcription can continue.

Elevated intracellular oxidative load reveals a repair and survival defect in Aptx$^{-/-}$ MEFs

Previous reports using human cells and primary neural cells (El-Khamisy et al. 2009) have found no repair defect in aprataxin-deleted cells, using comet assays. In order to test the hypothesis that Aptx repairs a subset of oxidative DNA breaks *in vivo*, which becomes critical for cell function and survival in situations of high rates of intracellular oxidative stress, Aptx$^{-/-}$ mice were generated in which a mutant form of superoxide dismutase SOD1^{G93A} was expressed to increase endogenous oxidative load. SOD1^{G93A} is associated with elevated levels of oxidative stress, oxidative DNA breaks and cellular dysfunction (Howland et al. 2002; Barbosa et al. 2010). MEFs were isolated and expression of normal murine Sod1 and mutant human SOD1 (SOD1^{G93A}), or not, was confirmed by immunoblotting (Figure 4.3 A). No Wt cell line was available as a result of the Aptx/SOD1^{G93A} breeding carried out but since experiments by myself and others had shown no difference in repair

of oxidative breaks in $Aptx^{-/-}$ cells relative to Wt cells by survival assay (Figure 4.1 D) (Clements et al. 2004) we went ahead with repair assays, focussing on the effect of aprataxin loss in a mutant SOD1 background in cells. We next compared $SOD1^{G93A}$ and $Aptx^{-/-}$ $SOD1^{G93A}$ cells for the ability to repair oxidative SSBs induced by IR or H_2O_2 using alkaline comet assays. No significant difference in repair rates was observed between $Aptx^{-/-}$ $SOD1^{G93A}$ compared to $SOD1^{G93A}$ cells following γ-irradiation (Figure 4.3 B-C), but a significant delay in repair was measured at 30 mins after H_2O_2 in the double mutants compared to aprataxin-proficient SOD1 mutants (Figure 4.3 D-E).

To test whether this delay in repair of oxidative damage at short time-points would translate into a survival defect, clonogenic survival assays were performed. A significant ($p = 0.03$, Student's T-test) survival defect after the maximum dose of X-ray irradiation used (5Gy) was measured in the double mutants compared with aprataxin-proficient SOD1 mutants (Figure 4.4 A). Interestingly though, even at moderate doses of H_2O_2 the double mutants showed a significant survival defect ($p = 0.015$, Student's T-test) at 100 μM and $p = 0.02$ at 200 μM) compared with aprataxin-proficient SOD1 mutants (Figure 4.4 B).

4.4 Discussion

Aprataxin-deletion alone conferred no survival defect following gamma-irradiation or H_2O_2, in agreement with previous reports (Figure 4.1 C and D)(Clements et al. 2004). Survival and comet assays demonstrated a small but signficant defect in aprataxin-deleted cells in a $SOD1^{G93A}$ background in MEFs following exposure to physiological levels of oxidizing agent (100-200 μM H_2O_2 in survival assays, 90 μM in comet assays), but not to X-ray or γ-irradiation, respectively. This likely reflects the different the types of damage inflicted by IR and H_2O_2. Although the extent and types of damage caused to DNA by each of these damaging agents is not well understood, H_2O_2 is believed to result in more oxidative base damage and a higher SSB:DSB ratio of damage than IR (Lindahl 1993). Further work is needed to establish whether or not the defects demonstrated here are relevant to AOA1 disease pathology. The cerebella of aged $SOD1^{G93A}Aptx^{-/-}$ mouse models should be analysed for evidence of enhanced sensitivity to oxidative damage.

It should be noted that the extent of the effect of the $SOD1^{G93A}$ mutant is not yet thoroughly understood. Elevated levels of highly toxic hydroxyl radicals produced by the mutant via the Fenton reaction (Mao et al. 1993) are associated with oxidative damage to DNA and hypersensitivity to oxidizing agents (Barbosa et al. 2010). But the oxidation of other biomolecules including lipids and proteins have also been observed, all eventually leading to neurodegeneration in a pathophysiology reminiscent of that of ALS in humans - hence it has been widely used around the world to as an ALS disease model (Gurney et al. 1994). Thus, we cannot rule out further neurotoxic effects of the mutant that may sensitise to aprataxin-deletion, besides DNA oxidation. Its induction of mitochondrial dysfunction may be especially relevant, as aprataxin is implicated in the repair of mtDNA (Sykora et al. 2011) and this may explain the heightened sensitivity to oxidising agents.

There may be a positive feedback loop whereby reactive oxygen species lead to mitochondrial dysfunction, which leads to respiratory burst, generating more reactive oxygen species. We may envisage a similar situation in aged cerebellar tissues with high metabolic rate and transcript turnover and a loss of aprataxin function. The finding that senescence is accelerated and transcription recovery following oxidative damage is impaired in aprataxin-deleted cells is intriguing. Further work is needed to establish whether or not the effects observed here in MEFs are reflective of the situation in vivo and whether or not they are relevant to AOA1 disease progression. Detailed analyses of the tissues affected and of the corresponding tissues in animal models will help to address these questions in the future.

Together, these data suggest that elevating endogenous oxidative stress by expressing $SOD1^{G93A}$ sensitises $Aptx^{-/-}$ cells to oxidative DNA damage and may provide a useful model of elevated oxidative stress levels in cycling cells.

Chapter Five: Results (3)

Analyses of the consequences of expression of a toxic form of SOD1 in aprataxin knockout models

5.1 Introduction

The DNA end processing abilities of aprataxin have been well characterized *in vitro* (Ahel et al. 2006; Takahashi et al. 2007; Reynolds, El-Khamisy, and Caldecott 2009) And there is growing evidence to suggest that it protects both nuclear and mitochondrial DNA against genotoxic stress (Gueven et al. 2004; Mosesso et al. 2005; Sykora et al. 2011) and has roles in the coordination of parallel pathways (Wei and Englander 2008; Rass, Ahel, and West 2007; Kijas et al. 2006; Daley, Wilson, and Ramotar 2010). But how these activities function in the context of DNA repair *in vivo*, what the downstream cellular effects are, and why aprataxin dysfunction results in cerebellar neurodegeneration remains largely unknown. To address this issue, we used the cell stress model described in the previous chapter (transgenic expression of human $SOD1^{G93A}$) to further examine the downstream effects of loss of aprataxin in cells under continuous oxidative stress.

5.2 Aims of this chapter

The aims of this chapter were to gain more insight into the observations that aprataxin deletion is associated with an accelerated senescence phenotype and a transcription recovery defect following oxidative damage in primary fibroblasts *in vitro* (Chapter 4).

Oxidative stress has been associated with telomeric instability and reduced telomerase activity (Makino et al. 2011), so the first aim of this chapter was to assess the impact of aprataxin loss on telomeric length/stability. Next: senescence is associated with cell cycle arrest in response to DNA damage, so cell cycle analysis was a natural next step in the investigation. Cellular senescence and somatic growth attenuation at the level of the whole organism has also been associated with persistent transcription-blocking lesions - via a decrease in IGF-1 and GH signalling (Garinis et al. 2009; Niedernhofer et al. 2006) so tissues from the livers from aged mice were harvested and examined for IGF1 expression.

5.3 Results

Effects of aprataxin-deletion are not due to major telomeric instability

Following the observation that Aptx$^{-/-}$ MEFs senesce faster than wild-type counterparts the mechanisms of cellular senescence were considered. Senescence can result from multiple different triggers and by several different pathways, as reviewed by (Collado and Serrano 2006), including telomeric instability. Senataxin, a putative DNA/RNA helicase related to aprataxin, has been suggested to play a role in telomere stability (De Amicis et al. 2010). To test whether a lack of aprataxin was affecting telomere stability the telomere length of 'aged' (P8) mutant MEFs was compared using the TeloTAGGG Telomere Length Assay (Roche). Although there were noticeable differences in the telomeric signals produced by each strain (Figure 5.1, triplicates 1 and 2 compared to triplicates 3 and 4) no difference was observed between Wt and Aptx$^{-/-}$; and SOD1^{G93A} and Aptx$^{-/-}$SOD1^{G93A}. To test whether telomere shortening might be triggered by exposure to exogenous sources of DNA damage, we repeated the analyses following exposure to 50μM H_2O_2 for 10 minutes for 3 consecutive days. Although a slightly longer smear of signal – suggesting the presence of shorter telomeric sequences was observed in the treated compared to untreated SOD1^{G93A} and Aptx$^{-/-}$SOD1^{G93A} cells, there was no dramatic difference in telomeric length detected between the Wt and Aptx$^{-/-}$ cells employed without and with H_2O_2 treatment (Fig. 5 (A+B)), suggesting that the observed senescence in Aptx-/- cells is not attributable to acute telomeric instability.

Effects of aprataxin-deletion are not due to major cell cycle disruption

Next, FACS analysis was performed on cultured MEFs (passage 4) to ascertain whether defective cell cycle progression was causing the observed senescence. All mutant populations had a lower proportion of cells in G1 phase and a higher proportion of dead cells than Wt cells (Fig. 5.3). The $SOD1^{G93A}$ populations had by far the highest proportion of dead cells in both experiments. The double mutant $Aptx^{-/-}SOD1^{G93A}$ cell populations showed a modest accumulation in S and G2 phase and a concurrently lower proportion of dead cells, relative to their aprataxin-proficient counterparts.

IGF-1 expression is down-regulated in Aptx-/-SOD1G93A mouse liver

Recent reports suggesting a link between DNA damage repair defects and somatotropic growth attenuation (measurable by IGF-1 expression levels) prompted questions as to whether this may be connected with the observed accelerated senescence and reduced transcription recovery rates in $Aptx^{-/-}$ cells (Fig. 4.2). To test this hypothesis samples of liver tissues from adult (3 months old) Wt, $Aptx^{-/-}$, $SOD1^{G93A}$, and $Aptx^{-/-}SOD1^{G93A}$ mice were tested for IGF-1 expression levels. PCR amplification of IGF-1 and β-actin, a housekeeping gene, revealed a possible reduction of IGF-1 expression in the $Aptx^{-/-}$ $SOD1^{G93A}$ tissues compared to Wt tissues (Fig. 5.5 A). These observations were confirmed by quantitative PCR analyses of cDNA generated from adult mouse livers (Fig. 5.5 B). Our data revealed a significant (Student's T-test: $p < 0.001$) down-regulation of IGF-1 in the double mutants compared to all the other genotypes.

5.4 Discussion

The telomeric length assays showed no observable difference between the mutants following treatment with - a concentration of 50μM H_2O_2 below those that produced a survival defect in double mutants (Figure 4.4 B) but capable of producing a transcription recovery defect (Figure 4.2 C). Possibly a different treatment regimen would have produced an observable difference but if telomeric instability were a major cause of the acceleration in senescence observed without the use of exogenous damaging agent (Figure 4.2 A and B), we would expect an observable effect after 3 consecutive days of 10 min 50μM H_2O_2 treatments. We cannot rule it out as a possible cause either, as the amount of telomeric instability necessary to trigger senescence relative to the sensitivity of the assay is not clear. What is clear is that there is no major destabilization of telomeres with loss of aprataxin, in a $SOD1^{G93A}$ background or not, and with oxidative damage, or not.

There did appear to be some modest disruption to cell cycle progression in the mutant MEFs according to the FACS analysis readouts (Figures 5.3 and 5.4). Interestingly, the double mutants' FACS profiles appeared 'healthier' than those of the $SOD1^{G93A}$ MEFs, prompting the question: Is the level of damage sustained in these aprataxin-deleted stressed cells reaching a threshold level at which a compensatory mechanism is protecting the cells from dying? Or is aprataxin involved in an apoptotic pathway induced by levels of damage sustained in $SOD1^{G93A}$ cells so that its deletion is protecting them from dying? If deletion of p53 were found to confer protection against cell death in mutant cells, then this would support the notion of a programmed cell death in response to elevated rates of DNA damage in mutant cells.

The down-regulation in IGF-1 expression observed in the double mutants offers a possible explanation, and adds strength to previous reports that persistent transcription-blocking DNA lesions trigger somatic growth attenuation (Garinis et al. 2009; Niedernhofer et al. 2006). This marked difference in IGF-1 expression suggests a specific effect signifying a switch from growth to somatic preservation associated with extended longevity and likely correlates with the accelerated senescence observed in aprataxin-deleted cells in vitro.

Chapter Six

Discussion

6.1 Effects of aprataxin loss *in vitro*

The observation that aprataxin facilitates gap filling by Pol β at single-strand breaks *in vitro* is intriguing, and supports previous reports that aprataxin acts in concert with parallel repair processes (Daley, Wilson, and Ramotar 2010). Aprataxin and Pol β both interact with the XRCC1/LigIII SSBR protein complex (Figure 3.9) so in cells, any interaction between them may be facilitated or impaired by the multi-protein complex in which they both operate at DNA breaks.

The XRCC1/LigIII complex control various aspects of SSBR, such as the rate of recruitment of further proteins to the complex and choice of short or long patch repair, via PAR chain synthesis by PARP1 (Caldecott et al. 1996, Caldecott 2003, Fisher et al. 2007, Petermann et al. 2005). The enhancement of 3' extension by Pol β in the presence of recombinant aprataxin and no lysate, however (Figure 3.8), suggests that they might interact directly. Further work could include yeast two-hybrid analyses and co-immunoprecipitations to investigate the interaction between aprataxin and polymerases, both DNA and RNA. Pol β deletion is embryonic lethal, but Pol β expression may be suppressed in specific tissues using Cre-Lox site-specific recombinase technology. It would be interesting to do brain-specific knockout of Pol β, to test whether this sensitises aprataxin deficient post-mitotic tissue in animal models.

Although this thesis has focussed on the role of aprataxin in SSBR, it should be noted that aprataxin is also active at double-strand breaks and present in the DSBR protein complex (Figure 3.10), as are the replicative polymerases, Pol λ, Pol μ and TdT. It would be interesting to find out if a similar interaction takes place between aprataxin and the polymerases involved in DSBR. This could be tested using a similar *in vitro* repair assays as described here. The repair of double-strand DNA substrates may be measured in the presence and absence of aprataxin.

Interactions between aprataxin and polymerases may be relevant to transcription-coupled repair; aprataxin may interact with RNA polymerase. SSBR is suggested to work in conjunction with transcription machinery (Banerjee et al. 2011; El-Khamisy 2011) and data presented in this thesis suggests that aprataxin facilitates transcription recovery following oxidative damage (Figure 4.2C). It would be interesting to further investigate this observation to find out whether aprataxin interacts with RNA polymerase II by yeast two-hybrid assay and/or co-immunoprecipitation.

Reynolds et al. showed that in the absence of aprataxin, short-patch repair of a 5’AMP SSB was blocked in the presence of elevated levels of ATP, due to low levels of non-adenylated ligase

(Reynolds et al. 2009). That suggests that aprataxin is of specific importance to SSBR at high levels at ATP, which may prove to be relevant to AOA1 pathology. It would be interesting to do similar *in vitro* experiments at a range of ATP concentrations to see if this has an effect on SSBR sub-pathway choice.

6.2 Effects of aprataxin loss in cells

The findings presented in this thesis show that loss of aprataxin has an impact on cell growth and senescence. Further findings from experiments in cells offer possible reasons for the slow growth observed. Namely, the delay in transcription recovery following damage (Figure 4.2C) and the DNA repair and survival defect in cells exposed to oxidative stress (Figures 4.3 and 4.4). The *in vitro* data presented in Chapter 3, which show that aprataxin facilitates gap filling by Pol β, suggest that the effects of aprataxin loss at SSBs may extend beyond the defective 5' end processing that has previously been associated with aprataxin loss and include an effect on gap filling. This may be due to direct interaction between the proteins, indirect interaction via one or more intermediaries, or steric hindrance. It is possible that a ligase may adenylate the 5' terminus of a SSB and remain attached until a proximal 3'P is available for ligation. If so, it may physically hinder the polymerase: an effect resolvable by the action of aprataxin. Electrophoretic mobility shift assays may be used to find out if this is the case.

The finding that IGF-1 expression is dramatically reduced in aprataxin-knockout animal models expressing a toxic SOD1 mutant is consistent with the observed slow growth and accelerated senescence. Of course, the slow growth observed in aprataxin-deleted cultured cells is not necessarily as a result of a similar down-regulation of IGF-1. Even so it represents a similar pattern: a deceleration of cell growth signalling with aprataxin-deletion.

This somatic growth attenuation is well tolerated, as evidenced by the lack of disease phenotype in animal models. Indeed this response to DNA damage has been observed by others to guard against further DNA damage, extending lifespan, alongside accelerating ageing (Van Der Pluijm et al. 2007; Niedernhofer et al. 2006; Hoeijmakers 2007). This may help to explain the lack of elevated mutation rate in AOA1 pathology, as slowed replication and growth would result in lowering the rate of mutation.

Regarding the single-strand break repair and survival defect, and the attenuation of IGF-1 expression presented in this thesis, it is tempting to surmise that the delay in repair of

single-strand breaks (and correlating survival defect) following oxidative damage is sufficient to produce the attenuation in IGF-1 expression observed in adult animal models. This may be the case, but the $SOD1^{G93A}$ mutant has other effects besides DNA oxidation. Therefore we cannot rule out the possibility that there is another unknown effect that, in combination with aprataxin loss leads to the observed somatic growth attenuation. Further evidence linking the IGF-1 expression suppression to oxidative damage would be necessary to rule out this possibility.

Transcription-coupled repair is understood to prioritise the repair of transcribed genes, thereby conserving DNA repair capacity for where its most needed (Tornaletti 2009). Aprataxin has been shown to associate with the nucleolar proteins nucleolin, nucleophosmin and upstream binding factor (UBF) that have been associated with transcription (Becherel et al. 2006; Gueven et al. 2004), presenting the possibility that aprataxin has a role at sites of high transcriptional demand. The cerebellum is thought to be extremely transcriptionally active so its role in transcription is likely to be especially important for the pathology of the disease. Further work is needed to investigate aprataxin's role in transcription-coupled repair. DNA microarray experiments using cell cultures or tissues from animal models could be very informative in measuring gene expression levels across the genome.

6.2.1 Importance of oxidative lesions in the brain

Since the brain is largely protected from exogenous DNA damage sources by the cranium and the blood-brain barrier, DNA lesions in the brain result predominantly from endogenous sources. The high rate of oxidative metabolism in the brain and the resulting high concentrations of reactive oxygen species produce high levels of DNA damage, especially single-strand breaks and oxidative damage (Lindahl 1993; De Bont 2004). Robust DNA repair processes are generally associated with replication in proliferating cells due to the presence of a sister chromatid to use as a template (Barnes and Lindahl 2004), so the post-mitotic neurons in the adult brain are believed to be especially reliant upon the repair mechanisms at their disposal. If AOA1 is indeed caused by defective DNA repair, then the tissue-specific neurodegeneration observed in the cerebellum of AOA1 patients suggests that the critical lesion is oxidative in nature and requires processing by aprataxin.

The synergistic toxicity of mutant SOD1 expression (which induces oxidative DNA damage) and aprataxin-deletion in cells is consistent with the above premise. Furthermore, it raises the

question: could SOD1-related activities play a role in AOA1 pathology? SOD1 and catalase are both important antioxidant enzymes that function in conjunction with one another. SOD1 is a scavenger of superoxide radicals but produces hydrogen peroxide. Under conditions where superoxide radicals are in excess and iron is available, the formation of toxic hydroxyl radicals from hydrogen peroxide by SOD1 via the Fenton reaction outweigh the beneficial effects of superoxide scavenging – a mechanism understood to be stimulated by the G93A mutation (Chang et al. 1988; Mao et al. 1993; Cleveland and Liu 2000) (Figure 1.22).

Transfection of mouse epidermal cells with catalase protects against toxicity associated with mutant SOD1 transfection, suggesting that catalase can compensate for harmful by-products of SOD1 activity (Amstad et al. 1991). Englander finds that catalase levels in the cerebellum are markedly elevated relative to other tissues - presumably as a cellular response to stress to mitigate the elevated levels of oxidative stress in these cells. Overexpression of catalase has been reported to increase life expectancy by almost 20% in mice (Schriner et al. 2005). It would be interesting to test catalase expression levels in $SOD1^{G93A}/Aptx^{-/-}$ animal models - in the brain and other tissues. We might expect an up-regulation in double mutants in response to higher levels of oxidative stress and impaired ability to repair oxidative DNA damage.

Further studies are required to understand the contribution of SOD1/catalase imbalance to toxic DNA oxidation by ROS and to investigate possible ways to slow the accumulation of damage. If SOD1/catalase imbalance and Fenton-derived ROS are found to be responsible for neuronal decline, then antioxidants and/or metal chelators may prove useful in extending the life of repair-defective neurons.

6.2.2 Downstream effects of aprataxin loss on cellular processes

The most note-worthy effects of aprataxin loss on downstream cellular processes presented in this thesis - namely, the slowed population doubling in cultured cells, the accelerated senescence, the delay in transcription recovery, and the attenuation of somatic growth signalling with concomitant expression of a toxic SOD1 mutant, all present promising avenues for further investigation. Conclusions from results obtained using the SOD1 mutant should be made with caution due to the unspecific nature of its effects. Still, all of the effects observed seem to be different readouts of the same overall cellular response to accumulating DNA damage - a switch to slow cell growth and other DNA-related processes in order to maintain genome stability.

This effect has also been observed in response to NAD^+ depletion in the nucleus and cytoplasm following caloric restriction or exercise (Yang et al. 2007) and is thought to be due to activation of the NAD^+ salvage pathway in the mitochondria. Before discussing this more, I will first consider the DNA repair role of aprataxin in the mitochondria.

6.2.3 Effects of mitochondrial dysfunction

The results presented in this thesis do not address the role of aprataxin specifically at mitochondrial DNA, but it should be noted that aprataxin has roles in repairing both nuclear and mitochondrial DNA (Sykora et al. 2011). Mitochondrial DNA is believed to be especially threatened by oxidative damage - due to the high levels of ROS present in the mitochondria, and the lack of protective histones bound to mtDNA. On the other hand, nuDNA is much more sensitive to oxidative damage, whereas the multiple copies of mtDNA and limited repair capacities thereof mean that a high level of oxidative breaks can persist without critically disrupting mitochondrial function. AOA1 shares some characteristics of one particular type of mitochondrial disease, known as Neuropathy, Ataxia, and Retinitis Pigmentosa (NARP), which results from a reduced ability of the ATP synthase enzyme in the mitochondria to generate ATP (Santorelli et al. 1997). It is likely that mitochondrial dysfunction accounts at least in part to AOA1 pathogenesis, although there is currently not enough evidence to be able to fully attribute the pathology to either compartment. Since aprataxin is present in both compartments, it is likely required for optimal function of both nuclear and mitochondrial processes.

6.2.4 PARylation, NAD^+, and sirtuin signalling

PARylation plays diverse roles in many molecular and cellular processes, including DNA damage recognition and repair, chromatin modification, transcription, and cell death pathways (Kim, Zhang, and Kraus 2005). These processes are involved in many physiological and pathophysiological outcomes, including genome maintenance, carcinogenesis, ageing, inflammation, and neuronal function (Kim, Zhang, and Kraus 2005). Generation of PAR for polymerisation by PARPs, is dependent upon NAD^+ (Nishizuka

1967). One of the major causes of cell death due to genotoxic stress is hyperactivation of the NAD^+-dependent PARP-1, leading to a depletion in nuclear and cytoplasmic NAD^+ and resulting in the translocation of apoptosis inducing factor (AIF) from the mitochondrial membrane to the nucleus, triggering apoptosis (Yu et al. 2002). This may explain the higher cell killing after damage observed in the double mutants (Figure 4.4).

Prolonged PARylation resulting from persisting SSBs such as those observed in the data presented in this thesis (Figure 4.3E) may be sufficient to deplete NAD^+ levels in neurons, to a level at which sirtuins are activated. The sirtuins are a highly conserved family of NAD^+-sensitive deacetylases and mono-ADP-ribosyltransferases that are implicated in transcriptional silencing and longevity under conditions of cell stress and caloric restriction (Imai et al. 2000). IGF-1 suppression has been associated with sirtuin activation (Niedernhofer et al. 2006; Mostoslavsky et al. 2006; Cohen et al. 2009).

Hence, the IGF-1 down-regulation observed in adult animal models (Figure 5.5) may be linked to the persisting SSBs observed in cultured cells of the same genotype (Figure 4.3E). Currently little is known about the exact amount of NAD^+ present in the cellular compartments, or the amount of DNA damage required to impact on NAD^+ levels. If mitochondrial dysfunction as a result of NAD^+ depletion is to blame for aprataxin-deficiency related pathology, then we might expect sirtuin agonists to prove useful in delaying symptom onset in patients. Several such compounds exist, including the Sirt1 agonist SRT1720, which has demonstrated improvement in mitochondrial capacity and oxidative metabolism in rats and mice (Milne et al. 2007; Feige et al. 2008; Yoshizaki et al. 2010).

6.3. Implications for understanding of aprataxin function and AOA1

The data presented in this thesis may prove to be helpful in developing understanding of aprataxin function and AOA1. Together, they suggest that although loss of aprataxin function is not harmful to cells under most conditions, concurrent oxidative damage can impact on cell function and accumulation of damage over long time periods can lead to several effects associated with ageing. I would therefore like to suggest that AOA1 disease progression may manifest due to reiterative cycles of DNA damage and response – leading to increasing loss of function and cell death: a cerebellum-specific progeroid syndrome (Figure 6.1).

Although this thesis has not addressed questions of aprataxin function at DSBs, it is recruited to DSBs and can bind and cleave blunt and 'sticky end' double stranded DNA-adenylate substrates (all be it with considerably lower affinity than single-strand break substrates). The vast majority of DNA strand breaks induced by oxidative damage (the principle type of damage believed to be responsible for AOA1 pathogenesis) are SSBs, but about one in 2000-3000 are DSBs (Olive and Johnston 1997; Bradley and Kohn 1979) More SSBs may be converted to DSBs by collision with the transcription machinery or by SSBs on opposite strands occurring close to one another. Although rare, these are likely to be highly toxic breaks and likely to contribute in part to AOA1 pathogenesis.

Treatment for AOA1 is currently very limited. Some AOA1 patients display coenzyme Q10 (CoQ10) deficiency. In these cases, oral CoQ10 supplementation can improve clinical outcome (Quinzii et al. 2005). Oral antioxidant supplements are used, with limited improvement in clinical outcome (Palau and Espinós 2006). Now that patients may be identified by genetic testing prior to the onset of symptoms, prophylactic treatment may significantly delay or even prevent disease onset, once the disease mechanism is clearly delineated. If oxidative breaks prove to be critical in AOA1 pathogenesis, antioxidant supplementation from infancy may prove useful in delaying symptom onset. If the absence of aprataxin and unavailability of non-adenylated ligase in cellular situations of elevated ATP levels proves to be critical, then pharmaceutical intervention favouring the non-adenylated ligase may be beneficial. If sirtuin signalling or SOD1/catalase imbalance prove to be relevant to the human disease, then pharmaceutical intervention may be designed to target these. In the longer term we may look to gene-therapy approaches to treat the disease. For example, tissue-specific antioxidant expression or DNA repair factor complementation.

6.3.1 Outstanding questions

Despite the progress that has been made over the last decade in understanding the molecular basis of AOA1, there are several important outstanding questions. The site-specific nature of the neurodegeneration observed in AOA1 remains to be explained. If the impact of aprataxin loss on cellular responses to oxidative damage presented here is true also in a human adult, then they may offer explanations to this question., It would be interesting to know what levels of oxidative damage may be tolerated in the human cerebellum to what extent defective

SSBR/transcription dysruption/accelerated senescence is tolerated before impacting on cell function. These issues are currently impossible to resolve absolutely due to the inaccessibility of human tissues but may be approximated using cellular and animal models.

The reason for the lack of elevated mutation rate and cancer predisposition in AOA1, a common feature of other human disorders associated with DNA repair defects, has not so far been resolved. The acceleration in senescence and attenuation of somatic growth, are consistent with a protection against expected elevated mutation rate. It would be interesting to find out if there are similar effects in human AOA1 patients. If a similar effect is found in human AOA1 patients, it may help to explain the lack of elevated malignancy and may even help to explain the site-specific nature of the neurodegeneration observed in AOA1. Further research into the role of growth hormone signalling on replicating cells and on complex neural systems will be necessary to address these questions.

6.3.2 Concluding remarks

The contribution of persisting DNA damage to ageing, and various age-related pathologies is a subject of intense interest. The DNA repair system shows remarkable capacity to adapt to specific situations and compensate for defects at the level of individual DNA strand breaks. The highly conserved metabolic response to persisting DNA damage, whereby attenuation of the IGF-1/GH somatic growth signalling pathway re-allocates resources from growth to somatic preservation and life extension, is an example of a compensatory response of a much larger scale, affecting the whole organism. Pharmaceutical or gene-therapy approaches to harnessing these processes may provide relief from progeroid syndromes and age-related disease.

Research into the mechanisms of neurological disease and efforts directed at slowing or preventing disease progression offer hope for treating debilitating neurodegenerative diseases. More generally, they offer hope for improving the robustness and extending the life span of the human brain.

References

Abraham, R.T., 2004. PI 3-kinase related kinases: “big” players in stress-induced signaling pathways. *DNA Repair*, 3(8-9), pp.883–887.

Adachi, N. et al., 2003. Hypersensitivity of nonhomologous DNA end-joining mutants to VP-16 and ICRF-193: implications for the repair of topoisomerase II-mediated DNA damage. *The Journal of biological chemistry*, 278(38), pp.35897–902.

Ahel, I. et al., 2006. The neurodegenerative disease protein aprataxin resolves abortive DNA ligation intermediates. *Nature*, 443(7112), pp.713–6.

Ahnesorg, P., Smith, P. & Jackson, S.P., 2006. XLF interacts with the XRCC4-DNA ligase IV complex to promote DNA nonhomologous end-joining. *Cell*, 124(2), pp.301–13.

Aicardi, J. et al., 1988. Ataxia-ocular motor apraxia: a syndrome mimicking ataxia-telangiectasia. *Annals of Neurology*, 24(4), pp.497–502.

Amstad, P. et al., 1991. The balance between Cu,Zn-superoxide dismutase and catalase affects the sensitivity of mouse epidermal cells to oxidative stress. *Biochemistry*, 30(38), pp.9305–9313.

Araki, M. et al., 2001. Centrosome protein centrin 2/caltractin 1 is part of the xeroderma pigmentosum group C complex that initiates global genome nucleotide excision repair. *The Journal of Biological Chemistry*, 276(22), pp.18665–18672.

Armanios, M., 2009. Syndromes of telomere shortening. *Annual Review of Genomics and Human Genetics*, 10(46), pp.45–61.

Audebert, M., Salles, B. & Calsou, P., 2004. Involvement of poly (ADP-ribose) polymerase-1 and XRCC1/DNA ligase III in an alternative route for DNA double-strand breaks rejoining. *Journal of Biological Chemistry*. 279(53):55117-26

Bakkenist, C.J. & Kastan, M.B., 2003. DNA damage activates ATM through intermolecular autophosphorylation and dimer dissociation. *Nature*, 421(6922), pp.499–506.

Balakrishnan, L. et al., 2009. Long patch base excision repair proceeds via coordinated stimulation of the multienzyme DNA repair complex. *The Journal of Biological Chemistry*, 284(22), pp.15158–15172.

Banerjee, D. et al., 2011. Preferential repair of oxidized base damage in the transcribed genes of mammalian cells. *The Journal of Biological Chemistry*, 286(8), pp.6006–6016.

Barbosa, L.F. et al., 2010. Increased SOD1 association with chromatin, DNA damage, p53 activation, and apoptosis in a cellular model of SOD1-linked ALS. *Biochimica et biophysica acta*, 1802(5), pp.462–71.

Barbot, C. et al., 2001. Recessive ataxia with ocular apraxia: review of 22 Portuguese patients. *Archives of Neurology*, 58(2), pp.201–205.

Barnes, D.E. et al., 1998. Targeted disruption of the gene encoding DNA ligase IV leads to lethality in embryonic mice. *Current Biology*, 8(25), pp.1395–1398.

Barnes, D.E. & Lindahl, T., 2004. Repair and genetic consequences of endogenous DNA base damage in mammalian cells. *Annual review of genetics*, 38, pp.445–76.

Barzilai, A., 2007. The contribution of the DNA damage response to neuronal viability. *Antioxidants redox signaling*, 9(2), pp.211–218.

Bayer, S.A. et al., 1991. Planar differences in nuclear area and orientation in the subventricular and intermediate zones of the rat embryonic neocortex. *Journal of Comparative Neurology*, 307(3), pp.487–498.

Beal, M.F., 1996. Mitochondria, free radicals, and neurodegeneration. *Current Opinion in Neurobiology*, 6(5), pp.661–666.

Bebenek, K. et al., 2001. 5'-Deoxyribose phosphate lyase activity of human DNA polymerase iota in vitro. *Science*, 291(5511), pp.2156–2159.

Becherel, O.J. et al., 2010. CK2 phosphorylation-dependent interaction between aprataxin and MDC1 in the DNA damage response. *Nucleic acids research*, 38(5), pp.1489–503.

Becherel, O.J. et al., 2006. Nucleolar localization of aprataxin is dependent on interaction with nucleolin and on active ribosomal DNA transcription. *Human molecular genetics*, 15(14), pp.2239–49.

Beckman, K.B. & Ames, B.N., 1997. Oxidative decay of DNA. *The Journal of Biological Chemistry*, 272(32), pp.19633–19636.

Benjamin, R.C. & Gillg, D.M., 1980. in Vitro. , pp.10502–10508.

Bernstein, N.K. et al., 2005. The molecular architecture of the mammalian DNA repair enzyme, polynucleotide kinase. *Molecular Cell*, 17(5), pp.657–70.

Bjelland, S., 2003. Mutagenicity, toxicity and repair of DNA base damage induced by oxidation. *Mutation Research/Fundamental and Molecular Mechanisms of Mutagenesis*, 531(1-2), pp.37–80.

Blackburn, E.H., 1990. Telomeres and their synthesis. *Science*, 249(4968), pp.489–490.

Blunt, T. et al., 1995. Defective DNA-dependent protein kinase activity is linked to V(D)J recombination and DNA repair defects associated with the murine scid mutation. *Cell*, 80(5), pp.813–23.

Bohgaki, T. et al., 2011. Genomic Instability, Defective Spermatogenesis, Immunodeficiency, and Cancer in a Mouse Model of the RIDDLE Syndrome M. Lichten, ed. *PLoS Genetics*, 7(4), p.17.

De Bont, R., 2004. Endogenous DNA damage in humans: a review of quantitative data. *Mutagenesis*, 19(3), pp.169–185.

Bradley, M.O. & Kohn, K.W., 1979. X-ray induced DNA double strand break production and repair in mammalian cells as measured by neutral filter elution. *Nucleic acids research*, 7(3), pp.793–804.

Bramson, J. et al., 1993. Poly(ADP-ribose) polymerase can bind melphalan damaged DNA. *Cancer Research*, 53(22), pp.5370–5373.

Brenner, C., 2002. Hint, Fhit, and GalT: Function, Structure, Evolution, and Mechanism of Three Branches of the Histidine Triad Superfamily of Nucleotide Hydrolases and Transferases. *Biochemistry*, 41(29), pp.9003–9014.

Brookman, K., Tebbs, R. & Allen, S., 1994. Isolation and Characterization of Mouse Xrcc-1, a DNA Repair Gene Affecting Ligation. *Genomics*, (22), pp.180–188.

Burma, S. et al., 2001. ATM phosphorylates histone H2AX in response to DNA double-strand breaks. *The Journal of Biological Chemistry*, 276(45), pp.42462–7.

Cadet, J., 2003. Oxidative damage to DNA: formation, measurement and biochemical features. *Mutation Research/Fundamental and Molecular Mechanisms of Mutagenesis*, 531(1-2), pp.5–23.

Cadet, J., Sage, E. & Douki, T., 2005. Ultraviolet radiation-mediated damage to cellular DNA. *Mutation Research*, 571(1-2), pp.3–17.

Caldecott, K., 2001. Mammalian DNA single-strand break repair: an X-ra(y)ted affair. *BioEssays news and reviews in molecular cellular and developmental biology*, 23(5), pp.447–455.

Caldecott, K.W. et al., 1994. An interaction between the mammalian DNA repair protein XRCC1 and DNA ligase III. *Molecular and Cellular Biology*, 14(1), pp.68–76.

Caldecott, K.W. et al., 1995. Characterization of the XRCC1-DNA ligase III complex in vitro and its absence from mutant hamster cells. *Nucleic Acids Research*, 23(23), pp.4836–43.

Caldecott, K.W., 2003a. DNA single-strand break repair and spinocerebellar ataxia. *Cell*, 112(1), pp.7–10.

Caldecott, K.W., 2008. Single-strand break repair and genetic disease. *Nature Reviews Genetics*, 9(8), pp.619–631.

Caldecott, K.W., 2003b. XRCC1 and DNA strand break repair. *DNA Repair*, 2(9), pp.955–969.

Caldecott, K.W. et al., 1996. XRCC1 polypeptide interacts with DNA polymerase beta and possibly poly (ADP-ribose) polymerase, and DNA ligase III is a novel molecular "nick-sensor" in vitro. *Nucleic acids research*, 24(22), pp.4387–94.

Calsou, P. et al., 2003. Coordinated Assembly of Ku and p460 Subunits of the DNA-dependent Protein Kinase on DNA Ends is Necessary for XRCC4–ligase IV Recruitment. *Journal of Molecular Biology*, 326(1), pp.93–103.

Campalans, A. et al., 2013. Distinct spatiotemporal patterns and PARP dependence of XRCC1 recruitment to single-strand break and base excision repair. *Nucleic acids research*, pp.1–15.

Campalans, A. et al., 2005. XRCC1 interactions with multiple DNA glycosylases: a model for its recruitment to base excision repair. *DNA Repair*, 4(7), pp.826–835.

Cappelli, E. et al., 1997. Involvement of XRCC1 and DNA ligase III gene products in DNA base excision repair. *The Journal of Biological Chemistry*, 272(38), pp.23970–5.

Carmichael, J. & Woods, C., 2006. Genetic defects of human brain development. *Current Neurology and Neuroscience Reports*, 6(5), pp.437–446.

Caspari, R. & Lee, S.-H., 2004. Older age becomes common late in human evolution. *Proceedings of the National Academy of Sciences of the United States of America*, 101(30), pp.10895–10900.

Celeste, A. et al., 2002. Genomic instability in mice lacking histone H2AX. *Science*, 296(5569), pp.922–927.

Chan, W.Y. et al., 2002. Proliferation and apoptosis in the developing human neocortex. *The Anatomical record*, 267(4), pp.261–276.

Chang, L.Y. et al., 1988. Molecular immunocytochemistry of the CuZn superoxide dismutase in rat hepatocytes. *The Journal of cell biology*, 107(6 Pt 1), pp.2169–79.

Chappell, C. et al., 2002. Involvement of human polynucleotide kinase in double-strand break repair by non-homologousend joining. *the The European Molecular Biology Organization Journal*, 21(11), pp.2827–2832.

Chatterjee, S., Berger, S.J. & Berger, N.A., 1999. Poly(ADP-ribose) polymerase: a guardian of the genome that facilitates DNA repair by protecting against DNA recombination. *Molecular and Cellular Biochemistry*, 193(1-2), pp.23–30.

Chen, D.S., Herman, T. & Demple, B., 1991. Two distinct human DNA diesterases that hydrolyze 3'-blocking deoxyribose fragments from oxidized DNA. *Nucleic Acids Research*, 19(21), pp.5907–5914.

Chen, X.B. et al., 2001. Human Mus81-associated endonuclease cleaves Holliday junctions in vitro. *Molecular Cell*, 8(5), pp.1117–1127.

Chiang, S.-C., Carroll, J. & El-Khamisy, S.F., 2010. TDP1 serine 81 promotes interaction with DNA ligase IIIalpha and facilitates cell survival following DNA damage. *Cell cycle (Georgetown, Tex.)*, 9(3), pp.588–595.

Chun, H.H. & Gatti, R. a, 2004. Ataxia-telangiectasia, an evolving phenotype. *DNA repair*, 3(8-9), pp.1187–96.

Clark, A.B. et al., 2000. Proliferating Cell Nuclear Antigen with MSH2-MSH6 and MSH2-MSH3 Complexes. *Yeast*, 275(47), pp.36498–36501.

Clements, P.M. et al., 2004. The ataxia-oculomotor apraxia 1 gene product has a role distinct from ATM and interacts with the DNA strand break repair proteins XRCC1 and XRCC4. *DNA repair*, 3(11), pp.1493–502.

Cleveland, D.W. & Liu, J., 2000. Oxidation versus aggregation [mdash] how do SOD1 mutants cause ALS? *Nat Med*, 6(12), pp.1320–1321.

Cloney, R.A., 2011. *Involvement of Human DNA Polymerase Kappa in Nucleotide Excision Repair*. University of Sussex.

Cohen, E. et al., 2009. Reduced IGF-1 signaling delays age-associated proteotoxicity in mice. *Cell*, 139(6), pp.1157–69.

Coleman, K.A. & Greenberg, R.A., 2011. The BRCA1-RAP80 complex regulates DNA repair mechanism utilization by restricting end resection. *The Journal of Biological Chemistry*, 286(15), pp.13669–13680.

Collado, M. & Serrano, M., 2006. The power and the promise of oncogene-induced senescence markers. *Nature Reviews Cancer*, 6(6), pp.472–476.

Cooke, M.S. et al., 2003. Oxidative DNA damage: mechanisms, mutation, and disease. *FASEB journal : official publication of the Federation of American Societies for Experimental Biology*, 17(10), pp.1195–214.

Cortes, U. et al., 2004. Depletion of the 110-Kilodalton Isoform of Poly (ADP-Ribose) Glycohydrolase Increases Sensitivity to Genotoxic and Endotoxic Stress in Mice. , 24(16), pp.7163–7178.

Cotner-Gohara, E. et al., 2008. Two DNA-binding and Nick Recognition Modules in Human DNA Ligase III. *The Journal of Biological Chemistry*, 283(16), pp.10764–10772.

Coverley, D.A., 1992. A role for the human single-stranded DNA binding protein HSSB/RPA in an early stage of nucleotide excision repair. *Nucleic Acids Research*, 20(15), pp.3873–80.

Crimella, C. et al., 2011. A novel nonsense mutation in the APTX gene associated with delayed DNA single-strand break removal fails to enhance sensitivity to different genotoxic agents. *Human mutation*, 32(4), pp.E2118–33.

Critchlow, S.E., Bowater, R.P. & Jackson, S.P., 1997. Mammalian DNA double-strand break repair protein XRCC4 interacts with DNA ligase IV. *Current Biology*, 7(8), pp.588–598.

Croteau, D.L. & Bohr, V.A., 1997. Repair of oxidative damage to nuclear and mitochondrial DNA in mammalian cells. *The Journal of Biological Chemistry*, 272(41), pp.25409–12.

Crut, A. et al., 2008. Dynamics of phosphodiester synthesis by DNA ligase. *Proceedings of the National Academy of Sciences of the United States of America*, 105(19), pp.6894–6899.

D'Amours, D. et al., 1999. Poly(ADP-ribosyl)ation reactions in the regulation of nuclear functions. *The Biochemical journal*, 342 (Pt 2, pp.249–68.

Daley, J.M., Wilson, T.E. & Ramotar, D., 2010. Genetic interactions between HNT3/Aprataxin and RAD27/FEN1 suggest parallel pathways for 5' end processing during base excision repair. *DNA repair*, 9(6), pp.690–9.

Danska, J.S. et al., 1994. Rescue of T cell-specific V(D)J recombination in SCID mice by DNA-damaging agents. *Science (New York, N.Y.)*, 266(5184), pp.450–5.

Darwin, C. & Peckham, M., 1959. The origin of species: a variorum text Morse Peckham, ed. *The Eugenics Review*, 51(3), p.170.

Das, A. et al., 2006. NEIL2-initiated, APE-independent repair of oxidized bases in DNA: Evidence for a repair complex in human cells. *DNA Repair*, 5(12), pp.1439–1448.

Date, H. et al., 2001. Early-onset ataxia with ocular motor apraxia and hypoalbuminemia is caused by mutations in a new HIT superfamily gene. *Nature Genetics*, 29(2), pp.184–188.

Date, H. et al., 2004. The FHA domain of aprataxin interacts with the C-terminal region of XRCC1. *Biochemical and Biophysical Research Communications*, 325(4), pp.1279–1285.

De Amicis, A. et al., 2010. Role of senataxin in DNA damage and telomeric stability. *DNA repair*.10 (2) 199-209

Deckbar, D. et al., 2007. Chromosome breakage after G2 checkpoint release. *The Journal of Cell Biology*, 176(6), pp.749–755.

DeFazio, L.G. et al., 2002. Synapsis of DNA ends by DNA-dependent protein kinase. *the The European Molecular Biology Organization Journal*, 21(12), pp.3192–3200.

Delacôte, F. & Lopez, B.S., 2008. Importance of the cell cycle phase for the choice of the appropriate DSB repair pathway for genome stability maintenance. January, pp.33–38.

Demple, B. & DeMott, M.S., 2002. Dynamics and diversions in base excision DNA repair of oxidized abasic lesions. *Oncogene*, 21(58), pp.8926–34.

Demple, B. & Harrison, L., 1994. Repair of oxidative damage to DNA: enzymology and biology. *Annual Review of Biochemistry*, 63(2), pp.915–948.

Dianov, G., Price, A. & Lindahl, T., 1992. Generation of Single-Nucleotide Repair Patches Following Excision of Uracil Residues from DNA. *Molecular and Cellular Biology*, 12(4).1605-1612

Dianov, G.L. et al., 2001. Base excision repair in nuclear and mitochondrial DNA. *Prog Nucleic Acid Res Mol Biol*, 68, pp.285–297.

Dianov, G.L. et al., 1999. Role of DNA polymerase beta in the excision step of long patch mammalian base excision repair. *The Journal of Biological Chemistry*, 274(20), pp.13741–3.

Dianova, I.I. et al., 2004. XRCC1-DNA polymerase beta interaction is required for efficient base excision repair. *Nucleic Acids Research*, 32(8), pp.2550–2555.

DiGiuseppe, J.A. & Dresler, S.L., 1989. Bleomycin-induced DNA repair synthesis in permeable human fibroblasts: mediation of long-patch and short-patch repair by distinct DNA polymerases. *Biochemistry*, 28(24), pp.9515–9520.

Dimri, G.P. et al., 1995. A biomarker that identifies senescent human cells in culture and in aging skin in vivo. *Proceedings of the National Academy of Sciences of the United States of America*, 92(20), pp.9363–7.

Doil, C. et al., 2009. RNF168 binds and amplifies ubiquitin conjugates on damaged chromosomes to allow accumulation of repair proteins. *Cell*, 136(3), pp.435–446.

Dresler, S.L. & Lieberman, M.W., 1983a. DNA polymerase function in repair synthesis in human fibroblasts. *Princess Takamatsu symposia*, 13, pp.253–265.

Dresler, S.L. & Lieberman, M.W., 1983b. Identification of DNA polymerases involved in DNA excision repair in diploid human fibroblasts. *Journal of Biological Chemistry*, 258(16), pp.9990–9994.

Dudley, D.D. et al., 2005. Mechanism and control of V(D)J recombination versus class switch recombination: similarities and differences. *Advances in Immunology*, 86(D), pp.43–112.

Dulic, A. et al., 2001. BRCT domain interactions in the heterodimeric DNA repair protein XRCC1-DNA ligase III. *Biochemistry*, 40(20), pp.5906–5913.

Durkacz, B.W. et al., 1980. (ADP-ribose)n participates in DNA excision repair. *Nature*, 283(5747), pp.593–596.

El-Khamisy, S.F. et al., 2003. A requirement for PARP-1 for the assembly or stability of XRCC1 nuclear foci at sites of oxidative DNA damage. *Nucleic Acids Research*, 31(19), pp.5526–5533.

El-khamisy, S.F. et al., 2005. Defective DNA single-strand break repair in spinocerebellar ataxia with axonal neuropathy-1. *Nature*, 434(7029), pp.108–113.

El-Khamisy, S.F. et al., 2009. Synergistic decrease of DNA single-strand break repair rates in mouse neural cells lacking both Tdp1 and aprataxin. *DNA repair*, 8(6), pp.760–6.

El-Khamisy, S.F., 2011. To live or to die: a matter of processing damaged DNA termini in neurons. *EMBO molecular medicine*, 3(2), pp.78–88.

Ellenberger, T. & Tomkinson, A.E., 2008. Eukaryotic DNA ligases: structural and functional insights. *Annual review of biochemistry*, 77, pp.313–38.

Englander, E.W., 2008. Brain capacity for repair of oxidatively damaged DNA and preservation of neuronal function. *Mechanisms of ageing and development*, 129(7-8), pp.475–482.

Fan, J. et al., 2004. XRCC1 co-localizes and physically interacts with PCNA. *Nucleic Acids Research*, 32(7), pp.2193–2201.

Fang, Y.-Z., Yang, S. & Wu, G., 2002. Free radicals, antioxidants, and nutrition. *Nutrition*, 18(10), pp.872–879.

Feige, J.N. et al., 2008. Specific SIRT1 activation mimics low energy levels and protects against diet-induced metabolic disorders by enhancing fat oxidation. *Cell Metabolism*, 8(5), pp.347–358.

Ferro, A.M., Higgins, N.P. & Olivera, B.M., 1983. Poly(ADP-ribosylation) of a DNA topoisomerase. *The Journal of Biological Chemistry*, 258(10), pp.6000–6003.

Finnie, N.J. et al., 1996. DNA-dependent protein kinase defects are linked to deficiencies in DNA repair and V(D)J recombination. *Philosophical Transactions of the Royal Society of London - Series B: Biological Sciences*, 351(1336), pp.173–179.

Fisher, A.E.O. et al., 2007. Poly(ADP-ribose) polymerase 1 accelerates single-strand break repair in concert with poly(ADP-ribose) glycohydrolase. *Molecular and cellular biology*, 27(15), pp.5597–605.

Fortini, P. et al., 1998. Different DNA polymerases are involved in the short- and long-patch base excision repair in mammalian cells. *Biochemistry*, 37(11), pp.3575–3580.

Frosina, G. et al., 1996. Two pathways for base excision repair in mammalian cells. *The Journal of Biological Chemistry*, 271(16), pp.9573–8.

Fukuhara, N., 1995. Clinicopathological features of MERRF. *Muscle nerve*, 3, pp.S90–S94.

Gali, H. et al., 2012. Role of SUMO modification of human PCNA at stalled replication fork. *Nucleic Acids Research*, 40(13), pp.1–11.

Gao, Y. et al., 2011. DNA ligase III is critical for mtDNA integrity but not Xrcc1-mediated nuclear DNA repair. *Nature*, 471(7337), pp.240–244.

Garinis, G.G. a et al., 2009. Persistent transcription-blocking DNA lesions trigger somatic growth attenuation associated with longevity. *Nature cell biology*, 11(5), pp.604–15.

Gatz, S.A. et al., 2011. Requirement for DNA ligase IV during embryonic neuronal development. *Journal of Neuroscience*, 31(27), pp.10088–10100.

Genschel, J., Bazemore, L.R. & Modrich, P., 2002. Human exonuclease I is required for 5’ and 3' mismatch repair. *Journal of Biological Chemistry*, 277(15), pp.13302–1311.

Gillet, L.C.J. & Schärer, O.D., 2006. Molecular mechanisms of mammalian global genome nucleotide excision repair. *Chemical Reviews*, 106(2), pp.253–276.

Godon, C. et al., 2008. PARP inhibition versus PARP-1 silencing: different outcomes in terms of single-strand break repair and radiation susceptibility. *Nucleic acids research*, 36(13), pp.4454–64.

Goodarzi, A.A. et al., 2006. DNA-PK autophosphorylation facilitates Artemis endonuclease activity. *The EMBO journal*, 25(16), pp.3880–9.

Van Gool, A.J. et al., 1997. The Cockayne syndrome B protein, involved in transcription-coupled DNA repair, resides in an RNA polymerase II-containing complex. *the The European Molecular Biology Organization Journal*, 16(19), pp.5955–5965.

Grawunder, U. et al., 1997. Activity of DNA ligase IV stimulated by complex formation with XRCC4 protein in mammalian cells. *Nature*, 388(6641), pp.492–495.

Grawunder, U. et al., 1998. Requirement for an interaction of XRCC4 with DNA ligase IV for wild-type V(D)J recombination and DNA double-strand break repair in vivo. *The Journal of Biological Chemistry*, 273(38), pp.24708–24714.

Gray, J.W. & Collins, C., 2000. Genome changes and gene expression in human solid tumors. *Carcinogenesis*, 21(3), pp.443–452.

Greider, C.W. & Blackburn, E.H., 1985. Identification of a specific telomere terminal transferase activity in Tetrahymena extracts. *Cell*, 43(2 Pt 1), pp.405–13.

Gu, J. et al., 2007. Single-stranded DNA ligation and XLF-stimulated incompatible DNA end ligation by the XRCC4-DNA ligase IV complex: influence of terminal DNA sequence. *Nucleic Acids Research*, 35(17), pp.5755–5762.

Gueven, N. et al., 2004. Aprataxin, a novel protein that protects against genotoxic stress. *Human molecular genetics*, 13(10), pp.1081–93.

Gumport, R.I. & Lehman, I.R., 1971. Structure of the DNA Ligase-Adenylate Intermediate: Lysine (ε-amino)-Linked Adenosine Monophosphoramidate. *Proceedings of the National Academy of Sciences of the United States of America*, 68(10), pp.2559–2563.

Gurney, M.E. et al., 1994. Motor neuron degeneration in mice that express a human Cu,Zn superoxide dismutase mutation. *Science (New York, N.Y.)*, 264(5166), pp.1772–5.

Gurney, M.E., 1997. The use of transgenic mouse models of amyotrophic lateral sclerosis in preclinical drug studies. *Journal of the Neurological Sciences*, 152 Suppl , pp.S67–S73.

Hammel, M. et al., 2011. XRCC4 Protein Interactions with XRCC4-like Factor (XLF) Create an Extended Grooved Scaffold for DNA Ligation and Double Strand Break Repair. *The Journal of Biological Chemistry*, 286(37), pp.32638–32650.

Hare, J.T. & Taylor, J.H., 1985. One role for DNA methylation in vertebrate cells is strand discrimination in mismatch repair. *Proceedings of the National Academy of Sciences of the United States of America*, 82(21), pp.7350–7354.

Harper, J.W. & Elledge, S.J., 2007. The DNA damage response: ten years after. *Molecular Cell*, 28(5), pp.739–45.

Harris, J.L. et al., 2009. Aprataxin, poly-ADP ribose polymerase 1 (PARP-1) and apurinic endonuclease 1 (APE1) function together to protect the genome against oxidative damage. *Human molecular genetics*, 18(21), pp.4102–17.

Hartlerode, A.J. & Scully, R., 2010. Mechanisms of double-strand break repair in somatic mammalian cells. *The Biochemical journal*, 426(3), p.389.

Harvey, C.L. et al., 1971. Enzymatic Breakage and Deoxyribonucleic Acid Joining of Deoxyribonucleic Acid. *Journal of Biological Chemistry*, 246(14), pp.4523–4530.

Hirano, M. et al., 2007. DNA single-strand break repair is impaired in aprataxin-related ataxia. *Annals of neurology*, 61(2), pp.162–74.

Hoeijmakers, J.H.J., 2001. Genome maintenance mechanisms for preventing cancer. , pp.366–374.

Hoeijmakers, J.H.J., 2007. Genome maintenance mechanisms are critical for preventing cancer as well as other aging-associated diseases. *Mechanisms of ageing and development*, 128(7-8), pp.460–2.

Hopfner, K.-P. et al., 2002. The Rad50 zinc-hook is a structure joining Mre11 complexes in DNA recombination and repair. *Nature*, 418(6897), pp.562–566.

Hoshino, K. & Kameyama, Y., 1988. Developmental-stage-dependent radiosensitivity of neural cells in the ventricular zone of telencephalon in mouse and rat fetuses. *Teratology*, 37(3), pp.257–262.

Hoshino, K., Kameyama, Y. & Inouye, M., 1991. Split-dose effect of X-irradiation on the induction of cell death in the fetal mouse brain. *Journal Of Radiation Research*, 32(1), pp.23–27.

Howland, D.S. et al., 2002. Focal loss of the glutamate transporter EAAT2 in a transgenic rat model of SOD1 mutant-mediated amyotrophic lateral sclerosis (ALS). *Proceedings of the National Academy of Sciences of the United States of America*, 99(3), pp.1604–9.

Huen, M.S.Y. et al., 2007. RNF8 transduces the DNA-damage signal via histone ubiquitylation and checkpoint protein assembly. *Cell*, 131(5), pp.901–914.

Huertas, P. & Jackson, S.P., 2009. Human CtIP mediates cell-cycle control of DNA-end resection and double-strand-break repair. *Journal of Biological Chemistry*. 284(14):9558-65

Hughes, A.L., 2002. Adaptive evolution after gene duplication. *Trends in Genetics*, 18(9), pp.433–434.

Imai, S. et al., 2000. Transcriptional silencing and longevity protein Sir2 is an NAD-dependent histone deacetylase. *Nature*, 403(6771), pp.795–800.

Interthal, H., Pouliot, J.J. & Champoux, J.J., 2001. The tyrosyl-DNA phosphodiesterase Tdp1 is a member of the phospholipase D superfamily. *Proceedings of the National Academy of Sciences of the United States of America*, 98(21), pp.12009–12014.

Izumi, T. et al., 2000. Requirement for human AP endonuclease 1 for repair of 3'-blocking damage at DNA single-strand breaks induced by reactive oxygen species. *Carcinogenesis*, 21(7), pp.1329–1334.

Izumi, T. et al., 2005. Two essential but distinct functions of the mammalian abasic endonuclease. *Proceedings of the National Academy of Sciences of the United States of America*, 102(16), pp.5739–5743.

Jackson, S.P. & Bartek, J., 2009. The DNA-damage response in human biology and disease. *Nature*, 461(7267), pp.1071–8.

Jilani, A. et al., 1999. Molecular cloning of the human gene, PNKP, encoding a polynucleotide kinase 3'-phosphatase and evidence for its role in repair of DNA strand breaks caused by oxidative damage. *The Journal of Biological Chemistry*, 274(34), pp.24176–24186.

Jin, S. et al., 1997. Binding of Ku and c-Abl at the kinase homology region of DNA-dependent protein kinase catalytic subunit. *The Journal of biological chemistry*, 272(40), pp.24763–6.

Jiricny, J., 2006. The multifaceted mismatch-repair system. *Nature Reviews Molecular Cell Biology*, 7(5), pp.335–46.

Karimi-Busheri, F. et al., 1998. Repair of DNA strand gaps and nicks containing 3'-phosphate and 5'-hydroxyl termini by purified mammalian enzymes. *Nucleic Acids Research*, 26(19), pp.4395–4400.

Kasai, H., Tanooka, H. & Nishimura, S., 1984. Formation of 8-hydroxyguanine residues in DNA by X-irradiation. *Gann*, 75(12), pp.1037–1039.

Katyal, S. & McKinnon, P.J., 2011. Disconnecting XRCC1 and DNA ligase III. *Cell cycle Georgetown Tex*, 10(14), pp.2269–2275.

Kerzendorfer, C. et al., 2010. Mutations in Cullin 4B result in a human syndrome associated with increased camptothecin-induced topoisomerase I-dependent DNA breaks. *Human Molecular Genetics*, 19(7), pp.1324–1334.

Kijas, A.W. et al., 2006. Aprataxin forms a discrete branch in the HIT (histidine triad) superfamily of proteins with both DNA/RNA binding and nucleotide hydrolase activities. *The Journal of biological chemistry*, 281(20), pp.13939–48.

Kim, J.K., Patel, D. & Choi, B.S., 1995. Contrasting structural impacts induced by cis-syn cyclobutane dimer and (6-4) adduct in DNA duplex decamers: implication in mutagenesis and repair activity. *Photochemistry and Photobiology*, 62(1), pp.44–50.

Kim, K., Biade, S. & Matsumoto, Y., 1998. Involvement of flap endonuclease 1 in base excision DNA repair. *The Journal of Biological Chemistry*, 273(15), pp.8842–8848.

Kim, M.Y., Zhang, T. & Kraus, W.L., 2005. Poly(ADP-ribosyl)ation by PARP-1: "PAR-laying" NAD+ into a nuclear signal. *Genes & development*, 19(17), pp.1951–67.

Klungland, A. & Lindahl, T., 1997. Second pathway for completion of human DNA base excision-repair: reconstitution with purified proteins and requirement for DNase IV (FEN1). *the The European Molecular Biology Organization Journal*, 16(11), pp.3341–3348.

Koch, C.A. et al., 2004. Xrcc4 physically links DNA end processing by polynucleotide kinase to DNA ligation by DNA ligase IV. *the The European Molecular Biology Organization Journal*, 23(19), pp.3874–3885.

Kolas, N.K. et al., 2007. Orchestration of the DNA-damage response by the RNF8 ubiquitin ligase. *Science*, 318(5856), pp.1637–1640.

Kouzminova, E.A. & Kuzminov, A., 2006. Fragmentation of replicating chromosomes triggered by uracil in DNA. *Journal of Molecular Biology*, 355(1), pp.20–33.

Kroeger, P.E. & Rowe, T.C., 1989. Interaction of topoisomerase 1 with the transcribed region of the Drosophila HSP 70 heat shock gene. *Nucleic Acids Research*, 17(21), pp.8495–8509.

Krokan, H.E., Drabløs, F. & Slupphaug, G., 2002. Uracil in DNA--occurrence, consequences and repair. *Oncogene*, 21(58), pp.8935–48.

Kubota, Y. et al., 1996. Reconstitution of DNA base excision-repair with purified human proteins: interaction between DNA polymerase beta and the XRCC1 protein. *the The European Molecular Biology Organization Journal*, 15(23), pp.6662–6670.

Kunkel, T.A. & Erie, D.A., 2005. DNA mismatch repair. *Annual Review of Biochemistry*, 74(1), pp.681–710.

Kusumoto, R. et al., 2001. Diversity of the damage recognition step in the global genomic nucleotide excision repair in vitro. *Mutation Research*, 485(3), pp.219–227.

Kuzminov, A., 2001. Single-strand interruptions in replicating chromosomes cause double-strand breaks. *Proceedings of the National Academy of Sciences of the United States of America*, 98(15), pp.8241–6.

Lagerwerf, S. et al., 2011. DNA damage response and transcription. *DNA Repair*, 10(7), pp.743–750.

Lakin, N.D. et al., 1996. Analysis of the ATM protein in wild-type and ataxia telangiectasia cells. *Oncogene*, 13(12), pp.2707–2716.

Lakshmipathy, U. & Campbell, C., 1999. The human DNA ligase III gene encodes nuclear and mitochondrial proteins. *Molecular and Cellular Biology*, 19(5), pp.3869–3876.

Lavin, M.F., 2008. Ataxia-telangiectasia: from a rare disorder to a paradigm for cell signalling and cancer. *Nature Reviews Molecular Cell Biology*, 9(10), pp.759–69.

Lavin, M.F., 2007. ATM and the Mre11 complex combine to recognize and signal DNA double-strand breaks. *Oncogene*, 26(56), pp.7749–7758.

Le Ber, I. et al., 2003. Cerebellar ataxia with oculomotor apraxia type 1: clinical and genetic studies. *Brain: A journal of neurology*, 126(Pt 12), pp.2761–2772.

Le Ber, I., Brice, A. & Dürr, A., 2006. Autosomal recessive cerebellar ataxias with oculomotor apraxia. *Revue Neurologique*, 162(2), pp.411–417.

Leber, R. et al., 1998. The XRCC4 gene product is a target for and interacts with the DNA-dependent protein kinase. *The Journal of Biological Chemistry*, 273(3), pp.1794–1801.

Lee, J.-B. et al., 2006. DNA primase acts as a molecular brake in DNA replication. *Nature*, 439(7076), pp.621–624.

Lehmann, A.R., 2003. DNA repair-deficient diseases, xeroderma pigmentosum, Cockayne syndrome and trichothiodystrophy. *Biochimie*, 85(11), pp.1101–11.

Lehmann, A.R., 1978. Repair processes for radiation-induced DNA damage. *Molecular biology, biochemistry, and biophysics*, 27, pp.312–34.

Lehmann, A.R. et al., 1975. Xeroderma pigmentosum cells with normal levels of excision repair have a defect in DNA synthesis after UV-irradiation. *Proceedings of the National Academy of Sciences of the United States of America*, 72(1), pp.219–223.

Levin, D.S. et al., 1997. An interaction between DNA ligase I and proliferating cell nuclear antigen: implications for Okazaki fragment synthesis and joining. *Proceedings of the National Academy of Sciences of the United States of America*, 94(24), pp.12863–12868.

Levin, D.S. et al., 2000. Interaction between PCNA and DNA ligase I is critical for joining of Okazaki fragments and long-patch base-excision repair. *Current Biology*, 10(15), pp.919–922.

Lieber, M.R. et al., 2003. Mechanism and regulation of human non-homologous DNA end-joining. *Nature Reviews Molecular Cell Biology*, 4(9), pp.712–720.

Lieber, M.R. & Karanjawala, Z.E., 2004. Ageing, repetitive genomes and DNA damage. *Nature Reviews Molecular Cell Biology*, 5(1), pp.69–75.

Lightowlers, R.N. et al., 1997. Mammalian mitochondrial genetics: heredity, heteroplasmy and disease. *Trends in Genetics*, 13(11), pp.450–455.

Limoli, C.L. et al., 1998. Induction of chromosome aberrations and delayed genomic instability by photochemical processes. *Photochemistry and photobiology*, 67(2), pp.233–8.

Lindahl, T., 1993a. Instability and decay of the primary structure of DNA. *Nature*.

Lindahl, T. & Nyberg, B., 1972. Rate of depurination of native deoxyribonucleic acid. *Biochemistry*, 11(19), pp.3610–3618.

Linford, N.J., Schriner, S.E. & Rabinovitch, P.S., 2006. Oxidative damage and aging: spotlight on mitochondria. *Cancer research*, 66(5), pp.2497–9.

Littlefield, L.G. et al., 1981. Chromosomal radiation sensitivity in ataxia telangiectasia long-term lymphoblastoid cell lines. *Cytogenetics and Cell Genetics*, 31(4), pp.203–213.

Liu, Y. et al., 2005. DNA polymerase beta and flap endonuclease 1 enzymatic specificities sustain DNA synthesis for long patch base excision repair. *The Journal of Biological Chemistry*, 280(5), pp.3665–3674.

Loizou, J.I. et al., 2004. The protein kinase CK2 facilitates repair of chromosomal DNA single-strand breaks. *Cell*, 117(1), pp.17–28.

Lou, Z. et al., 2006. MDC1 maintains genomic stability by participating in the amplification of ATM-dependent DNA damage signals. *Molecular Cell*, 21(2), pp.187–200.

Lukas, C. et al., 2004. Mdc1 couples DNA double-strand break recognition by Nbs1 with its H2AX-dependent chromatin retention. *the The European Molecular Biology Organization Journal*, 23(13), pp.2674–2683.

Luo, H. et al., 2004. A new XRCC1-containing complex and its role in cellular survival of methyl methanesulfonate treatment. *Molecular and Cellular Biology*, 24(19), pp.8356–8365.

Lynch, M. & Conery, J.S., 2000. The evolutionary fate and consequences of duplicate genes. *Science*, 290(5494), pp.1151–1155.

Ma, Y. et al., 2002. Hairpin opening and overhang processing by an Artemis/DNA-dependent protein kinase complex in nonhomologous end joining and V(D)J recombination. *Cell*, 108(6), pp.781–794.

Mackey, Z.B. et al., 1997. An alternative splicing event which occurs in mouse pachytene spermatocytes generates a form of DNA ligase III with distinct biochemical properties that may function in meiotic recombination. *Molecular and Cellular Biology*, 17(2), pp.989–998.

Macrae, C.J. et al., 2008. APLF (C2orf13) facilitates nonhomologous end-joining and undergoes ATM-dependent hyperphosphorylation following ionizing radiation. *DNA Repair*, 7(2), pp.292–302.

Mailand, N. et al., 2007. RNF8 ubiquitylates histones at DNA double-strand breaks and promotes assembly of repair proteins. *Cell*, 131(5), pp.887–900.

Makino, N. et al., 2011. Antioxidant therapy attenuates myocardial telomerase activity reduction in superoxide dismutase-deficient mice. *Journal of molecular and cellular cardiology*, 50(4), pp.670–7.

Mani, R.S. et al., 2010. Dual modes of interaction between XRCC4 and polynucleotide kinase/phosphatase: implications for nonhomologous end joining. *The Journal of Biological Chemistry*, 285(48), pp.37619–37629.

Mao, G.D. et al., 1993. Superoxide Dismutase (SOD) -Catalase Conjugates. 268(1), pp.0–4.

Maresca, B. & Schwartz, J.H., 2006. Sudden Origins : A General Mechanism of Evolution Based on Stress Protein Concentration and Rapid Environmental Change. , (1942), pp.38–46.

Marintchev, A. et al., 2000. Domain specific interaction in the XRCC1-DNA polymerase beta complex. *Nucleic Acids Research*, 28(10), pp.2049–2059.

Marsin, S. et al., 2003. Role of XRCC1 in the coordination and stimulation of oxidative DNA damage repair initiated by the DNA glycosylase hOGG1. *The Journal of Biological Chemistry*, 278(45), pp.44068–44074.

Martin, G.M. et al., 1985. Increased chromosomal aberrations in first metaphases of cells isolated from the kidneys of aged mice. *Israel journal of medical sciences*, 21(3), pp.296–301.

Masson, M. et al., 1998. XRCC1 Is Specifically Associated with Poly(ADP-Ribose) Polymerase and Negatively Regulates Its Activity following DNA Damage. *Molecular and Cellular Biology*, 18(6), pp.3563–3571.

Matsumoto, Y. et al., 1999. Reconstitution of proliferating cell nuclear antigen-dependent repair of apurinic/apyrimidinic sites with purified human proteins. *The Journal of Biological Chemistry*, 274(47), pp.33703–33708.

Matsunaga, T. et al., 1995. Human DNA repair excision nuclease. Analysis of the roles of the subunits involved in dual incisions by using anti-XPG and anti-ERCC1 antibodies. *Journal of Biological Chemistry*, 270(35), pp.20862–20869.

McClintock, B., 1941. The Stability of Broken Ends of Chromosomes in Zea Mays. *Genetics*, 26(2), pp.234–82.

McEachern, M.J., Krauskopf, A. & Blackburn, E.H., 2000. Telomeres and their control. *Annual Review of Genetics*, 34(1), pp.331–358.

McKinnon, P.J., 2009. DNA repair deficiency and neurological disease. *Nature reviews. Neuroscience*, 10(2), pp.100–12.

McKinnon, P.J. & Caldecott, K.W., 2007. DNA strand break repair and human genetic disease. *Annual review of genomics and human genetics*, 8, pp.37–55.

Meek, K. et al., 2007. trans Autophosphorylation at DNA-dependent protein kinase's two major autophosphorylation site clusters facilitates end processing but not end joining. *Molecular and cellular biology*, 27(10), pp.3881–90.

Mehrotra, P.V. et al., 2011. DNA repair factor APLF is a histone chaperone. *Molecular Cell*, 41(1), pp.46–55.

Miao, Z.-H. et al., 2006. Hereditary ataxia SCAN1 cells are defective for the repair of transcription-dependent topoisomerase I cleavage complexes. *DNA Repair*, 5(12), pp.1489–1494.

Milne, J.C. et al., 2007. Small molecule activators of SIRT1 as therapeutics for the treatment of type 2 diabetes. *Nature*, 450(7170), pp.712–6.

Mimitou, E.P. & Symington, L.S., 2008. Sae2, Exo1 and Sgs1 collaborate in DNA double-strand break processing. *Nature*, 455(7214), pp.770–774.

Moreira, M.C. et al., 2001. The gene mutated in ataxia-ocular apraxia 1 encodes the new HIT/Zn-finger protein aprataxin. *Nature Genetics*, 29(2), pp.189–193.

Morrison, C. et al., 1997. Genetic interaction between PARP and DNA-PK in V(D)J recombination and tumorigenesis. *Nature Genetics*, 17(4), pp.479–482.

Mosbaugh, D.W. & Linn, S., 1984. Excision repair and DNA synthesis with a combination of HeLa DNA polymerase beta and DNase V. *The Journal of Biological Chemistry*, 258(1), pp.108–118.

Moser, J. et al., 2007. Sealing of chromosomal DNA nicks during nucleotide excision repair requires XRCC1 and DNA ligase III alpha in a cell-cycle-specific manner. *Molecular Cell*, 27(2), pp.311–323.

Mosesso, P. et al., 2005. The novel human gene aprataxin is directly involved in DNA single-strand-break repair. *Cellular and molecular life sciences : CMLS*, 62(4), pp.485–91.

Mostoslavsky, R. et al., 2006. Genomic instability and aging-like phenotype in the absence of mammalian SIRT6. *Cell*, 124(2), pp.315–329.

Mueller, G.A. et al., 2008. A comparison of BRCT domains involved in nonhomologous end-joining: introducing the solution structure of the BRCT domain of polymerase lambda. *DNA Repair*, 7(8), pp.1340–1351.

Muller, H., 1938. The remaking of chromosomes. *Collecting Net.*, 13, pp.181–195. 198.

Murphy, W.J. et al., 1994. Induction of T cell differentiation and lymphomagenesis in the thymus of mice with severe combined immune deficiency (SCID). *Journal of immunology (Baltimore, Md. : 1950)*, 153(3), pp.1004–14.

Nagai, A. et al., 1995. Enhancement of damage-specific DNA binding of XPA by interaction with the ERCC1 DNA repair protein. *Biochem Biophys Res Commun*, 211(3), pp.960–966.

Nair, P.A. et al., 2007. Structural basis for nick recognition by a minimal pluripotent DNA ligase. *Nature structural & molecular biology*, 14(8), pp.770–8.

Nash, R.A. et al., 1997. XRCC1 protein interacts with one of two distinct forms of DNA ligase III. *Biochemistry*, 36(17), pp.5207–5211.

Negrini, M. & Calin, G.A., 2010. Involvement of MicroRNAs in Human Cancer: Discovery and Expression Profiling. In *An Omics Perspective on Cancer Research*. pp. 69–104.

Nick McElhinny, S.A. et al., 2000. Ku recruits the XRCC4-ligase IV complex to DNA ends. *Molecular and Cellular Biology*, 20(9), pp.2996–3003.

Niedernhofer, L.J. et al., 2006. A new progeroid syndrome reveals that genotoxic stress suppresses the somatotroph axis. *Nature*, 444(7122), pp.1038–43.

Nishizuka, Y., 1967. Studies on the Polymer of Adenosine Diphosphate Ribose. 242(13), pp.3164–3171.

Nitiss, J.L., 2009. DNA topoisomerase II and its growing repertoire of biological functions. *Nature Reviews Cancer*, 9(5), pp.327–337.

Nouspikel, T., 2009. DNA repair in mammalian cells : Nucleotide excision repair: variations on versatility. *Cellular and molecular life sciences CMLS*, 66(6), pp.994–1009.

O'Connor, T.R. & Laval, J., 1989. Physical association of the 2,6-diamino-4-hydroxy-5N-formamidopyrimidine-DNA glycosylase of Escherichia coli and an activity nicking DNA at apurinic/apyrimidinic sites. *Proceedings of the National Academy of Sciences of the United States of America*, 86(14), pp.5222–5226.

O'Donovan, A. et al., 1994. XPG endonuclease makes the 3' incision in human DNA nucleotide excision repair [see comments]. *Nature*, 371(6496), pp.432–435.

O'Driscoll, M. et al., 2001. DNA Ligase IV mutations identified in patients exhibiting development delay and immunodeficiency. *Molecular Cell*, 8(6), pp.1175–1185.

O'Driscoll, M. & Jeggo, P.A., 2008. The role of the DNA damage response pathways in brain development and microcephaly: insight from human disorders. *DNA Repair*, 7(7), pp.1039–1050.

Odell, M. et al., 2000. Crystal structure of eukaryotic DNA ligase-adenylate illuminates the mechanism of nick sensing and strand joining. *Molecular Cell*, 6(5), pp.1183–1193.

Okazaki, R. et al., 1968. Mechanism of DNA chain growth. I. Possible discontinuity and unusual secondary structure of newly synthesized chains. *Proceedings of the National Academy of Sciences USA*, 1100, pp.598–605.

Olive, P.L. & Johnston, P.J., 1997. DNA damage from oxidants: influence of lesion complexity and chromatin organization. *Oncology Research*, 9(6-7), pp.287–294.

Olivera, B. et al., 1968. On the mechanism of the polynucleotide joining reaction. *Harbor Symposia*, 33, pp.27–24.

Otterlei, M. et al., 1999. Post-replicative base excision repair in replication foci. *the The European Molecular Biology Organization Journal*, 18(13), pp.3834–44.

Le Page, F. et al., 2003. Poly(ADP-ribose) polymerase-1 (PARP-1) is required in murine cell lines for base excision repair of oxidative DNA damage in the absence of DNA polymerase beta. *The Journal of biological chemistry*, 278(20), pp.18471–7.

Painter, R.B., 1981. Radioresistant DNA synthesis: an intrinsic feature of ataxia telangiectasia. *Mutation Research*, 84(1), pp.183–190.

Palau, F. & Espinós, C., 2006. Autosomal recessive cerebellar ataxias. *Orphanet Journal of Rare Diseases*, 1(3), p.47.

Pâques, F. & Haber, J.E., 1999. Multiple Pathways of Recombination Induced by Double-Strand Breaks in Saccharomyces cerevisiae. *Microbiology and Molecular Biology Reviews*, 63(2), pp.349–404.

Park, C.H. et al., 1995. Purification and characterization of the XPF-ERCC1 complex of human DNA repair excision nuclease. *Journal of Biological Chemistry*, 230, pp.22657–22660.

Park, C.H. & Sancar, A., 1994. Formation of a ternary complex by human XPA, ERCC1, and ERCC4(XPF) excision repair proteins. *Proceedings of the National Academy of Sciences of the United States of America*, 91(11), pp.5017–5021.

Parlanti, E. et al., 2004. Aphidicolin-resistant and -sensitive base excision repair in wild-type and DNA polymerase beta-defective mouse cells. *DNA Repair*, 3(7), pp.703–710.

Parlanti, E. et al., 2007. Human base excision repair complex is physically associated to DNA replication and cell cycle regulatory proteins. *Nucleic acids research*, 35(5), pp.1569–77.

Pascucci, B. et al., 1999. Long patch base excision repair with purified human proteins. DNA ligase I as patch size mediator for DNA polymerases delta and epsilon. *The Journal of Biological Chemistry*, 274(47), pp.33696–33702.

Pascucci, B. et al., 2002. Reconstitution of the base excision repair pathway for 7,8-dihydro-8-oxoguanine with purified human proteins. *Nucleic Acids Research*, 30(10), pp.2124–2130.

Payne, A. & Chu, G., 1994. Xeroderma pigmentosum group E binding factor recognizes a broad spectrum of DNA damage. *Mutation Research*, 310(1), pp.89–102.

Pellegrini, L. et al., 2002. Insights into DNA recombination from the structure of a RAD51-BRCA2 complex. *Nature*, 420(6913), pp.287–293.

Peltonen, K. & Dipple, A., 1995. Polycyclic aromatic hydrocarbons: chemistry of DNA adduct formation. *Journal of occupational and environmental medicine American College of Occupational and Environmental Medicine*, 37(1), pp.52–58.

Perez-Jannotti, R.M., Klein, S.M. & Bogenhagen, D.F., 2001. Two forms of mitochondrial DNA ligase III are produced in Xenopus laevis oocytes. *The Journal of Biological Chemistry*, 276(52), pp.48978–48987.

Petermann, E., Keil, C. & Oei, S.L., 2005. Importance of poly(ADP-ribose) polymerases in the regulation of DNA-dependent processes. *Cellular and molecular life sciences*, 62(7-8), pp.731–8.

Petta, T.B. et al., 2008. Human DNA polymerase iota protects cells against oxidative stress. *the The European Molecular Biology Organization Journal*, 27(21), pp.2883–2895.

Van Der Pluijm, I. et al., 2007. Correction: Impaired Genome Maintenance Suppresses the Growth Hormone–Insulin-Like Growth Factor 1 Axis in Mice with Cockayne Syndrome P. Cooper, ed. *PLoS Biology*, 5(1), p.1.

Podlutsky, A.J. et al., 2001. Human DNA polymerase β initiates DNA synthesis during long-patch repair of reduced AP sites in DNA. *the The European Molecular Biology Organization Journal*, 20(6), pp.1477–1482.

Pommier, Y. et al., 2003. Repair of and checkpoint response to topoisomerase I-mediated DNA damage. *Mutation ResearchFundamental and Molecular Mechanisms of Mutagenesis*, 532(1-2), pp.173–203.

Popanda, O. & Thielmann, H.W., 1992. The function of DNA topoisomerases in UV-induced DNA excision repair: studies with specific inhibitors in permeabilized human fibroblasts. *Carcinogenesis*, 13(12), pp.2321–2328.

Pourquier, P. et al., 1997. Trapping of mammalian topoisomerase I and recombinations induced by damaged DNA containing nicks or gaps. Importance of DNA end phosphorylation and camptothecin effects. *The Journal of Biological Chemistry*, 272(42), pp.26441–26447.

Prakash, S., Johnson, R.E. & Prakash, L., 2005. Eukaryotic translesion synthesis DNA polymerases: specificity of structure and function. *Annual Review of Biochemistry*, 74(1), pp.317–353.

Prasad, R. et al., 2001. DNA polymerase beta -mediated long patch base excision repair. Poly(ADP-ribose)polymerase-1 stimulates strand displacement DNA synthesis. *The Journal of Biological Chemistry*, 276(35), pp.32411–32414.

Prasad, R. et al., 2000. FEN1 stimulation of DNA polymerase beta mediates an excision step in mammalian long patch base excision repair. *The Journal of Biological Chemistry*, 275(6), pp.4460–4466.

Prasad, R. et al., 2003. Localization of the deoxyribose phosphate lyase active site in human DNA polymerase iota by controlled proteolysis. *The Journal of Biological Chemistry*, 278(32), pp.29649–29654.

Prasad, R. et al., 1996. Specific interaction of DNA polymerase beta and DNA ligase I in a multiprotein base excision repair complex from bovine testis. *The Journal of Biological Chemistry*, 271(27), pp.16000–7.

Prize, N., Muller, H. & Mcclintock, B., 2009. Maintenance of chromosomes by telomeres and the enzyme telomerase. *Medicine*, 1(12), pp.1–12.

Quinzii, C.M. et al., 2005. Coenzyme Q deficiency and cerebellar ataxia associated with an aprataxin mutation. *Neurology*, 64(3), pp.539–541.

Rass, U. et al., 2010. Mechanism of Holliday junction resolution by the human GEN1 protein. *Genes & development*, 24(14), pp.1559–69.

Rass, U., Ahel, I. & West, S.C., 2007a. Actions of aprataxin in multiple DNA repair pathways. *The Journal of biological chemistry*, 282(13), pp.9469–74.

Rass, U., Ahel, I. & West, S.C., 2007b. Defective DNA repair and neurodegenerative disease. *Cell*, 130(6), pp.991–1004.

Reynolds, J.J., El-Khamisy, S.F., Katyal, S., et al., 2009. Defective DNA ligation during short-patch single-strand break repair in ataxia oculomotor apraxia 1. *Molecular and Cellular Biology*, 29(5), pp.1354–1362.

Reynolds, J.J., 2011. Investigating the link between defective DNA end-processing and human neurological disease. *Doctoral Thesis*, University of Sussex.

Reynolds, J.J., El-Khamisy, S.F. & Caldecott, K.W., 2009. Short-patch single-strand break repair in ataxia oculomotor apraxia-1. *Biochemical Society transactions*, 37(Pt 3), pp.577–81.

Riballo, E. et al., 2009. XLF-Cernunnos promotes DNA ligase IV–XRCC4 re-adenylation following ligation. *Nucleic Acids Research*, 37(2), pp.482–492.

Rich, T., Allen, R.L. & Wyllie, A.H., 2000. Defying death after DNA damage. *Nature*, 407(6805), pp.777–783.

Roca, J., 1995. The mechanisms of DNA topoisomerases. *Trends in biochemical sciences*, 20, pp.156–160.

Rodier, F. et al., 2005. Cancer and aging: the importance of telomeres in genome maintenance. *The international journal of biochemistry & cell biology*, 37(5), pp.977–90.

Rossi, M.L. & Bambara, R. a, 2006. Reconstituted Okazaki fragment processing indicates two pathways of primer removal. *The Journal of biological chemistry*, 281(36), pp.26051–61.

Rulten, S.L. et al., 2008. APLF (C2orf13) Is a Novel Component of Poly(ADP-Ribose) Signaling in Mammalian Cells. *Molecular and Cellular Biology*, 28(14), pp.4620–4628.

Rulten, S.L. et al., 2011. PARP-3 and APLF function together to accelerate nonhomologous end-joining. *Molecular cell*, 41(1), pp.33–45.

Saldanha, S.N., Andrews, L.G. & Tollefsbol, T.O., 2003. Assessment of telomere length and factors that contribute to its stability. *European Journal of Biochemistry*, 270(3), pp.389–403.

San Filippo, J. et al., 2006. Recombination mediator and Rad51 targeting activities of a human BRCA2 polypeptide. *The Journal of Biological Chemistry*, 281(17), pp.11649–11657.

Sander, M. et al., 2005. Proceedings of a workshop on DNA adducts: biological significance and applications to risk assessment Washington, DC, April 13-14, 2004. *Toxicology and applied pharmacology*, 208(1), pp.1–20.

Sano, Y. et al., 2004. Aprataxin, the causative protein for EAOH is a nuclear protein with a potential role as a DNA repair protein. *Annals of neurology*, 55(2), pp.241–9.

Santorelli, F.M. et al., 1997. Heterogeneous clinical presentation of the mtDNA NARP/T8993G mutation. *Neurology*, 49(1), pp.270–273.

Sartori, A.A. et al., 2007. Human CtIP promotes DNA end resection. *Nature*, 450(7169), pp.509–514.

Satoh, M. et al., 2008. Association between oxidative DNA damage and telomere shortening in circulating endothelial progenitor cells obtained from metabolic syndrome patients with coronary artery disease. *Atherosclerosis*, 198(2), pp.347–53.

Schlissel, M.S., Kaffer, C.R. & Curry, J.D., 2006. Leukemia and lymphoma: a cost of doing business for adaptive immunity. *Genes & development*, 20(12), pp.1539–44.

Schriner, S.E. et al., 2005. Extension of murine life span by overexpression of catalase targeted to mitochondria. *Science*, 308(5730), pp.1909–1911.

Sedgwick, B., Robins, P. & Lindahl, T., 2006. Direct removal of alkylation damage from DNA by AlkB and related DNA dioxygenases. *Methods in Enzymology*, 408(06), pp.108–120.

Segal-Raz, H. et al., 2011. ATM-mediated phosphorylation of polynucleotide kinase/phosphatase is required for effective DNA double-strand break repair. *EMBO reports*, 12(7), pp.713–9.

Shen, J. et al., 2010. Mutations in PNKP cause microcephaly, seizures and defects in DNA repair. *Nature Genetics*, 42(3), pp.245–249.

Shibutani, S., Takeshita, M. & Grollman, A.P., 1991. Insertion of specific bases during DNA synthesis past the oxidation-damaged base 8-oxodG. *Nature*, 349(6308), pp.431–434.

Shimazaki, H. et al., 2002. Early-onset ataxia with ocular motor apraxia and hypoalbuminemia: the aprataxin gene mutations. *Neurology*, 59(4), pp.590–595.

Shivji, K.K., Kenny, M.K. & Wood, R.D., 1992. Proliferating cell nuclear antigen is required for DNA excision repair. *Cell*, 69(2), pp.367–374.

Simsek, D. et al., 2011. Crucial role for DNA ligase III in mitochondria but not in Xrcc1-dependent repair. *Nature*, 471(7337), pp.245–8.

Sinauer Associates Sadava, D. *et al*. *Life: The Science of Biology*, 8th ed. (2008) (Sunderland, MA: Sinauer Associates and W. H. Freeman & Company), 248.

Singhal, R.K., Prasad, R. & Wilson, S.H., 1995. DNA polymerase beta conducts the gap-filling step in uracil-initiated base excision repair in a bovine testis nuclear extract. *Journal of Biological Chemistry*, 270(2), pp.949–957.

Sleeth, K.M., Robson, R.L. & Dianov, G.L., 2004. Exchangeability of mammalian DNA ligases between base excision repair pathways. *Biochemistry*, 43(40), pp.12924–30.

Slupphaug, G., 2003. The interacting pathways for prevention and repair of oxidative DNA damage. *Mutation Research/Fundamental and Molecular Mechanisms of Mutagenesis*, 531(1-2), pp.231–251.

Sobol, R.W. et al., 1996. Requirement of mammalian DNA polymerase-beta in base-excision repair. *Nature*, 379(6561), pp.183–186.

Von Sonntag, C., 1987. New aspects in the free-radical chemistry of pyrimidine nucleobases. *Free Radical Research Communications*, 2(4-6), pp.217–224.

Sonoda, E. et al., 2006. Differential usage of non-homologous end-joining and homologous recombination in double strand break repair. *DNA Repair*, 5(9-10), pp.1021–9.

Sozou, P.D. & Kirkwood, T.B., 2001. A stochastic model of cell replicative senescence based on telomere shortening, oxidative stress, and somatic mutations in nuclear and mitochondrial DNA. *Journal of theoretical biology*, 213(4), pp.573–86.

Stewart, G.S. et al., 2007. RIDDLE immunodeficiency syndrome is linked to defects in 53BP1-mediated DNA damage signaling. *Proceedings of the National Academy of Sciences of the United States of America*, 104(43), pp.16910–16915.

Stewart, G.S. et al., 1999. The DNA double-strand break repair gene hMRE11 is mutated in individuals with an ataxia-telangiectasia-like disorder. *Cell*, 99(6), pp.577–587.

Stucki, M. et al., 1998. Mammalian base excision repair by DNA polymerases delta and epsilon. *Oncogene*, 17(7), pp.835–843.

Stucki, M. & Jackson, S.P., 2004. MDC1/NFBD1: a key regulator of the DNA damage response in higher eukaryotes. *DNA Repair*, 3(8-9), pp.953–957.

Sugasawa, K. et al., 2001. A multistep damage recognition mechanism for global genomic nucleotide excision repair. *Genes & Development*, 15(5), pp.507–521.

Sung, P. & Klein, H., 2006. Mechanism of homologous recombination : mediators and helicases take on regulatory functions. *Group*, 7(10), pp.739–750.

Suraweera, A. et al., 2009. Functional role for senataxin, defective in ataxia oculomotor apraxia type 2, in transcriptional regulation. *Human Molecular Genetics*, 18(18), pp.3384–3396.

Suwa, A. et al., 1994. DNA-dependent protein kinase (Ku protein-p350 complex) assembles on double-stranded DNA. *Proceedings of the National Academy of Sciences of the United States of America*, 91(15), pp.6904–6908.

Sykora, P. et al., 2011. Aprataxin localizes to mitochondria and preserves mitochondrial function. *Proceedings of the National Academy of Sciences of the United States of America*, 2011, pp.1–6.

Takahashi, T. et al., 2007. Aprataxin, causative gene product for EAOH/AOA1, repairs DNA single-strand breaks with damaged 3′-phosphate and 3′-phosphoglycolate ends. *Nucleic Acids Research*, 35(11), pp.3797–3809.

Takashima, H. et al., 2002. Mutation of TDP1, encoding a topoisomerase I-dependent DNA damage repair enzyme, in spinocerebellar ataxia with axonal neuropathy. *Nature Genetics*, 32(2), pp.267–272.

Takata, M. et al., 1998. Homologous recombination and non-homologous end-joining pathways of DNA double-strand break repair have overlapping roles in the maintenance of chromosomal integrity in vertebrate cells. *The EMBO journal*, 17(18), pp.5497–508.

Tanaka, K. et al., 1990. Analysis of a human DNA excision repair gene involved in group A xeroderma pigmentosum and containing a zinc-finger domain. *Nature*, 348(6296), pp.73–6.

Tapias, A. et al., 2004. Ordered conformational changes in damaged DNA induced by nucleotide excision repair factors. *The Journal of Biological Chemistry*, 279(18), pp.19074–19083.

Taylor, R.M. et al., 2000. A Cell Cycle-Specific Requirement for the XRCC1 BRCT II Domain during Mammalian DNA Strand Break Repair. *Molecular and Cellular Biology*, 20(2), pp.735–740.

Taylor, R.M. et al., 1998. Role of a BRCT domain in the interaction of DNA ligase III-alpha with the DNA repair protein XRCC1. *Current Biology*, 8(15), pp.877–880.

Tebbs, R.S. et al., 1999. Requirement for the Xrcc1 DNA base excision repair gene during early mouse development. *Developmental biology*, 208(2), pp.513–29.

Tebbs, R.S., Thompson, L.H. & Cleaver, J.E., 2003. Rescue of Xrcc1 knockout mouse embryo lethality by transgene-complementation. *DNA Repair*, 2(12), pp.1405–1417.

Tornaletti, S., 2009. DNA repair in mammalian cells: Transcription-coupled DNA repair: directing your effort where it's most needed. *Cellular and molecular life sciences CMLS*, 66(6), pp.1010–1020.

Tranchant, C. et al., 2003. Phenotypic variability of aprataxin gene mutations. *Neurology*, 60(5), pp.868–870.

Tu, Y., Bates, S. & Pfeifer, G.P., 1997. Sequence-specific and domain-specific DNA repair in xeroderma pigmentosum and Cockayne syndrome cells. *Journal of Biological Chemistry*, 272(33), pp.20747–20755.

Uematsu, N. et al., 2007. Autophosphorylation of DNA-PKCS regulates its dynamics at DNA double-strand breaks. *The Journal of Cell Biology*, 177(2), pp.219–229.

Uziel, T. et al., 2003. Requirement of the MRN complex for ATM activation by DNA damage. *the The European Molecular Biology Organization Journal*, 22(20), pp.5612–5621.

Van Loon, B., Markkanen, E. & Hübscher, U., 2010. Oxygen as a friend and enemy: How to combat the mutational potential of 8-oxo-guanine. *DNA repair*, 9(6), pp.604–16.

Vens, C., Hofland, I. & Begg, A.C., 2007. Involvement of DNA polymerase beta in repair of ionizing radiation damage as measured by in vitro plasmid assays. *Radiation Research*, 168(3), pp.281–291.

Vermeulen, C. et al., 2008. Cell cycle phase dependent role of DNA polymerase beta in DNA repair and survival after ionizing radiation. *Radiotherapy & Oncology*, 86(3), pp.391–398.

Vermeulen, C. et al., 2007. Role for DNA polymerase beta in response to ionizing radiation. *DNA Repair*, 6(2), pp.202–212.

Vermeulen, W. et al., 2000. Nucleotide excision repair and human syndromes. *Biochemical Society Transactions*, 21(3), pp.453–460.

Vidal, A.E. et al., 2001. XRCC1 coordinates the initial and late stages of DNA abasic site repair through protein-protein interactions. *the The European Molecular Biology Organization Journal*, 20(22), pp.6530–9.

Vijg, J. & Dollé, M.E.T., 2002. Large genome rearrangements as a primary cause of aging. *Mechanisms Of Ageing And Development*, 123(8), pp.907–915.

Volker, M. et al., 2001. Sequential assembly of the nucleotide excision repair factors in vivo. *Molecular Cell*, 8(1), pp.213–224.

Waga, S. & Stillman, B., 1998. The DNA replication fork in eukaryotic cells. *Annual Review of Biochemistry*, 67, pp.721–751.

Wallace, D.C., 2001. Mouse models for mitochondrial disease. *American Journal of Medical Genetics*, 106(1), pp.71–93.

Wang, J.C., 2002. Cellular roles of DNA topoisomerases: a molecular perspective. *Nature Reviews Molecular Cell Biology*, 3(6), pp.430–440.

Wang, X.W. et al., 1996. The XPB and XPD DNA helicases are components of the p53-mediated apoptosis pathway. *Genes & Development*, 10(10), pp.1219–1232.

Ward, J.F. et al., 1987. Radiation and hydrogen peroxide induced free radical damage to DNA. *The British journal of cancer. Supplement*, 8, pp.105–12.

Watson, J.D. & Crick, F.H., 1953. Molecular structure of nucleic acids; a structure for deoxyribose nucleic acid. *Nature*, 171(4356), pp.737–738.

Wei, W. & Englander, E.W., 2008. DNA polymerase beta-catalyzed-PCNA independent long patch base excision repair synthesis: a mechanism for repair of oxidatively damaged DNA ends in post-mitotic brain. *Journal of neurochemistry*, 107(3), pp.734–44.

Weiss, B. & Jacquemin-Sablon, A., 1968. Breakage and Joining of Deoxyribonucleic Acid VI. Further purification and properties of polynucleotide ligase from Escherichia Coli infected with bacteriophage T4. *Journal of Biological Sciences*, 248(17), pp.4543–4555.

Weiss, B., Thompson, A. & Richardson, C., 1968. Ezymatic breakage and joining of deoxyribonucleic acid. VII. Properties of the enzyme-adenylate intermediate in the polynucleotide ligase reaction. *The Journal of Biological Sciences*, 248(17), pp.4556–4563.

Weissman, L. et al., 2007. DNA repair, mitochondria, and neurodegeneration. *Neuroscience*, 145(4), pp.1318–1329.

Whitehouse, C.J. et al., 2001. XRCC1 stimulates human polynucleotide kinase activity at damaged DNA termini and accelerates DNA single-strand break repair. *Cell*, 104(1), pp.107–17.

Williams, R.S. et al., 2008. Mre11 dimers coordinate DNA end bridging and nuclease processing in double-strand-break repair. *Cell*, 135(1), pp.97–109.

Williams, R.S., Williams, J.S. & Tainer, J.A., 2007. Mre11-Rad50-Nbs1 is a keystone complex connecting DNA repair machinery, double-strand break signaling, and the chromatin template. *Cell*, 85(4), pp.509–520.

Winters, T.A. et al., 1999. Determination of human DNA polymerase utilization for the repair of a model ionizing radiation-induced DNA strand break lesion in a defined vector substrate. *Nucleic Acids Research*, 27(11), pp.2423–2433.

Wong, A.K. et al., 1997. RAD51 interacts with the evolutionarily conserved BRC motifs in the human breast cancer susceptibility gene brca2. *The Journal of Biological Chemistry*, 272(51), pp.31941–31944.

Wu, J. & Liu, L.F., 1997. Processing of topoisomerase I cleavable complexes into DNA damage by transcription. *Nucleic Acids Research*, 25(21), pp.4181–4186.

Wu, L. & Hickson, I.D., 2003. The Bloom's syndrome helicase suppresses crossing over during homologous recombination. *Nature*, 426(6968), pp.870–4.

Xanthoudakis, S. et al., 1996. The redox/DNA repair protein, Ref-1, is essential for early embryonic development in mice. *Proceedings of the National Academy of Sciences of the United States of America*, 93(17), pp.8919–8923.

Yang, H. et al., 2007. Nutrient-sensitive mitochondrial NAD+ levels dictate cell survival. *Cell*, 130(6), pp.1095–107.

Yano, K. et al., 2008. Ku recruits XLF to DNA double-strand breaks. *EMBO Reports*, 9(1), pp.91–96.

Yoshizaki, T. et al., 2010. SIRT1 inhibits inflammatory pathways in macrophages and modulates insulin sensitivity. *American Journal of Physiology - Endocrinology And Metabolism*, 298(3), pp.E419–E428.

Yu, S.-W. et al., 2002. Mediation of poly(ADP-ribose) polymerase-1-dependent cell death by apoptosis-inducing factor. *Science*, 297(5579), pp.259–263.

Yüce-Petronczki, O. & West, S.C., 2012. Senataxin, defective in the neurogenerative disorder AOA-2, lies at the interface of transcription and the DNA damage response. *Molecular and cellular biology*.

Zahradka, P. & Ebisuzaki, K., 2005. A Shuttle Mechanism for DNA-Protein Interactions. *European Journal of Biochemistry*, 127(3), pp.579–585.

Zelko, I.N., Mariani, T.J. & Folz, R.J., 2002. Superoxide dismutase multigene family: a comparison of the CuZn-SOD (SOD1), Mn-SOD (SOD2), and EC-SOD (SOD3) gene structures, evolution, and expression. *Free Radical Biology & Medicine*, 33(3), pp.337–349.

Zeng, Z. et al., 2011. TDP2/TTRAP is the major 5'-tyrosyl DNA phosphodiesterase activity in vertebrate cells and is critical for cellular resistance to topoisomerase II-induced DNA damage. *The Journal of biological chemistry*, 286(1), pp.403–9.

Von Zglinicki, T., 2002. Oxidative stress shortens telomeres. *Trends in biochemical sciences*, 27(7), pp.339–44.

Zhou, W. & Doetsch, P.W., 1994. Transcription bypass or blockage at single-strand breaks on the DNA template strand: effect of different 3' and 5' flanking groups on the T7 RNA polymerase elongation complex. *Biochemistry*, 33(49), pp.14926–34.

Zhu, C. et al., 1996. Ku86-deficient mice exhibit severe combined immunodeficiency and defective processing of V(D)J recombination intermediates. *Cell*, 86(3), pp.379–389.

Zhu, Z. et al., 2008. Sgs1 helicase and two nucleases Dna2 and Exo1 resect DNA double-strand break ends. *Cell*, 134(6), pp.981–994.

Appendix I

Figures and Tables

Chapter One

Introduction

Figures

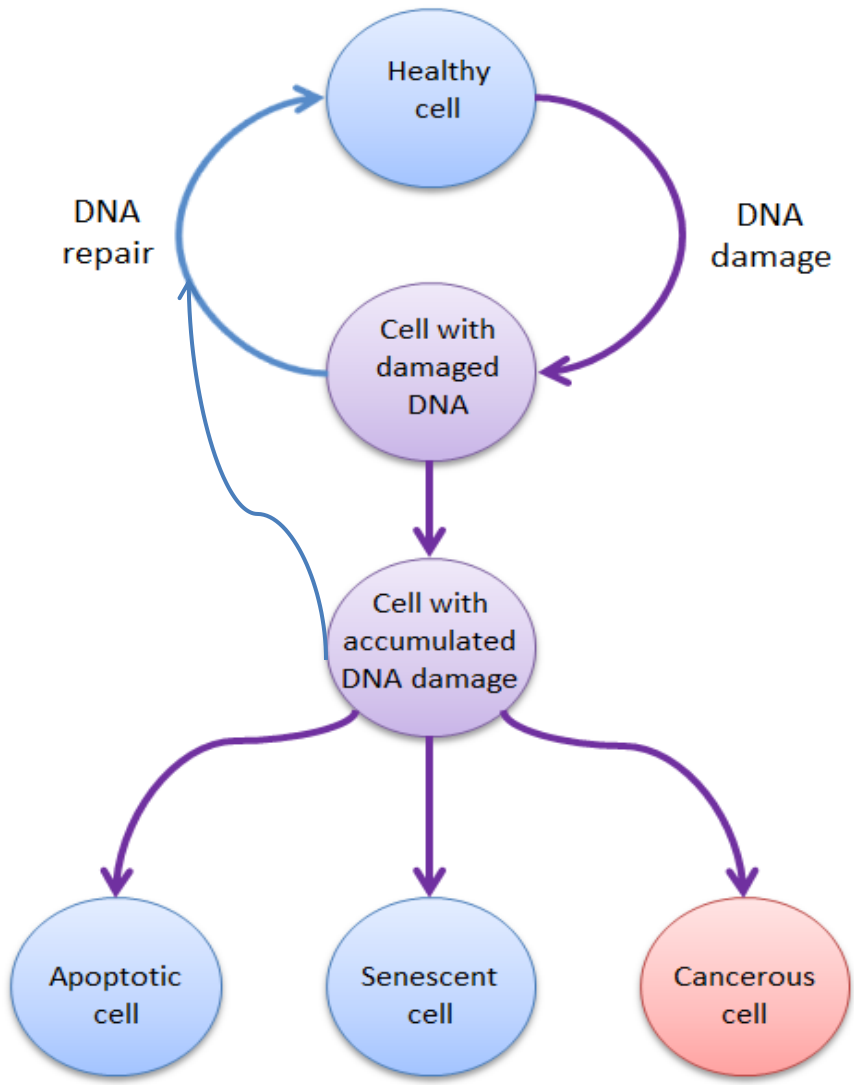

Figure 1.1 Cellular outcomes of DNA damage.

If left unrepaired, accumulated DNA damage may cause a cell to become apoptotic, senescent, or cancerous. The rate at which a cell is able to efficiently repair DNA is contingent on many factors including cell type and age.

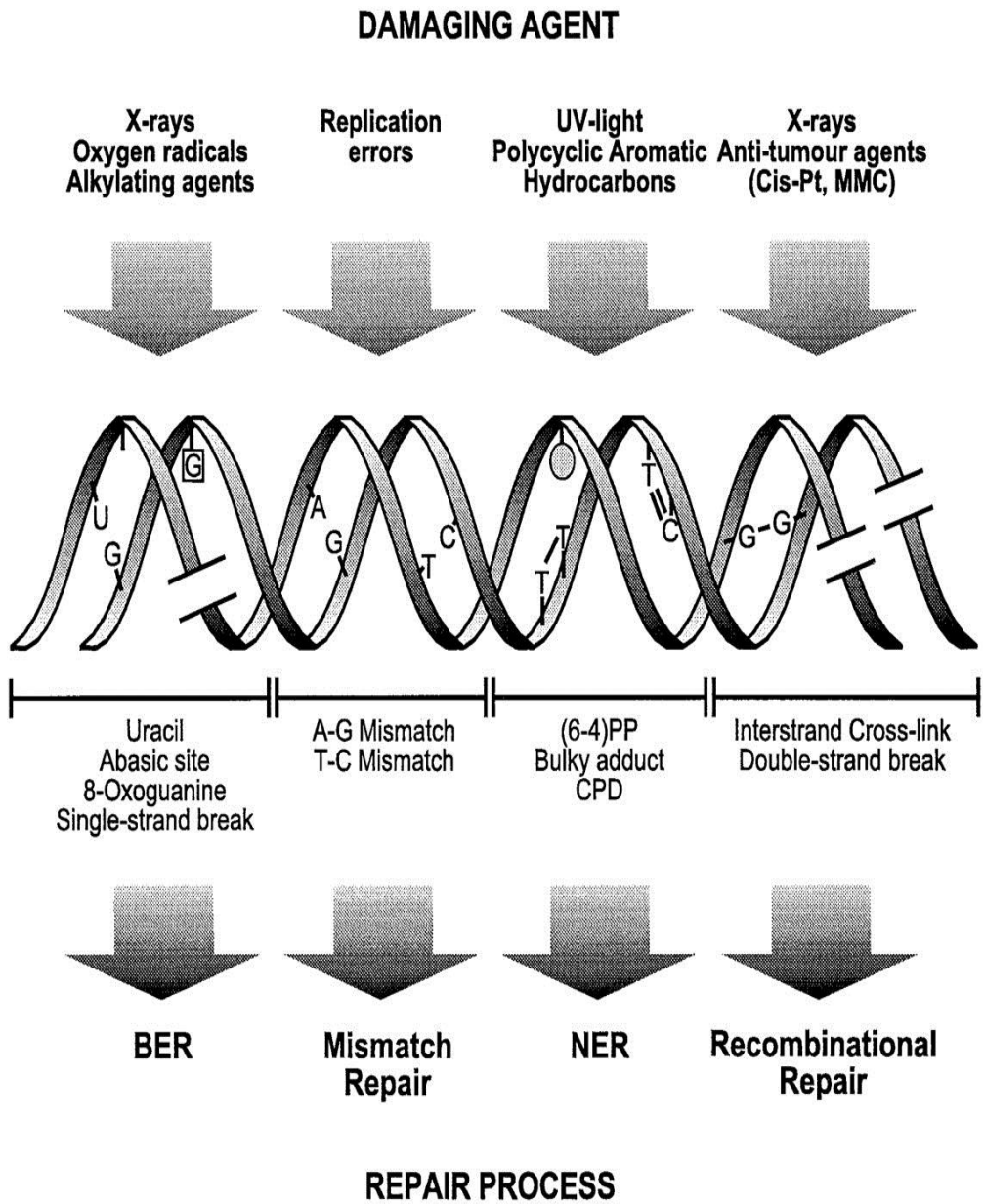

Figure 1.2 DNA lesions and their predominant repair mechanisms

The nature and extent of DNA damage depends upon the source of the damage. Under normal circumstances the nature of the lesion dictates which repair pathway will repair it.

From Vermeulen et al. 2000

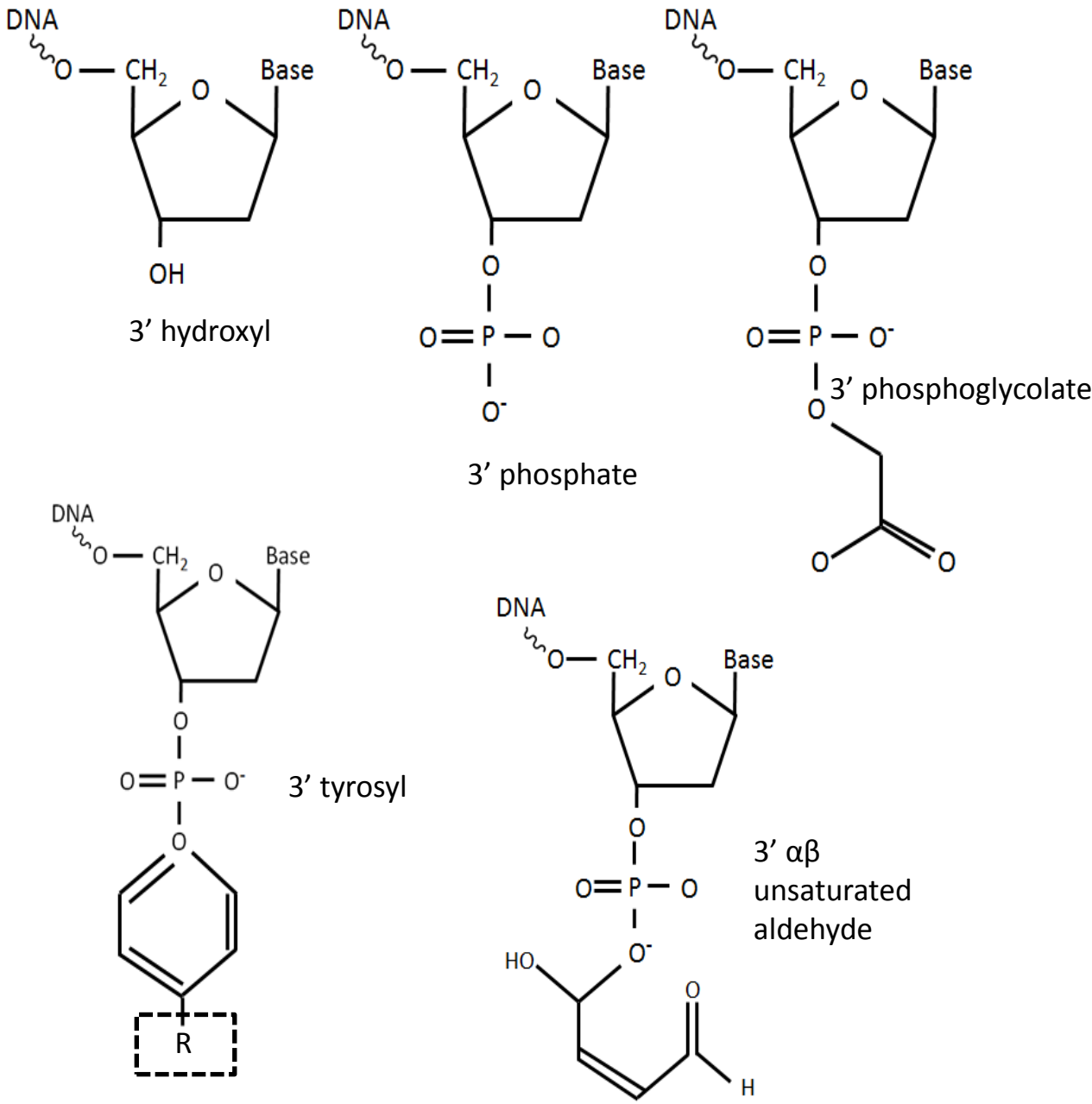

Figure 1.3 Structures of the most common chemical moieties at the 3’ termini of SSBs

3’hydroxyl (3’OH), 3’phosphate (3’P), 3’phosphoglycolate (3’PG), 3’tyrosyl (3’Y) - which may include a variably degraded Top1 polypeptide (R), and 3’αβ unsaturated aldehyde (3’PUA) are all common 3’ SSB termini.

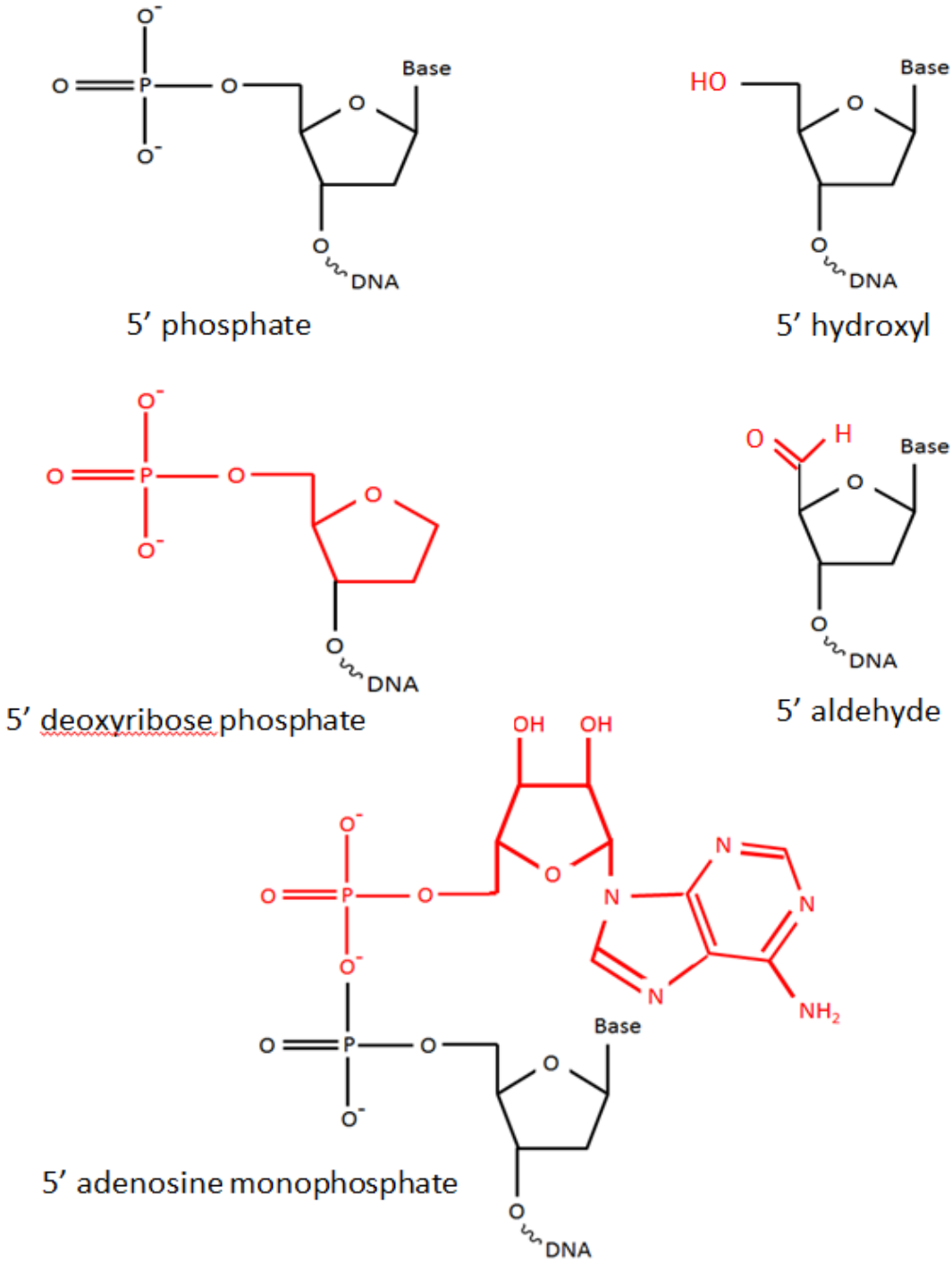

Figure 1.4 Structures of the most common chemical moieties present at the 5' termini of DNA SSBs

5'phosphate (5'P), 5'hydroxyl (5'OH), 5' deoxyribose phosphate, (5'dRP), 5'aldehyde (5'AH) and 5'adenosine monophosphate (5'AMP). Structures in red indicate unligatable damaged termini that require processing before ligation.

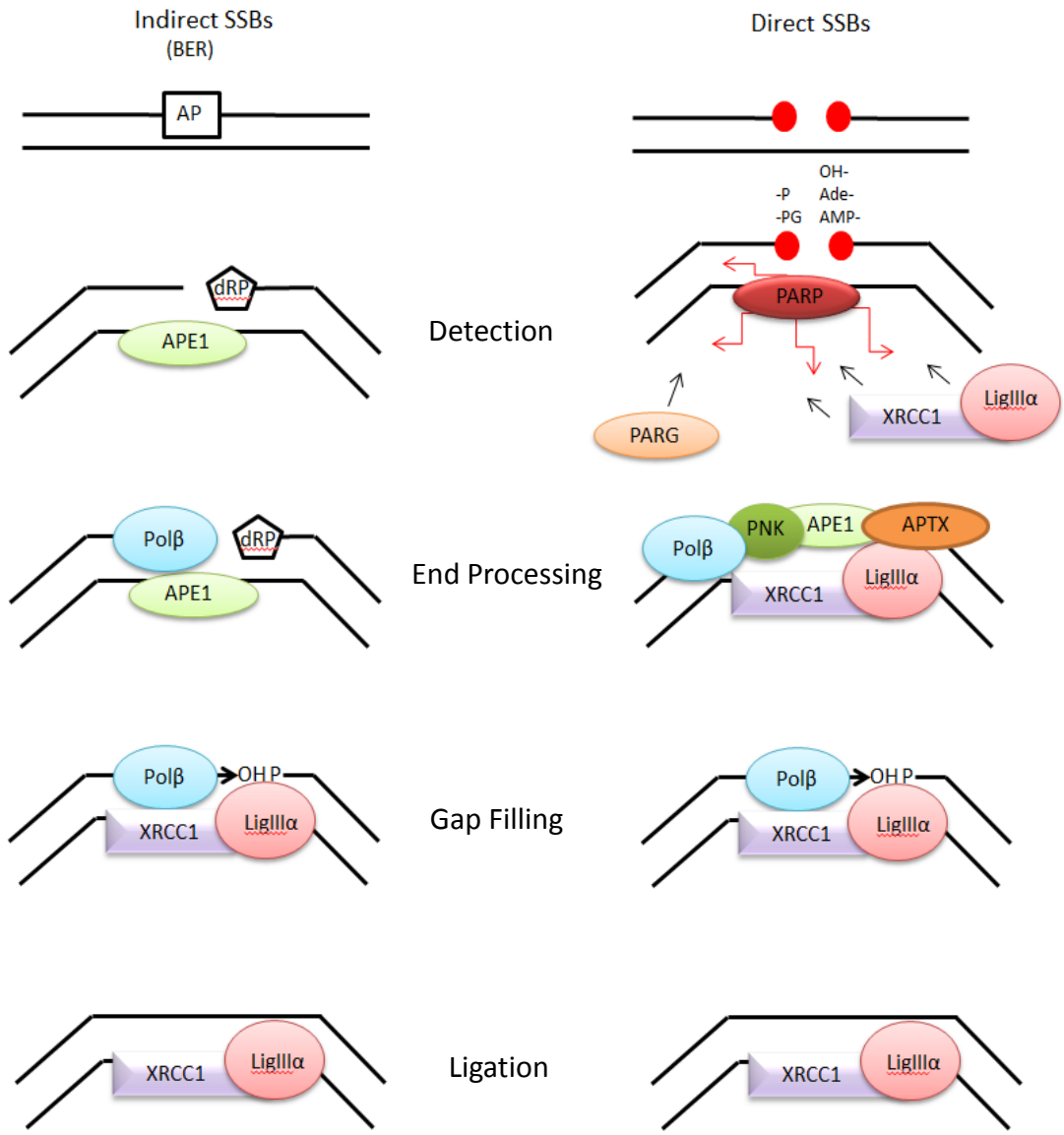

Figure 1.5 Model for mammalian SSBR at indirect and direct short-patch single strand breaks

The main repair proteins involved in the repair of indirect (in this case BER-induced) and direct 'short patch' single strand breaks are depicted at the common steps of repair, Detection, End Processing, Gap Filling and Ligation. The end processing factors used depend on the chemistry of the termini at the break. AP = Abasic site APE1 = Apurinic/apyrimidinc endonuclease 1 dRP=deoxyribose phosphate Polβ = polymerase β APTX = aprataxin PNK = polynucleotide kinase. The processes involved are reviewed in detail in Caldecott, 2003.

Adapted from Caldecott, *Cell*, 2003

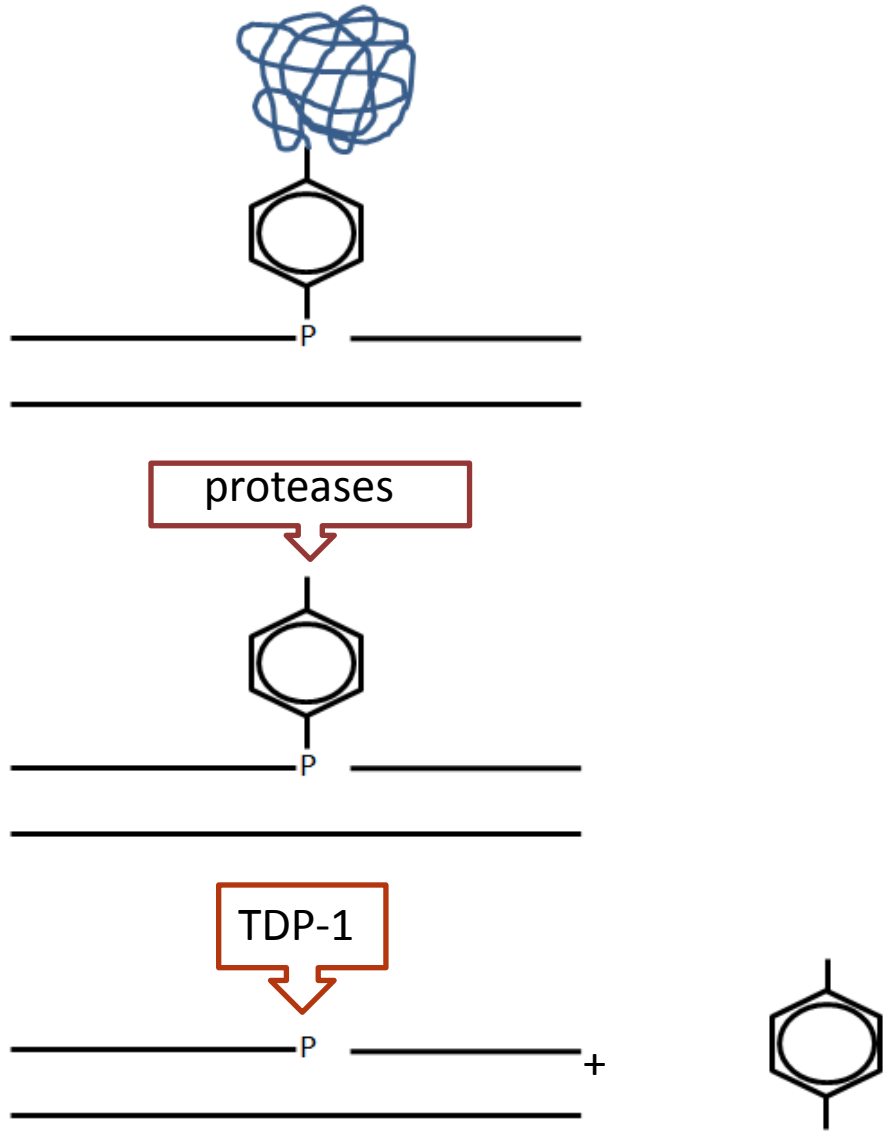

Figure 1.6 Repair of Topoisomerase 1 cleavage complexes by proteases and TDP-1

Proteases degrade the Top1 protein to leave a tyrosine bound on the 3' terminus of the lesion. TDP-1 cleaves the phophotyrosyl bond to release tyrosine and restore the ligatable 3'P terminus. In cells TDP-1 performs this action in concert with the SSBR complex.

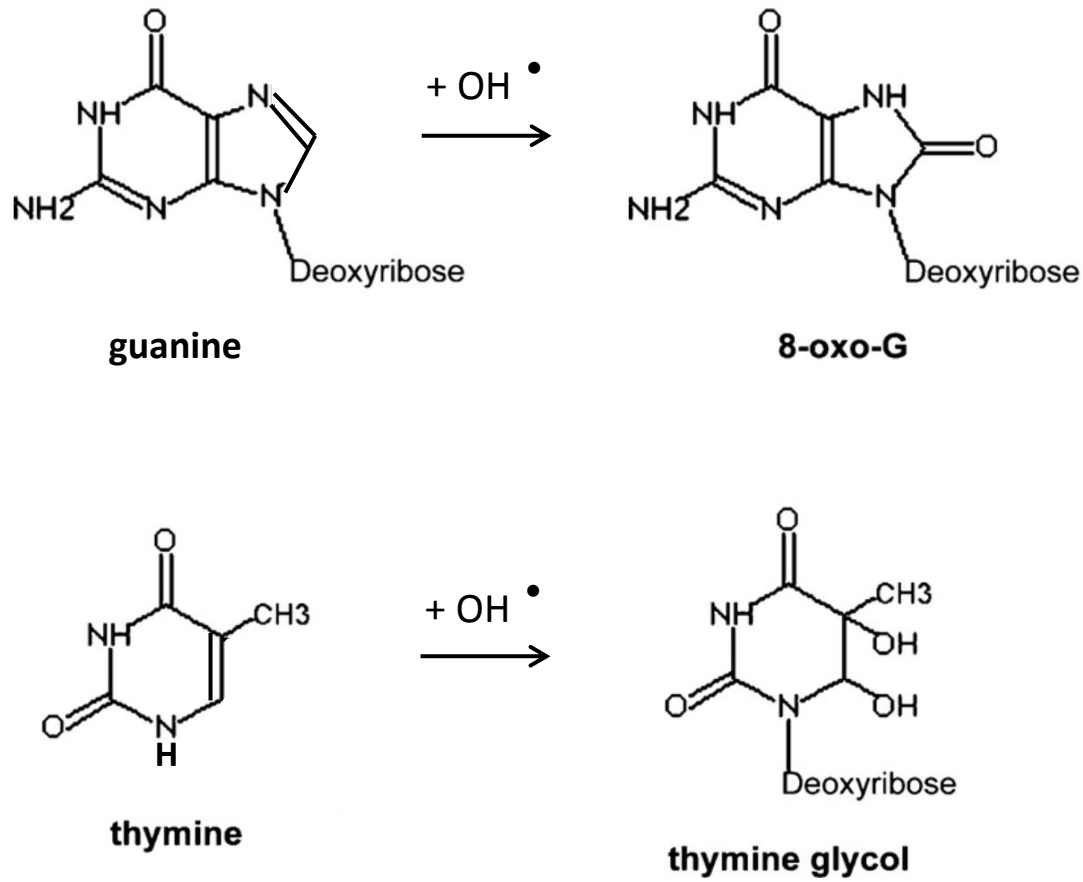

Figure 1.7 Formation of 8-oxo-G and thymine glycol by hydroxyl radical attack of guanine and thymine

The most common oxidative base damage, 7,8-dihydro-8-oxoguanine (8-oxo-G); and thymine glycol; are produced by the attack of guanine and thymine by hydroxyl radicals.

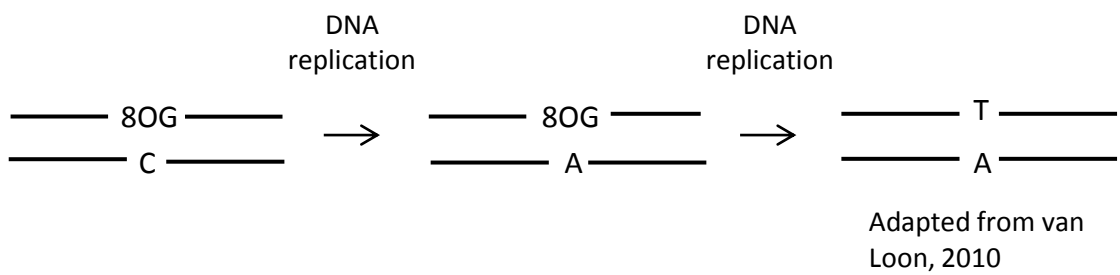

Figure 1.8 The mutagenic potential of 3-oxo-guanine

The incorporation of adenine opposite 8-oxo-G can lead to a G → T mutation after two rounds of replication.

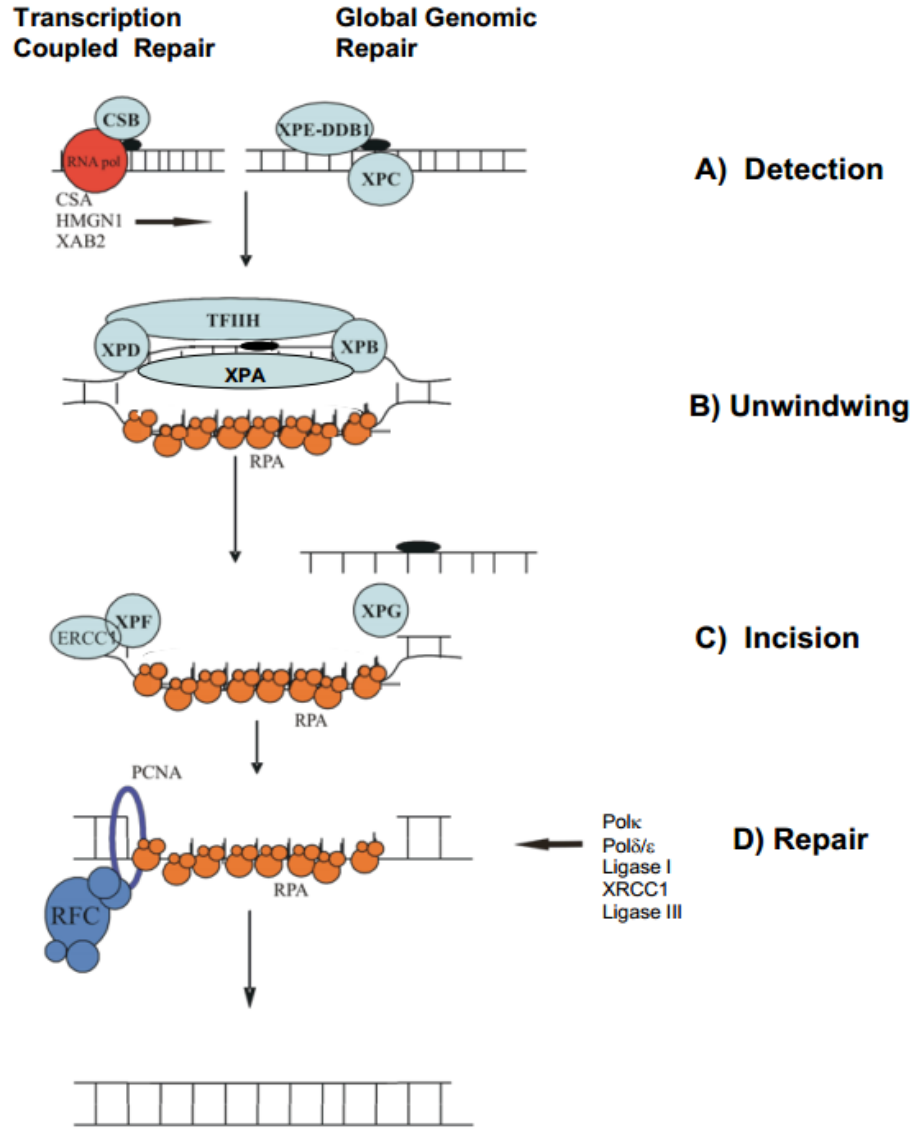

Figure 1.9 Eukaryotic (Mammalian) Nucleotide Excision Repair

A) Damage is sensed through either the detection of stalled polymerase by the CS proteins (Transcription Coupled Repair) or through the detection of helical distortions by XPE and/or XPC (Global Genomic Repair). Chromatin remodelers, not shown here for simplicity, are inolved in reshaping the chromatin landscape to facilitate downstream processes.

B) The two pathways converge with the recruitment of TFIIH, carrying the helicases XPB and XPD which serve to unwind the double helix and allowing the recruitment of RPA, XPA and XPG.

C) The hucleases XPF-ERCC1 and XPG coordinate their incisions on the lesion containing strand with the 5' incision by XPF preceding the 3' incision by XPG (5' and 3' are in relation to the position of the lesion).

D) The resulting gap in the DNA double helix is then resynthesized by DNA polymerases: Polδ, Polε, and Polκ. This is then followed by ligation and the restoration of the chromatin structure. The choice of polymerase and ligase is influenced by whether the cell is actively cycling or in a non-cycling state.

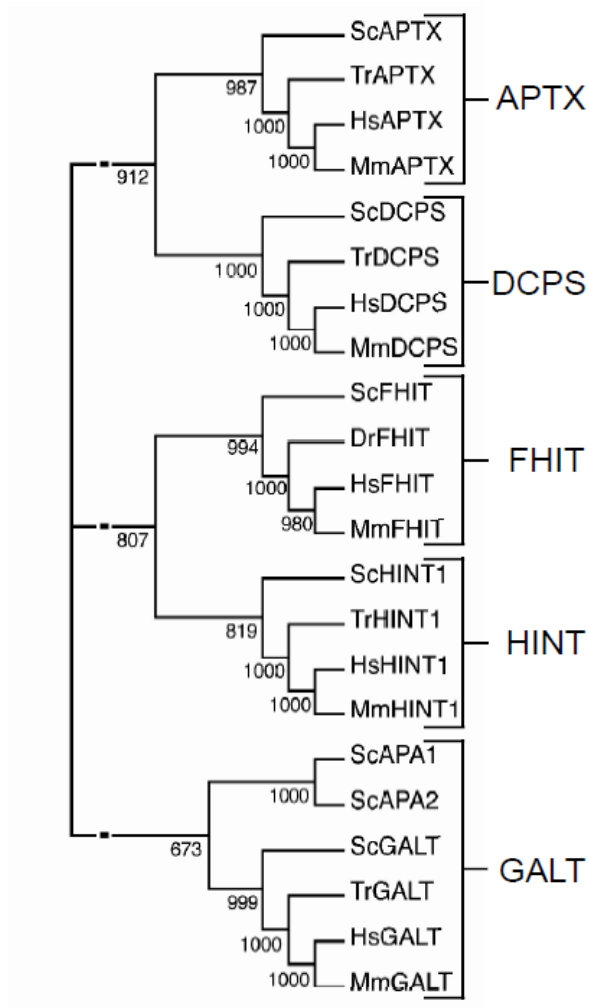

Figure 1. 10 Phylogenetic tree of aprataxin, a member of the histidine triad family of nucleotide hydrolases and transferases

Numbers refer to confidence of shared ancestry, out of 1000.

The protein sequences from each branch (indicated by the bracket) including aprataxin were aligned by ClustalW then used to build a Neighbor Joining tree (with pairwise deletion) to investigate how these sequences relate to each other using human CHK2 protein as the root. The boot- strap test was applied with 1000 replicates, and the values are indicated on the top at each node.

Kijas 2006

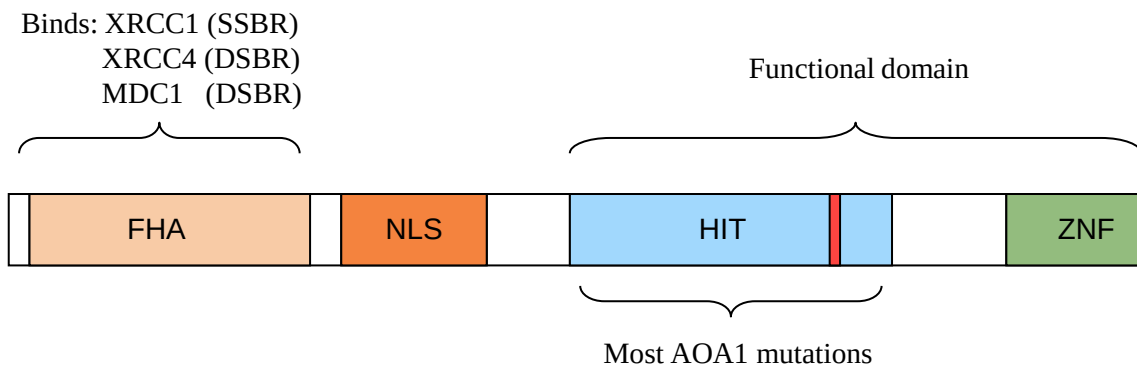

Adapted from Caldecott, 2008

Figure 1.11 Illustration of the aprataxin protein with known domains indicated

FHA = Forkhead Associated domain, responsible for binding to XRCC1 during SSBR and XRCC4 during DSBR. NLS = Nuclear Localizing Signal HIT = Histidine Triad, contains the catalytic histidine triad (indicated by a red box). ZNF = Zinc Finger, important for optimal function.

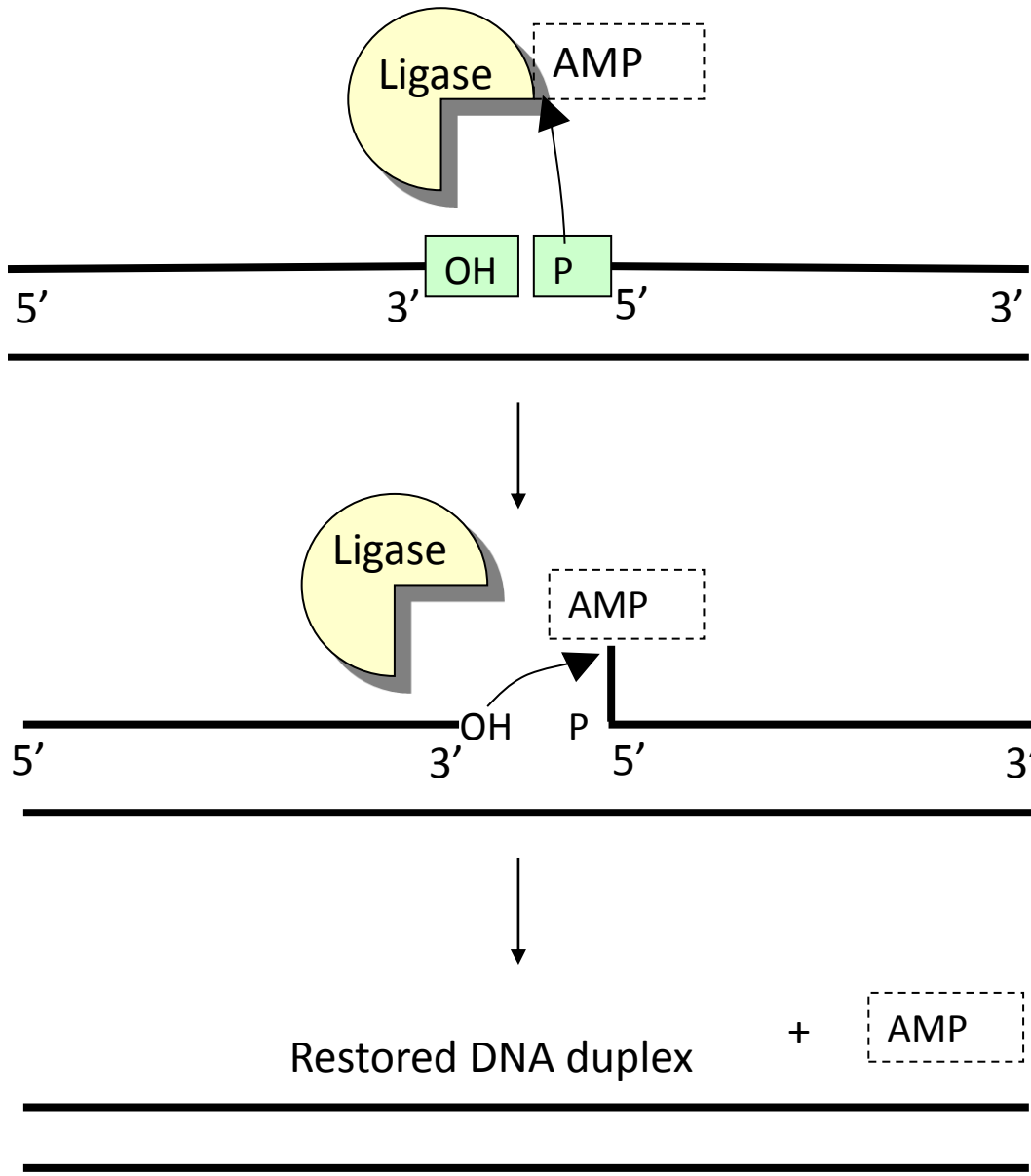

Figure 1.12 Normal ligation of a DNA nick by DNA ligase

At a DNA nick containing a 5’P and a 3’OH, an adenylated ligase transfers an AMP group to the 5’ terminus of the nick, which is then attacked by the 3’OH to reseal the nick.

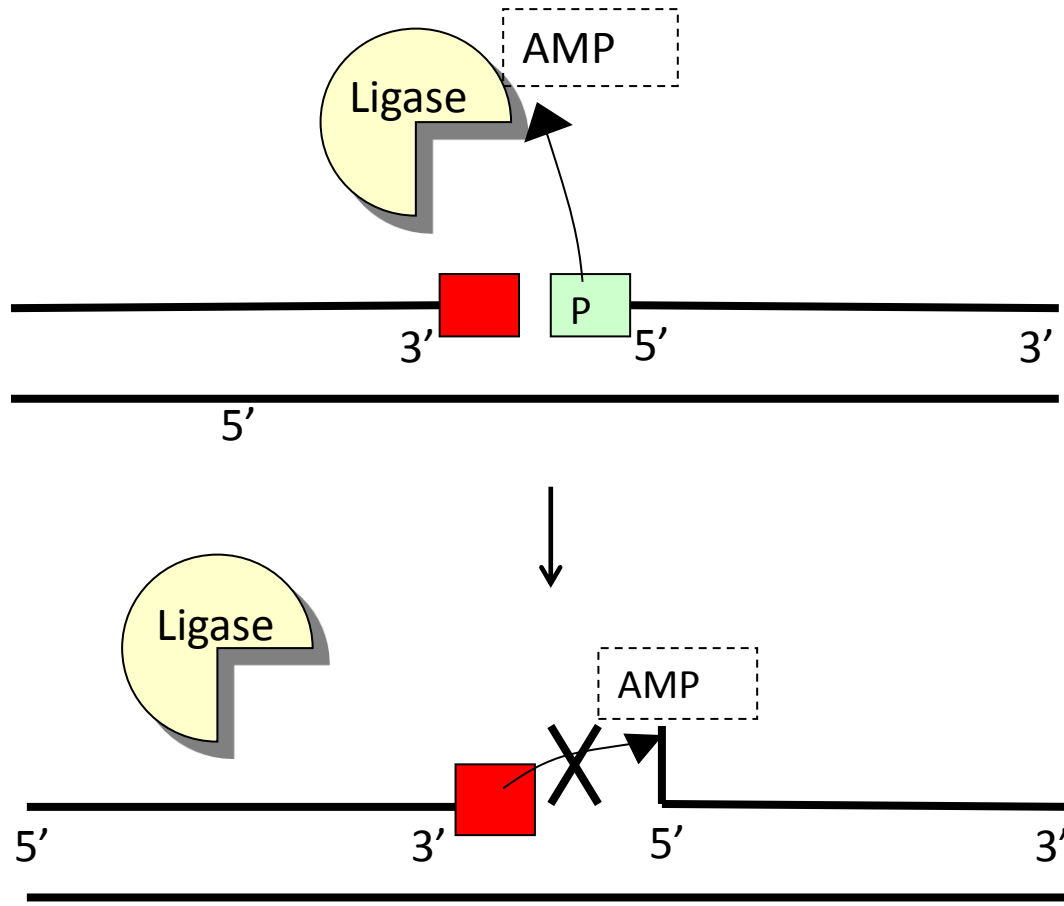

Figure 1.13 Abortive nick ligation and formation of a 5’AMP

During an abortive ligation reaction, an AMP group is transferred from an adenylated ligase to the 5’P of a single strand break containing a damaged 3’ terminus – shown in red.
The damaged 3’ terminus may be any moiety other than a 3’OH.

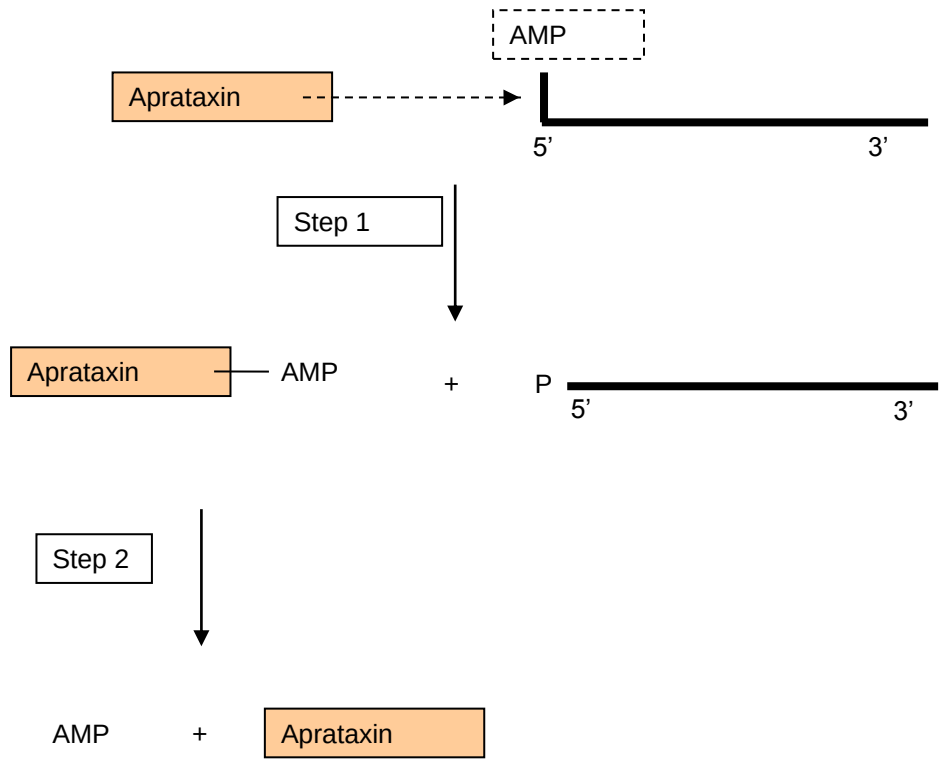

Figure 1.14 Schematic to illustrate the resolution of abortive ligation intermediates by aprataxin

Step 1: Attack of the 5’ adenylated phosphate and transfer of the AMP onto aprataxin’s active site histidine triad. Step 2: Hydrolysis of the 5’phosphohistidine to release AMP and recycle aprataxin.

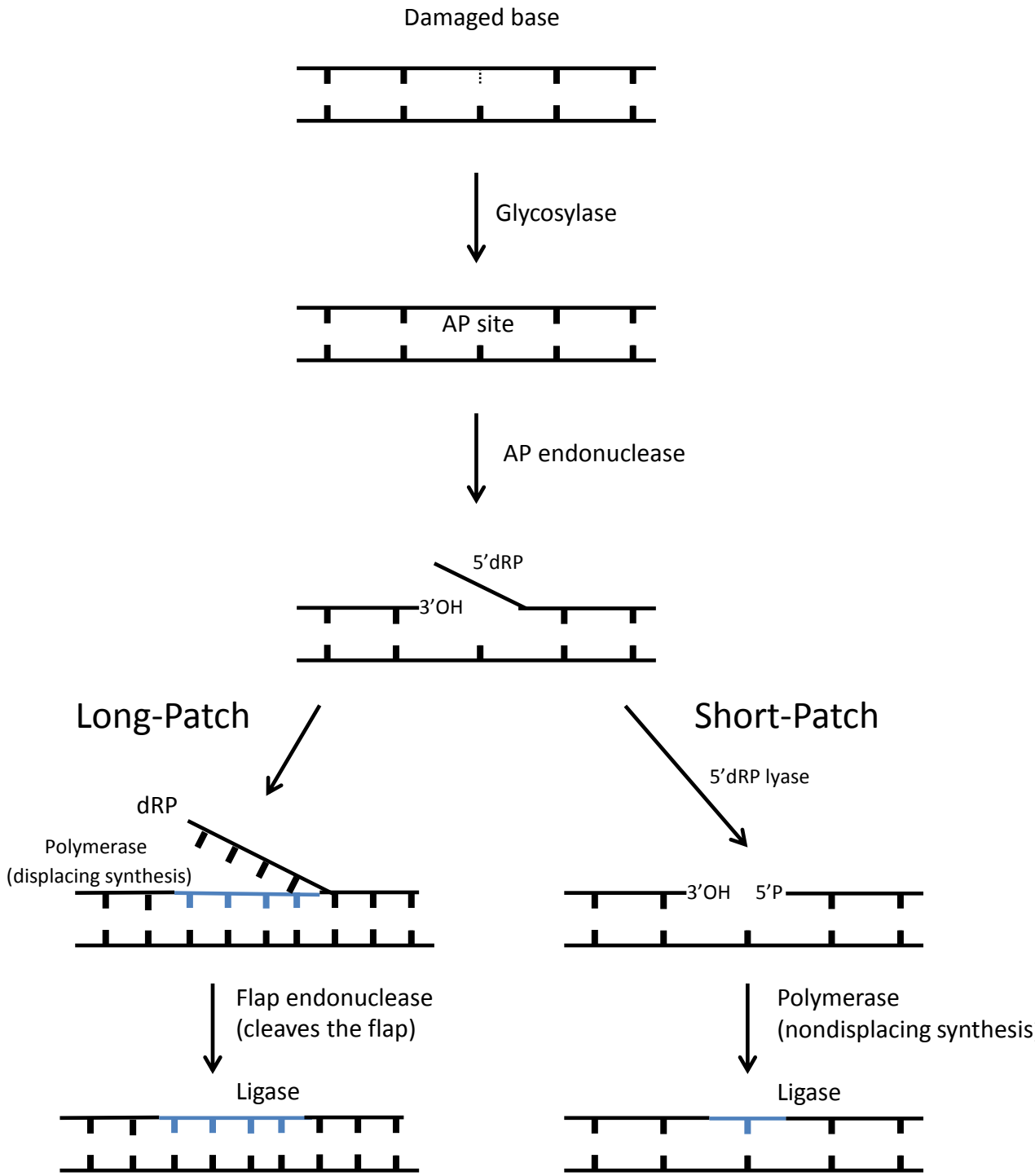

Figure 1.15 Schematic to show long-patch and short-patch repair of a single strand break

During long-patch repair, the polymerase fills the gap and displaces the 5' dRP and several nucleotides. The resulting flap is cleaved by a flap endonuclease before a ligase seals the remaining nick. During short patch repair the polymerase simply fills the gap and a ligase seals the nick.

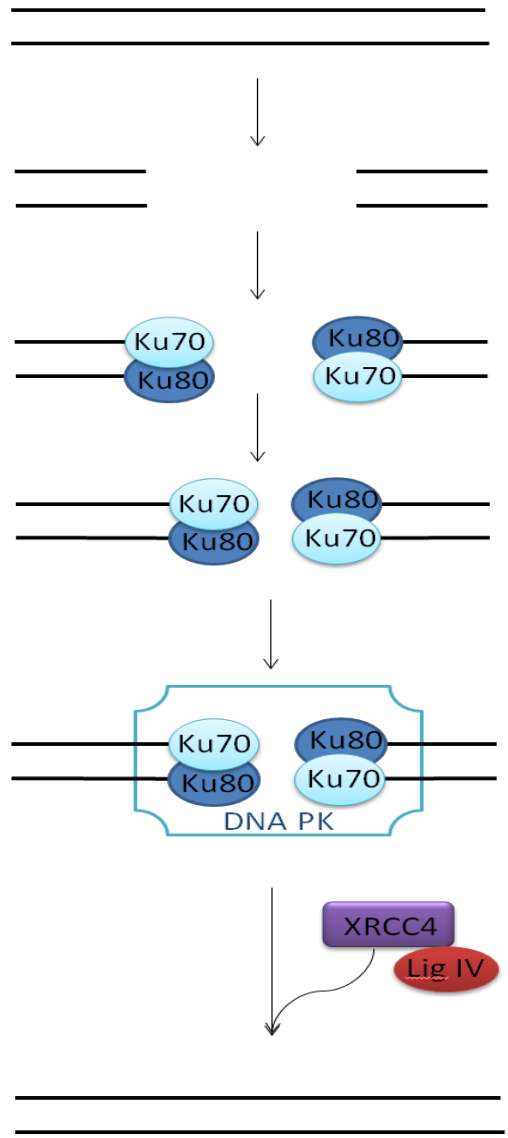

Figure 1.16 General scheme of classical non-homologous end-joining

DNA double strand breaks are detected by the Ku 70/80 heterodimer, resulting in the recruitment of DNA-PKcs and the XRCC4/DNA ligase IV complex. DNA ends processed by nucleases during the synaptic complex if necessary (not shown here for simplicity). Leber, 1998.

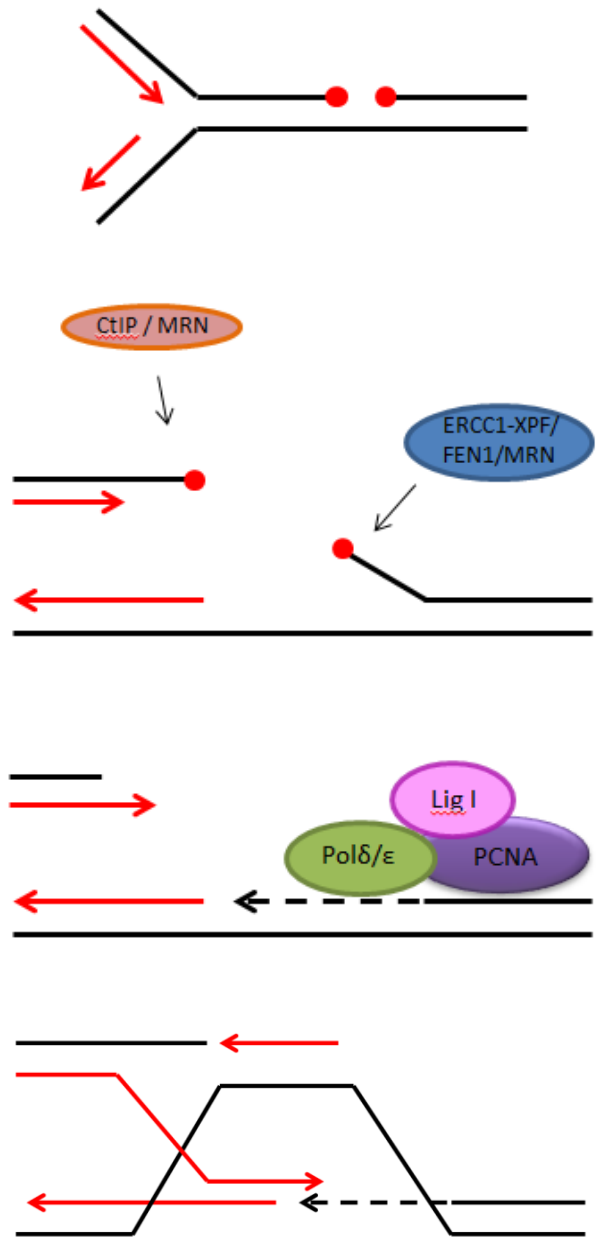

Figure 1.17 General scheme of homology-directed repair of DNA double strand breaks

DNA double strand breaks are detected by the Ku 70/80 heterodimer, resulting in the recruitment of DNA-PKcs and the XRCC4/DNA ligase IV complex. DNA ends processed by nucleases during the synaptic complex if necessary (not shown here for simplicity).

Summarized from Hartlerode and Scully, 2010

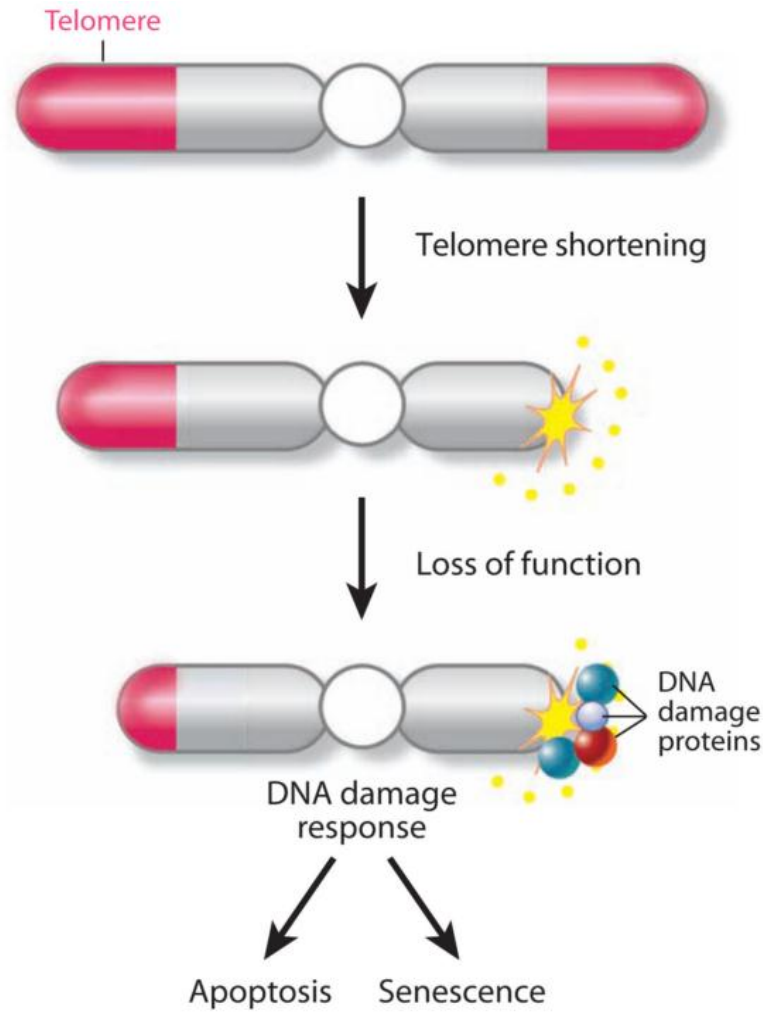

From Armanios, *Annual Review of Genomics and Human Genetics*, 2009

Figure 1.18 Telomeres protect genomic information

Short telomeres activate a DNA-damage response that leads to apoptosis and senescence. As cells divide, telomeres shorten because of the end-replication problem. Critically, short telomeres recruit DNA damage proteins that activate cellular programs of apoptosis or senescence. This cellular response manifests as organ failure in clinically recognisable syndromes of telomere shortening.

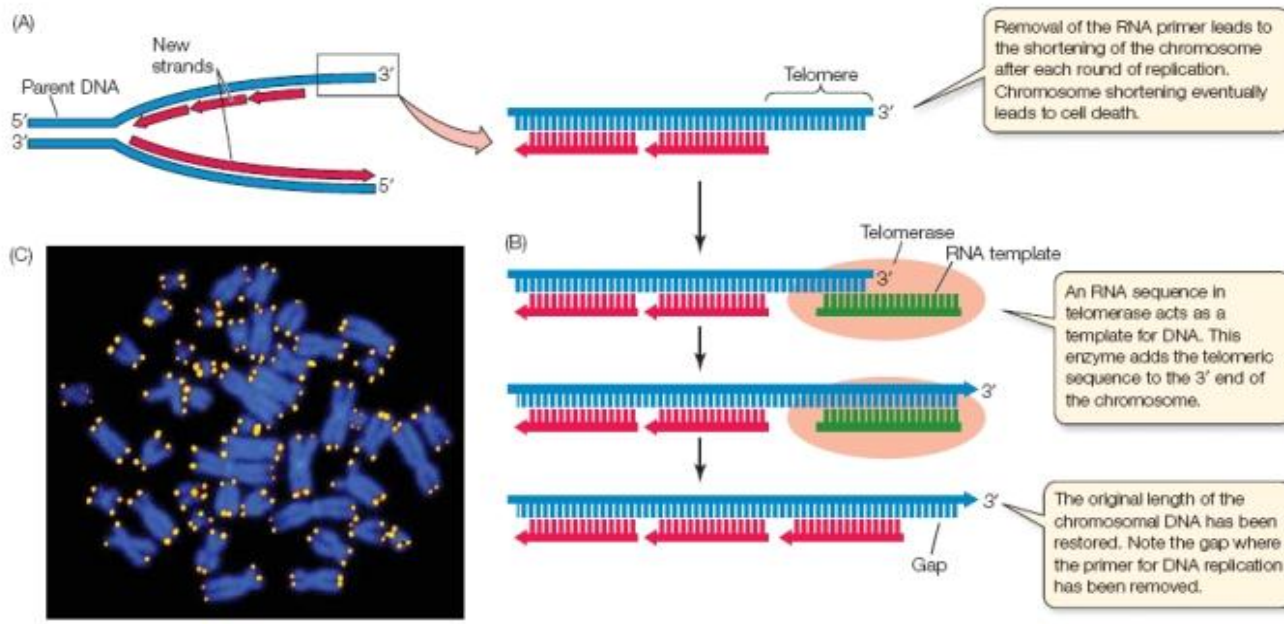

Figure 1.19 Telomeres and telomerase

(A) Removal of the RNA primer at the 3' end of the lagging strand leaves a region of DNA at the end of the telomere unreplicated. (B) The enzyme telomerase binds to the 3' end and extends the lagging strand of DNA. An RNA sequence embedded in telomerase provides a template so that, overall, the DNA does not get shorter. (C) Bright fluorescent staining marks the telomeric regions on these blue-stained human chromosomes.

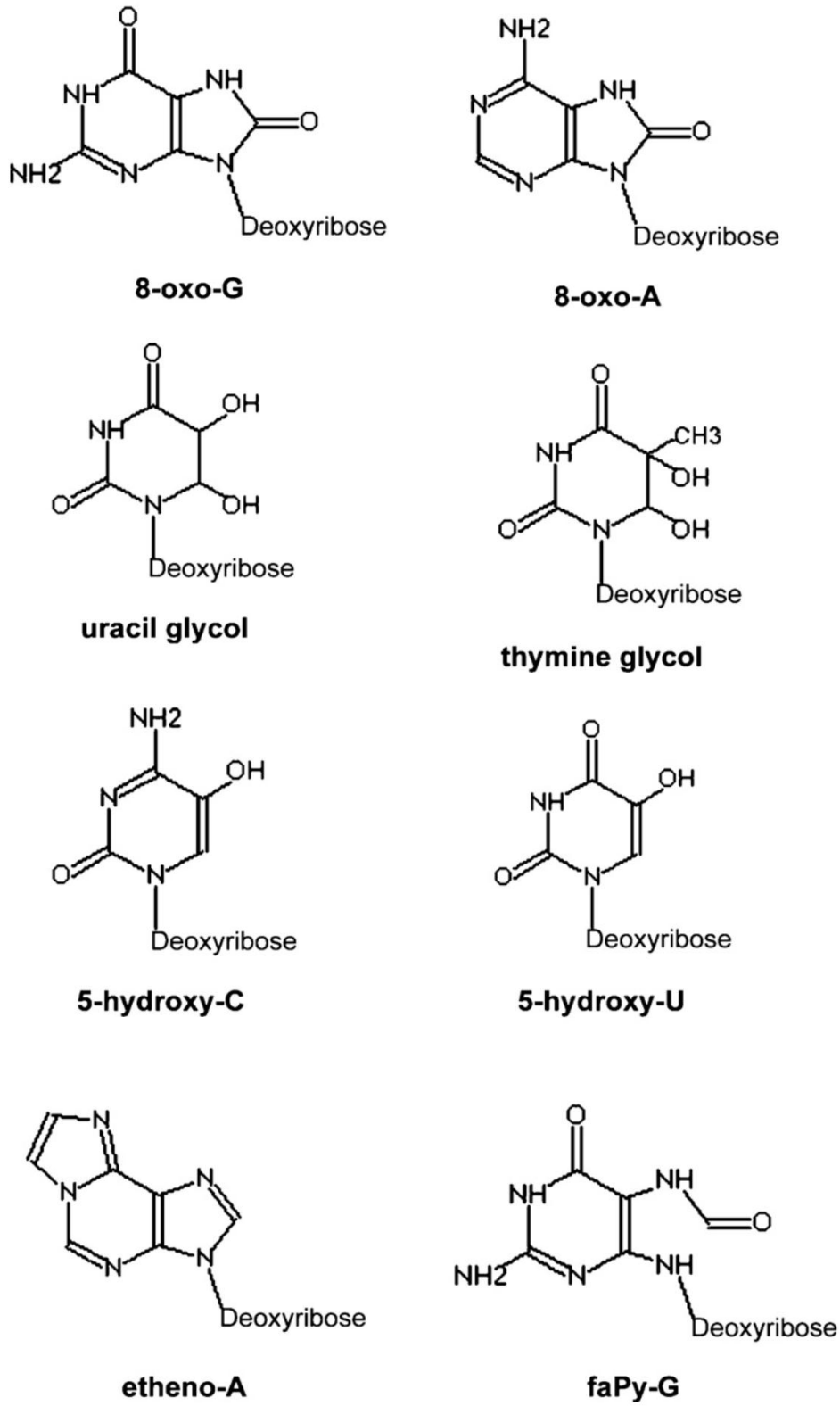

Figure 1.20 The most common oxidative DNA lesions

7,8-dihydro-8-oxoguanine (8-oxo-G);7,8-dihydro-8-oxo-adenine (8-oxo-adenine (8-oxo-A); uracil glycol; thymine glycol; 5-hydroxycytosine (5-hydroxy-C); 5-hydoxyuracil (5-hydroxy-U); ethenoadenine (etheno-A); 2,6-diamino-4-hydroxy-5-formamidopyrimidine (faPy-G) and 4,6-diamino-5-formamidopyrimidine (faPy-A).

Adapted from van Loon, 2010

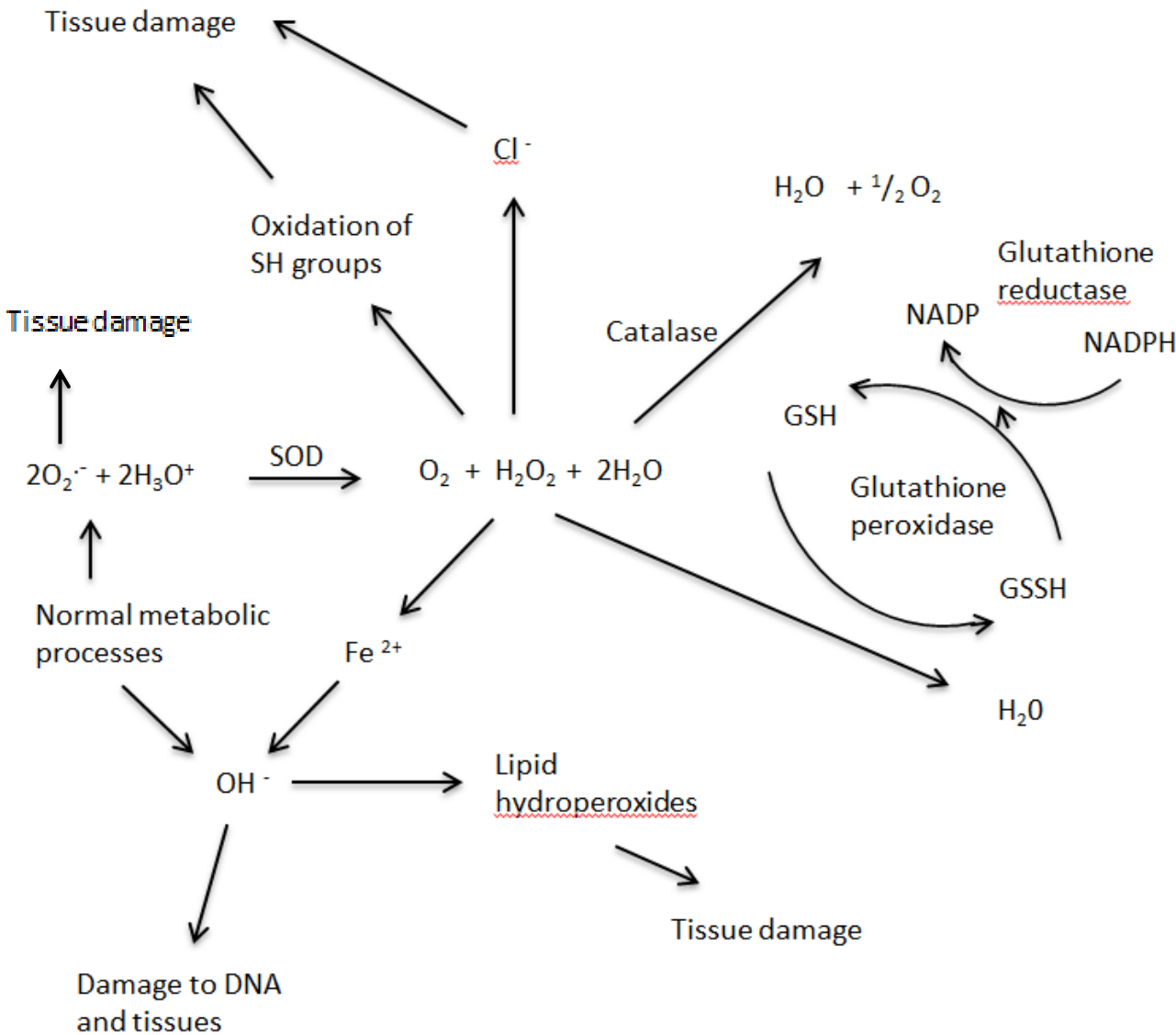

Figure 1.21 a) Diagram of some key redox reactions involved in oxidative toxicity

Enzymatic inactivation of superoxide in performed by superoxide dismutase (SOD) . Two superoxide radicals and two protons generate the less toxic hydrogen peroxide and oxygen.

a) $O_2^- + Fe^{3+} \longrightarrow Fe^{2+} + O_2$

b) $Fe^{2+} + H_2O_2 \longrightarrow Fe^{3+} + OH^- + OH\cdot$

c) $O_2^- + H_2O_2 \longrightarrow O_2\ OH^- + OH\cdot$

Figure 1.21 b) Fenton-type reactions undertaken by the mutant SOD1^{G93A}

The SOD1^{G93A} mutant is understood to exert its oxidative damage to DNA by the conversion of hydrogen peroxide to highly toxic hydroxyl radicals by way of these Fenton-type reactions.

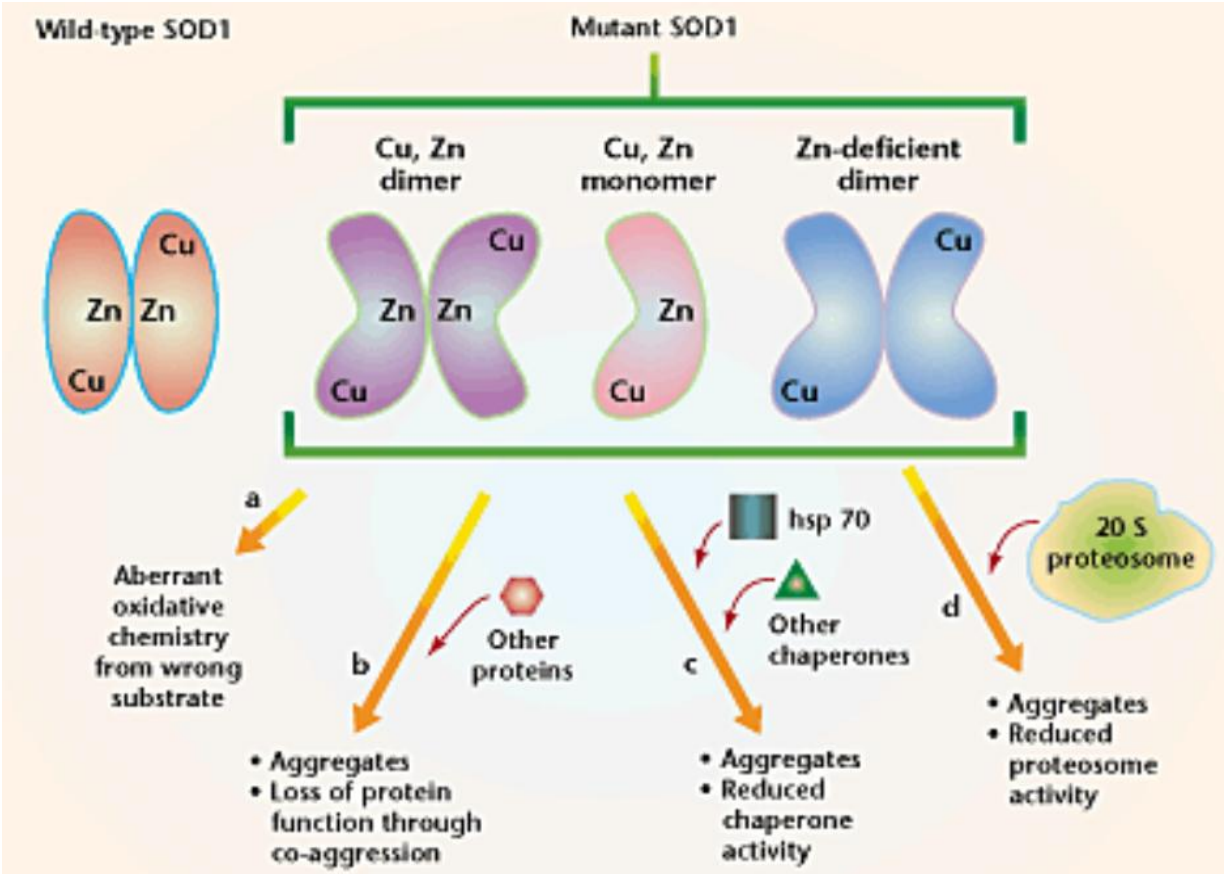

Figure 1. 22 Proposed models for SOD1-mediated toxicity linked to altered conformation and/or aggregation of mutant SOD1 subunits

Wild-type SOD1 exists as a dimer with bound Cu and Zn, while mutants are misfolded, unable to dimerize or unable to efficiently bind Zn. ***a)*** Mutant SOD1 toxicity may result from aberrant oxidative chemistry. Misfolded enzymatic subunits admit access of improper substrates to the catalytic copper site of SOD1. ***b−d)*** Neuronal toxicity arises from protein aggregation. Diffuse or focal aggregates sequester key cellular components[3] ***b***). Aggregates place an increased burden on protein chaperones, which continually try to fold or refold mutant SOD1, leading to c) a reduction in overall protein-folding chaperone activity d) Accumulation of mutant SOD1 overwhelms the capacity of the ubiquitin proteasome pathway to degrade misfolded SOD molecules, but also other critical substrates.

Cleveland and Liu, *Nature Medicine*, 2000

Chapter Two

Materials and Methods

Tables

Chapter Two

Materials and Methods

Tables

	WT	APTX$^{-/-}$	APTX $^{+/-}$	SOD1 ^{G93A}	APTX$^{-/-}$ SOD1 ^{G93A}
1	A60/61-8	A60-61-2			
2		DAS58/64-5		DAS58/64-3	DAS58/64-4
3	SA276/267-7	SA275/269-4	SA275/269-7		

Table 2.i Codes of MEFs used for survival, comet and senescence assays

	WT	APTX$^{-/-}$	SOD1 ^{G93A}	APTX$^{-/-}$ SOD1 ^{G93A}
1	SA47-417	SA50-494	SA46-448	SA46-459
2	SA47-420	SA50-497		SA46-464
3	C57BL/6J -1	A19-117	SOD/C6-50L	SA50-495

Table 2.ii Codes of adult mice used for comparison of liver IGF1 levels relative to β-actin

	Sequence
APTX 1	5’ – AGCAAGTGGCCTCACATACACATGC – 3’
APTX 2	5’ – CTCCTTGCCTGCTTACACTCCAGC – 3’
APTX 3	5’ – TTCTCTCCATGACTGGTCATGGC – 3’
SOD 1 Forward	5’ - CTAGGCCACAGAATTGAAAGATCT - 3’
SOD 1 Reverse	5’ – GTAGGTGGAAATTCTAGCATCATC - 3’
SOD 1^{G93A} Forward	5’ – CATCAGCCCTAATCCATCTGA – 3’
SOD 1^{G93A} Reverse	5’ – CGCGACTAACAATCAAAGTGA – 3’

Table 2.iii Details of primers used for genotyping biopsies

Oligonucleotide	Sequence
25mer	5’-GACATACTAACTTGAGCGAAACGGT-3’
18mer	5’-TCCGTTGAAGCCTGCTTT-3’
14mer	5’-AACTCGCTTTGCCA-3’
36mer	5’-TAGGCAACTTCGGACGAAACTGTTGAGCGAAACGGT-3’
43mer	5’-CCGTTTCGCTCAAGTTAGTATGTCAAAGCAGGCTTCAACGGAT-3’
Competitor oligonucleotide	5’-TCTGCTAGCATCGATCCATG-3’

Table 2.iv Sequences of the oligonucleotides used to prepare model SSB substrates

Primer	Sequence
β-actin Forward	5’-GACGTTGACATCCGTAAAGA-3’
β-actin Reverse	5’-AATCTCCTTCTGCATCCTGT-3’
IGF-1 Forward	5’-TGCTTGCTCACCTTCACCA-3’
IGF-1 Reverse	5’-CAACACTCATCCACAATGCC-3’

Table 2.v Sequences of the primers used for Q-PCR

Chapter 3

Results (1)

Aprataxin facilitates gap filling at DNA single-strand breaks *in vitro*

Figures

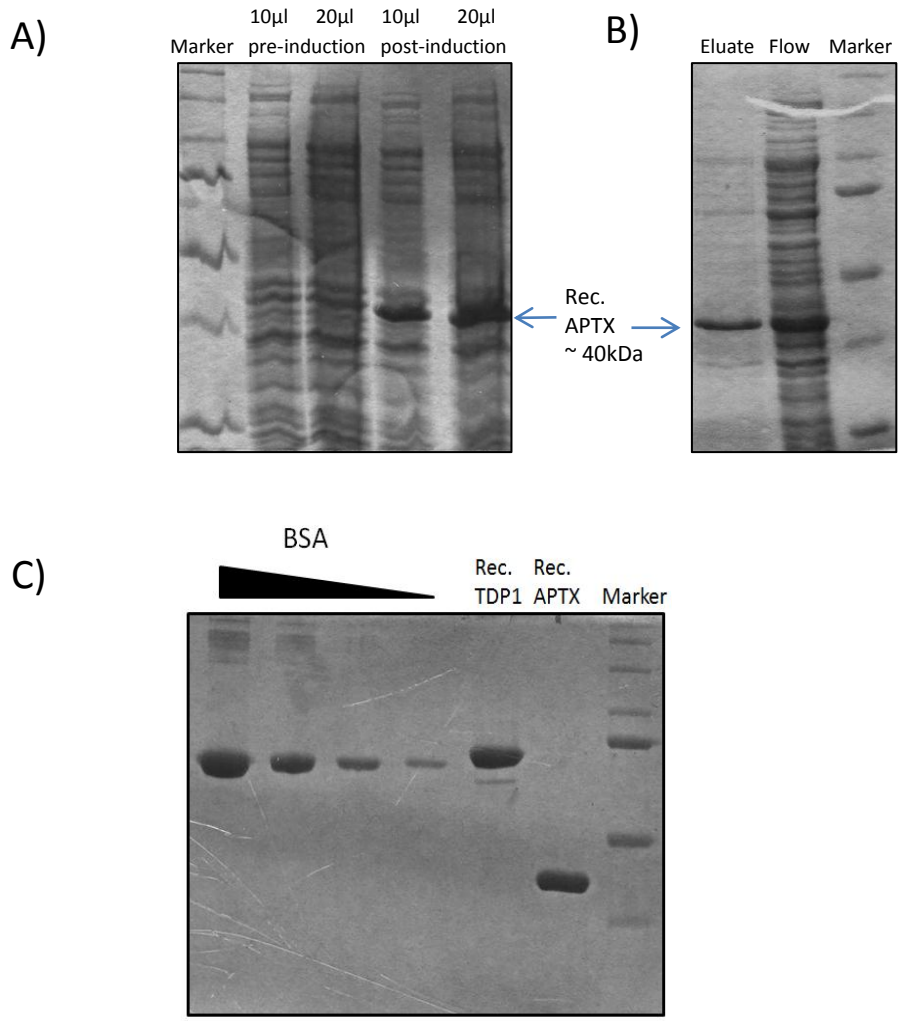

Figure 3.1 Overexpression and purification of recombinant His-tagged human APTX

A) Western blot of 10 and 20 µl supernatant samples of BL21 *E.Coli* culture transformed with the pB352_hAPTX bacterial expression vector, pre- and post-induction with 1 M IPTG. His-tagged recombinant APTX runs above the 37 kDa marker at approx. 40 kDa.

B) Flow-through and peak fraction from IMAC show presence of His-APTX.

C) Peak recombinant APTX fraction from IMAC was purified by cation exhange chromatography. Concentration was calculated to be 6.4 µM using BSA standards of 1,2,4,8 µg (Recombinant TDP1 was also prepared but was not used in this study).

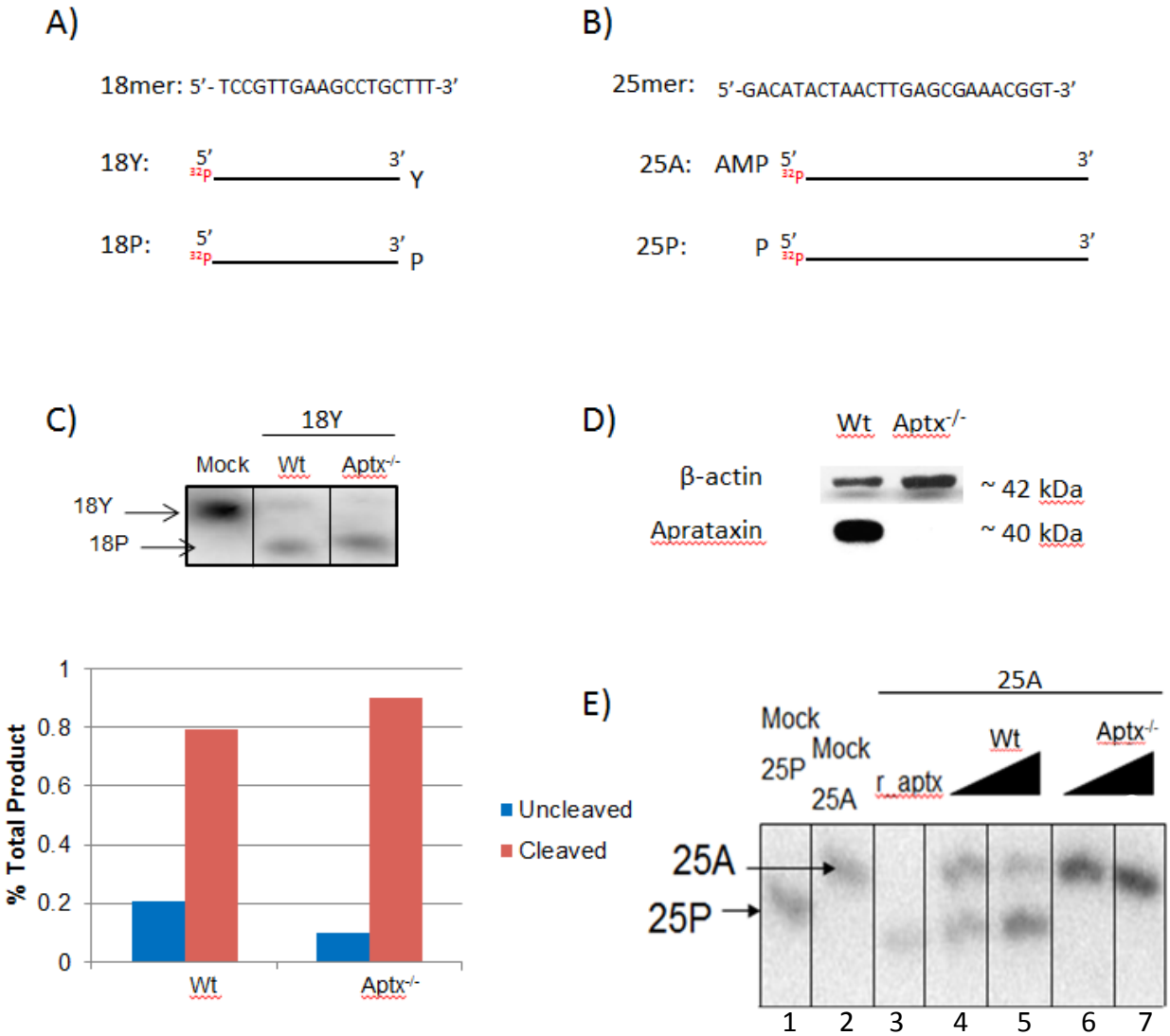

Figure 3.2 MEF lysate, DNA substrate and recombinant protein activity controls

A) Diagram of the 18mer oligonucleotide used with 3' phosphotyrosine (18Y) or 3' phosphate (18P) end.

B) Diagram showing the 25mer oligonucleotide used with 5' adenosine monophosphate (25A) or phosphate (25P).

C) Lysate activity control. *In vitro* repair assay: 3ug Wt and Aptx$^{-/-}$ lysates both cleaved 3'tyrosine from 18Y substrate, confirming enzymatic activity in both. The bar chart is a quantification of the products of each reaction, showing similar enzyme activity. The signal intensity of the 'product' band and the 'substrate' band were quantified as percentages of the total signal intensity, using ImageQuant.

D) Western blot: aprataxin protein present in Wt, and absent in Aptx$^{-/-}$ cell lysate, β-actin present in both.

E) Mutant MEF, recombinant APTX and DNA substrate control: Radiograph showing electrolysed DNA substrates alone 1: Mock 25P and 2: Mock 25A, and product of the in vitro repair reactions in with 25nmol 25A substrate was incubated with 3: Recombinant APTX and 4+5: 0.5 µg and 1.0 µg Wt MEF lysate show DNA-adenylate cleavage activity to convert the 25A substrate into the 25P product. 6+7: Similar concentrations of Aptx$^{-/-}$ lysate show no evidence of DNA-adeynlate cleavage activity, the 25A substrate remains unprocessed, confirming a lack of aprataxin activity.

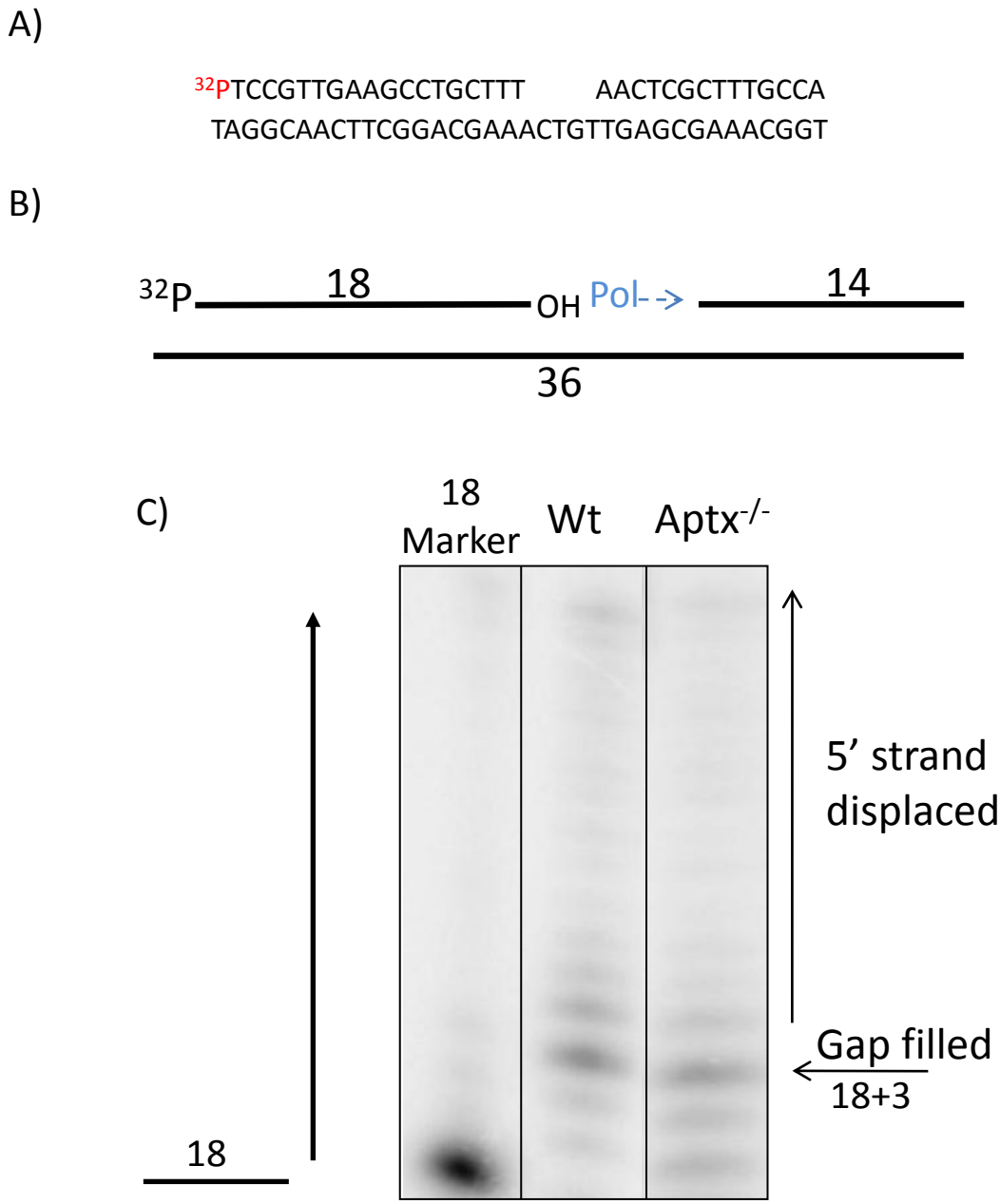

Figure 3.3 *In vitro* DNA single-strand repair assay showing 3' extension by Wt and Aptx$^{-/-}$ lysate

A) Diagram to show the gap substrate used in all further *in vitro* repair assays. An 18mer and 14mer is annealed to a 36mer, forming a DNA duplex with a 3 nucleotide gap.

B) Simplified diagram of the gap substrate showing the 18mer 3' hydroxyl – a potential substrate for gap-filling by a polymerase.

C) *In vitro* DNA single strand repair experiments: 25nmoles gap substrate were incubated with 1µg MEF cell-free extract, for 30min at 37^{o}C in reaction buffer containing 10 µM deoxynucleoside triphosphates (dNTPs), 1 mM ATP, 1000-fold molar excess of competitor oligonucleotide. The image is a radiograph showing the products of a gap-filling *in vitro* experiment, separated by urea electrophoresis DNA gel. Radiolabelled DNA products were visualised on a phosphorimager. This is a representative radiograph of three repeats.

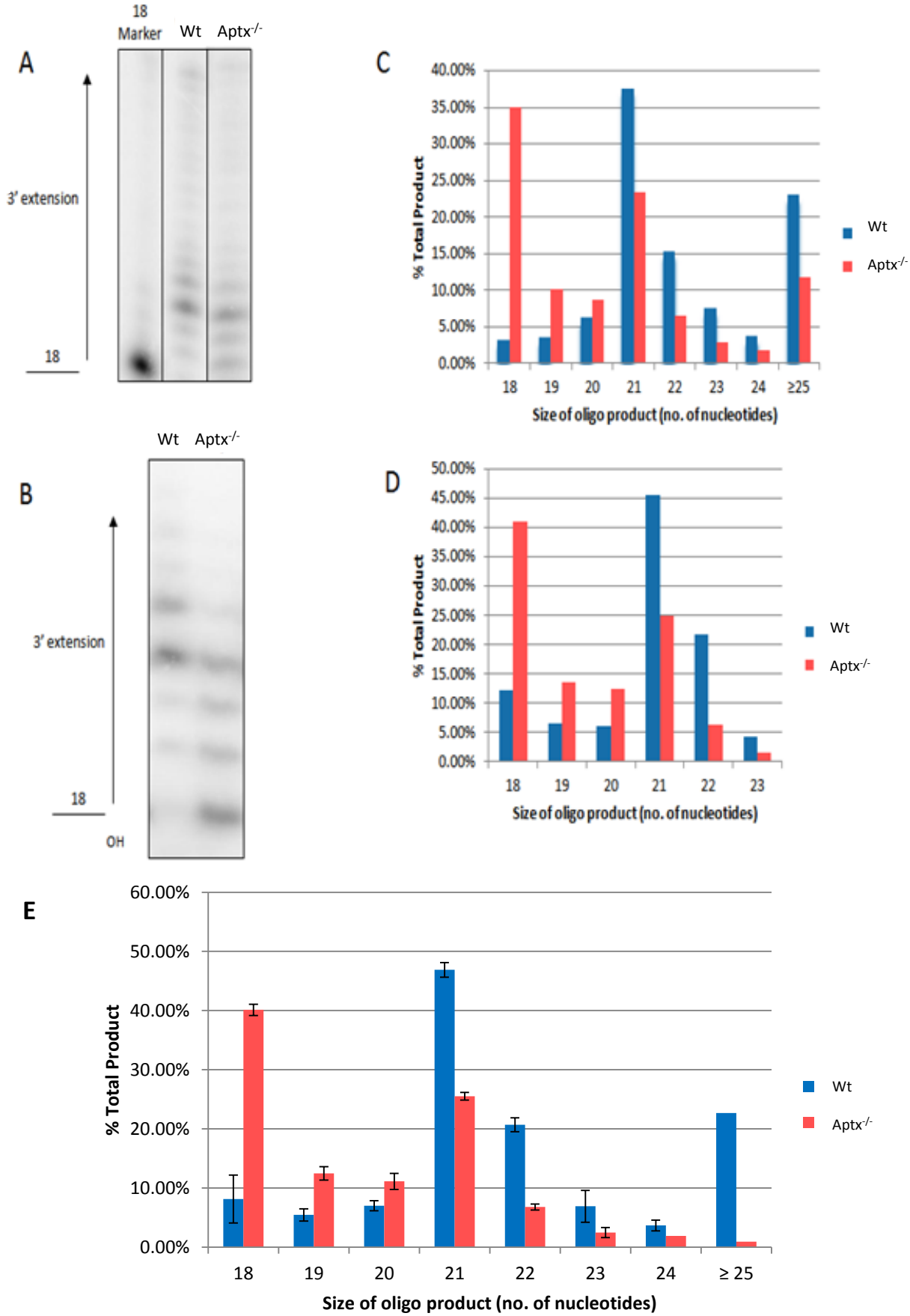

Figure 3.4: Effect of Wt or Aptx$^{-/-}$ lysate on 3' extension of a DNA gap substrate *in vitro*

A and **B:** Radiographs of electrolysed products of two similar experiments. 100nm gap substrate was incubated with either Wt or Aptx$^{-/-}$ lysate for 30 min at 37^{o}C. **C** and **D** are quantifications of **A** and **B** calculated using ImageQuant. **E:** Data from **C** and **D** combined SD calculated and plotted as error bars.

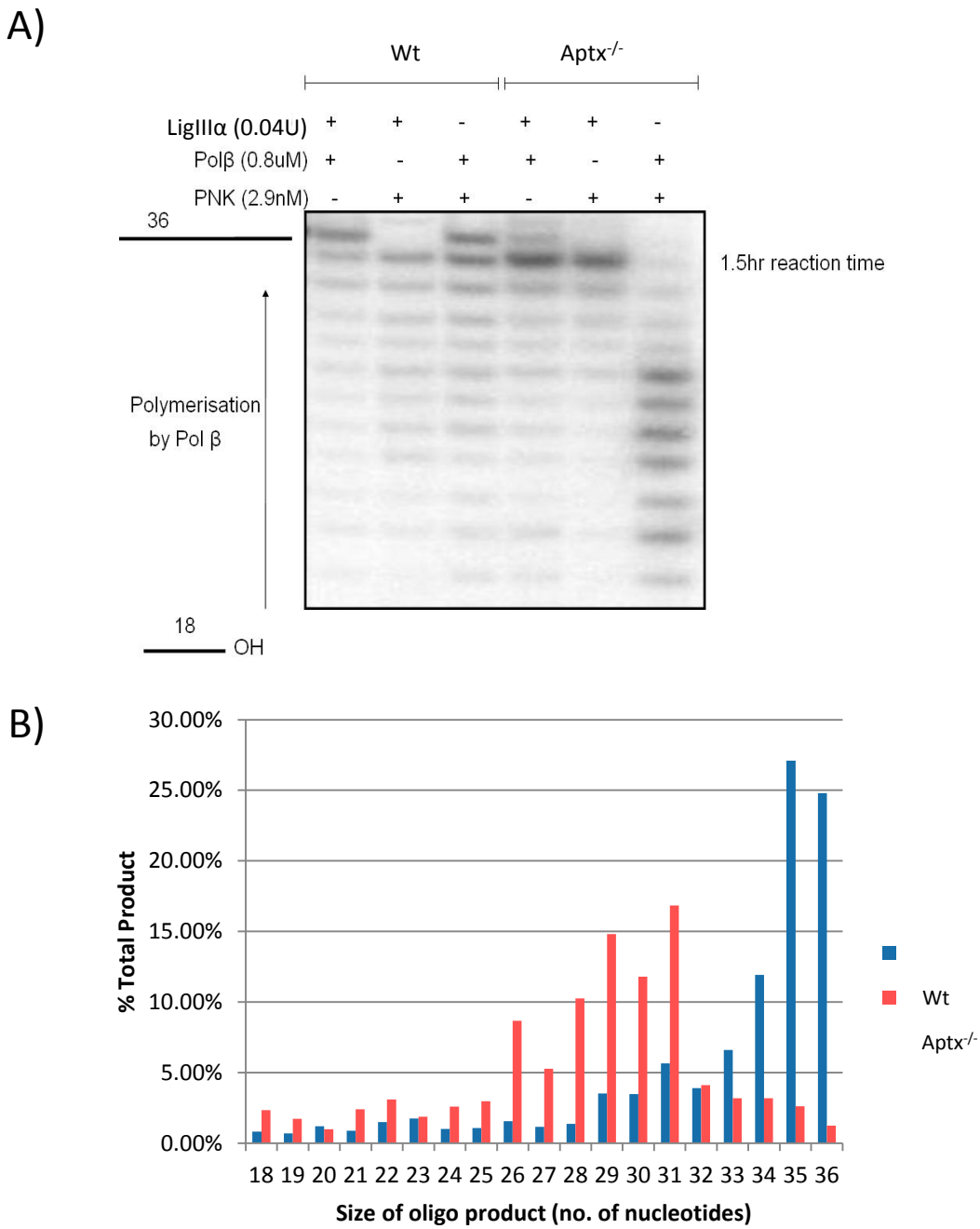

Figure 3.5: Effect of recombinant proteins on 3' extension of a DNA gap substrate, in the presence of either Wt or Aptx$^{-/-}$ lysate *in vitro*

A) Radiograph showing eletrolysed products of *in vitro* repair reactions in which 100nm gap substrate were incubated with 1µg MEF lysates, Wt or Aptx$^{-/-}$, with the addition of recombinant PNK (1nM), and/or Pol-β (0.8µM) and/or DNA Ligase III α (10nM). Reactions were run for 1.5 hrs and stopped with 90% formamide stop buffer. Products were run on a 15% denaturing PAGE gel.

B) Quantification of lanes 3 and 6, which show the gel-separated products of reactions containing PNK and Pol-β and either Wt or Aptx-/- lysates, were calculated using ImageQuant software and plotted as a bar chart.

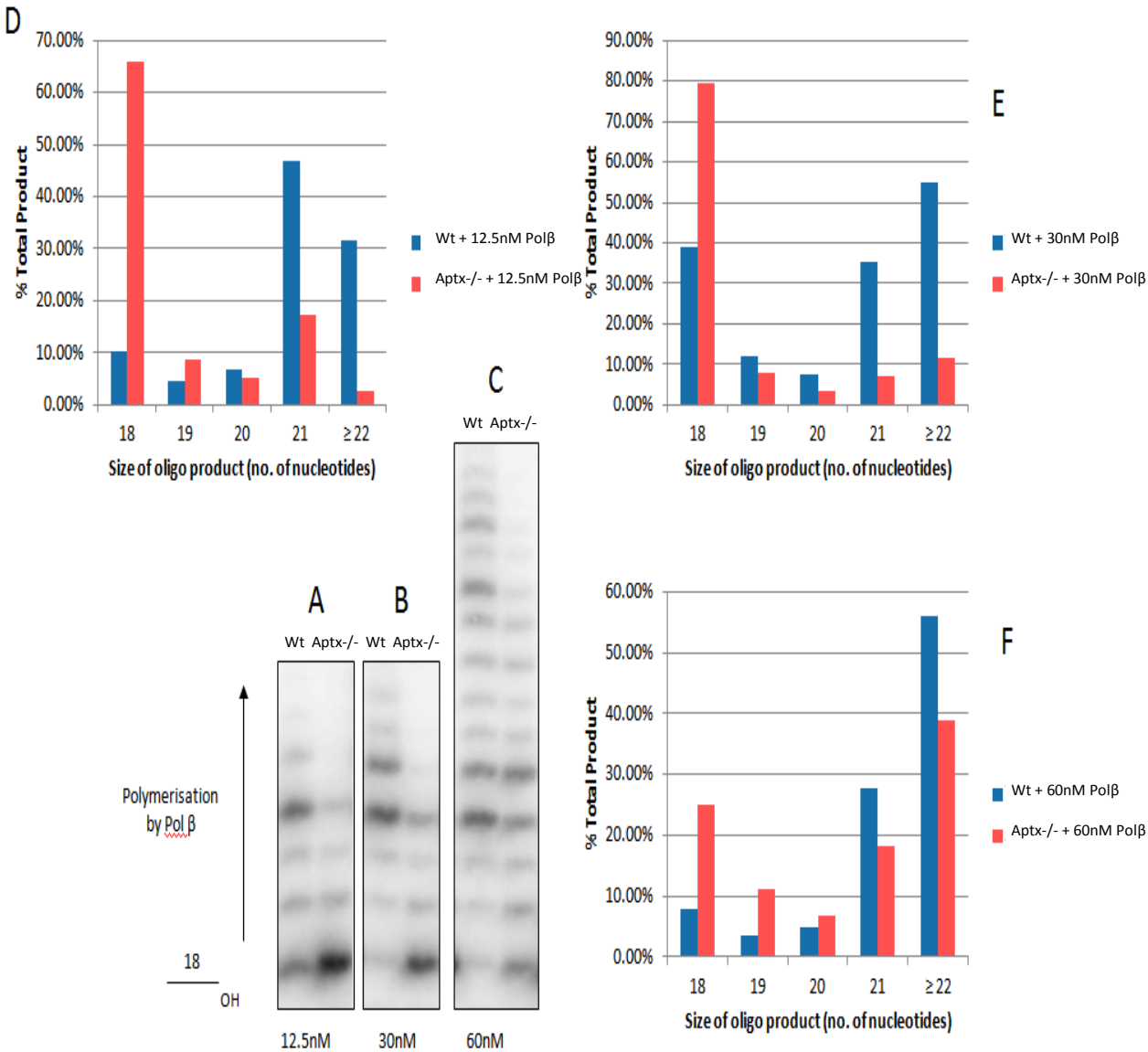

Figure 3.6: Effect of recombinant Pol β and Wt or Aptx$^{-/-}$ lysate on DNA gap substrate *in vitro*

A, **B** and **C:** Radiographs showing electrolysed products of *in vitro* repair assays in which 100nm gap substrate, incubated with a range of Pol β concentrations, from 12.5nM to 60nM in the presence of either Wt or Aptx$^{-/-}$ lysate for 30 min at 37^{o}C. 3' extension was facilitated in the presence of Wt lysate, compared with 3' extension in the presence of Aptx$^{-/-}$ lysate, over a range of concentrations of Pol-β. **D**, **E** and **F** are quantifications of **A**, **B** and **C**, respectively, calculated with ImageQuant.

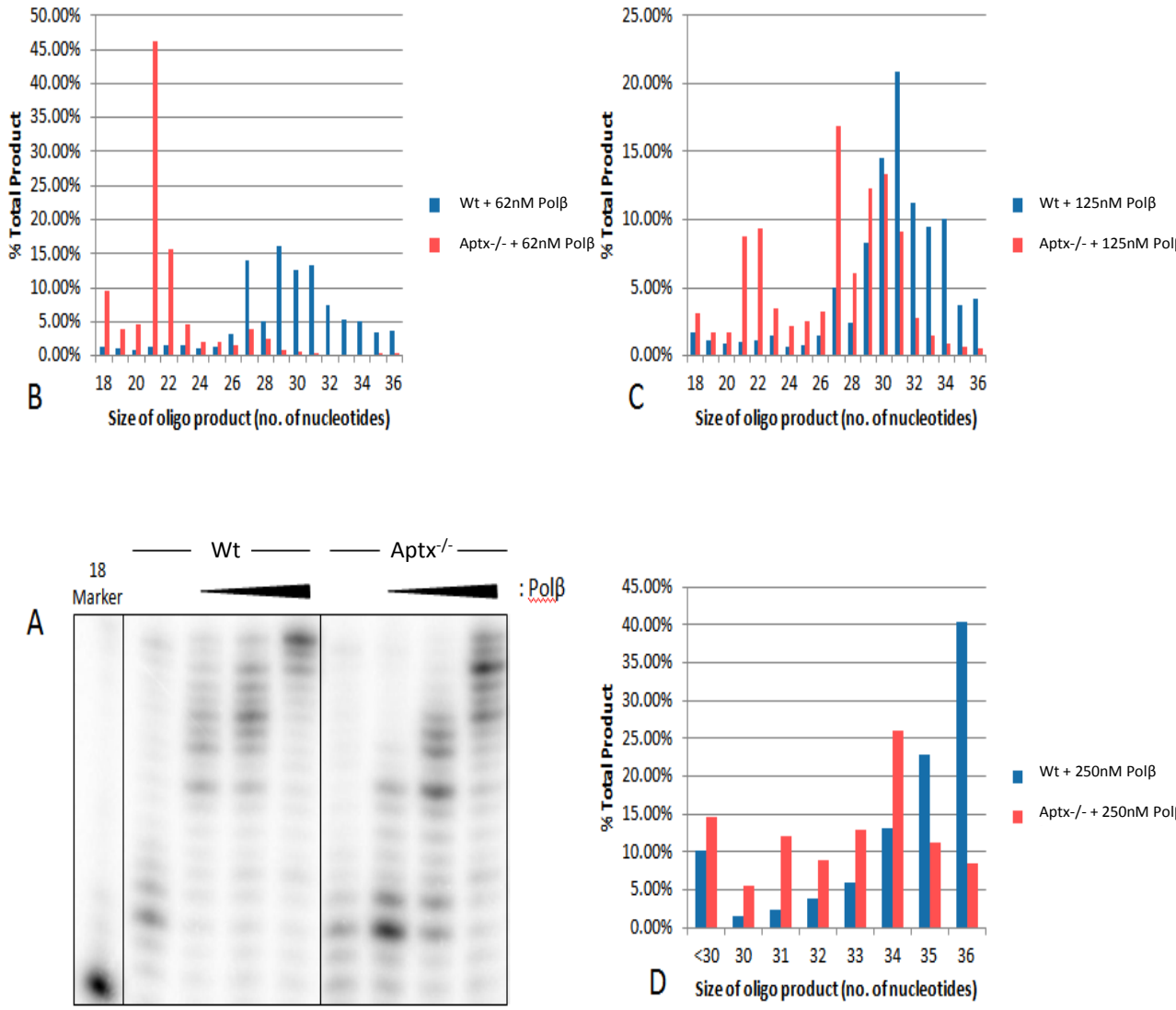

Figure 3.7: Effect of recombinant Pol-β and Wt or Aptx$^{-/-}$ lysate on DNA gap substrate *in vitro*

A: Radiograph showing electrolysed products of *in vitro* repair assays in which100nm gap substrate were incubated with either Wt or Aptx$^{-/-}$ lysate alone or with recombinant Pol β at concentrations ranging from 62nM to 250nM, for 30 min at 37^{o}C. 3' extension was facilitated in the presence of Wt lysate, compared with 3' extension in the presence of Aptx$^{-/-}$ lysate, over a range of concentrations of Pol β.

B, **C** and **D** are quantifications of the Pol β titration in **A**.

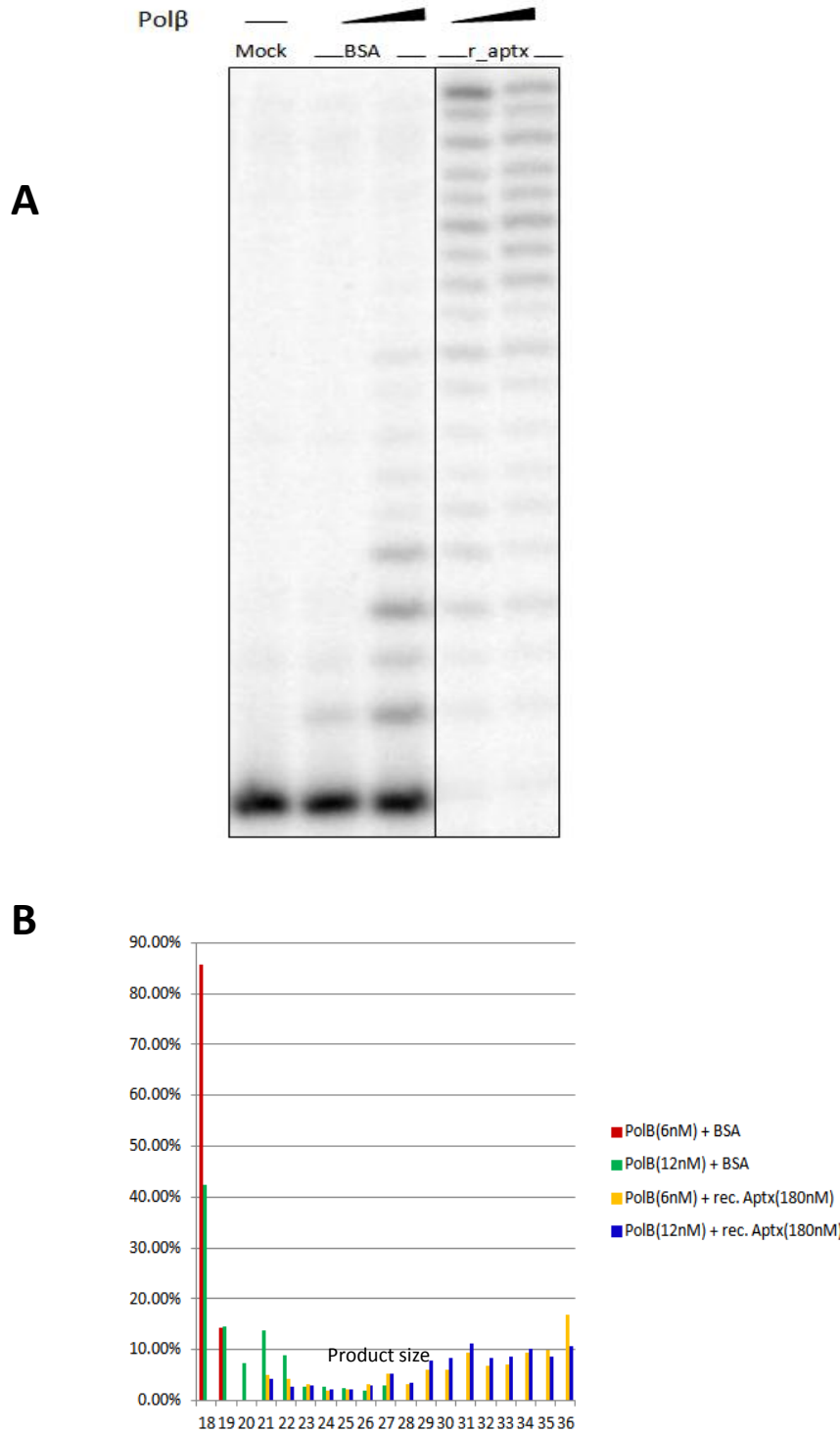

Figure 3.8: Recombinant aprataxin promotes 3' extension by recombinant Pol β

A: Radiograph showing electrolysed products of *in vitro* repair assays in which 100nm gap substrate was incubated with 6 or 12 nM Pol-β in the presence of either 180nM APTX or 180nM BSA, for 30 mins at 37°C. Reactions were stopped with formamide stop buffer and products were separated on a 15% urea gel. **B** is a quantification of % signal intensity of each product size using ImageQuant and plotted on a bar chart.

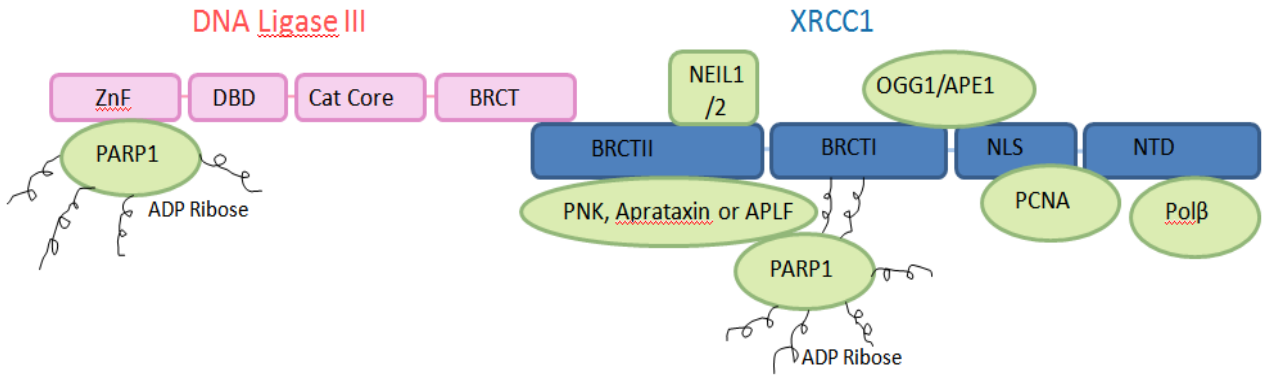

Figure 3.9: Aprataxin and Pol β both interact with XRCC1-LigIII in the major multi-protein complex of the SSBR machinery

DNA Ligase IIIα interacts with the NEIL1 and NEIL2 - DNA glycosylases that repair oxidized bases in a sub-pathway of BER, which is dependent upon PNK but not APE1. PNK, Aprataxin and APLF all have overlapping binding sites on XRCC1. Pol β also interacts with XRCC1, at the NTD. Data presented in this chapter suggest that they might interact directly in vitro. Further studies are necessary to investigate their interaction in cells.

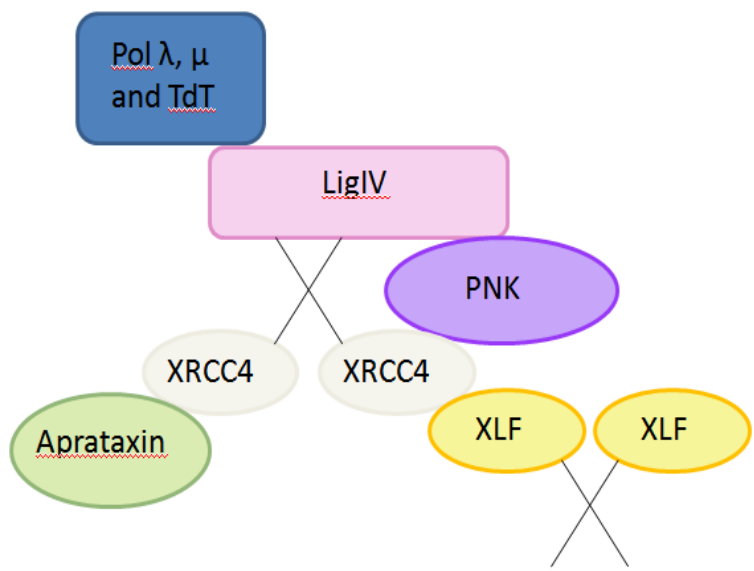

Figure 3.10: Diagram showing the interaction of aprataxin with the DSBR machinery

The X family of polymerases include Pol λ and μ terminal deoxynucleotidyl transferase (TdT). TdT is expressed only in lymphoid tissue, and adds "n nucleotides" to double-strand breaks formed during V(D)J recombination to promote immunological diversity. An interaction between aprataxin and Pol β may indicate additional interactions with other polymerases, which would suggest a role in other processes.

Chapter 4

Results (2)

How does loss of aprataxin affect growth, survival,senescence, and DNA repair in cells?

Figures

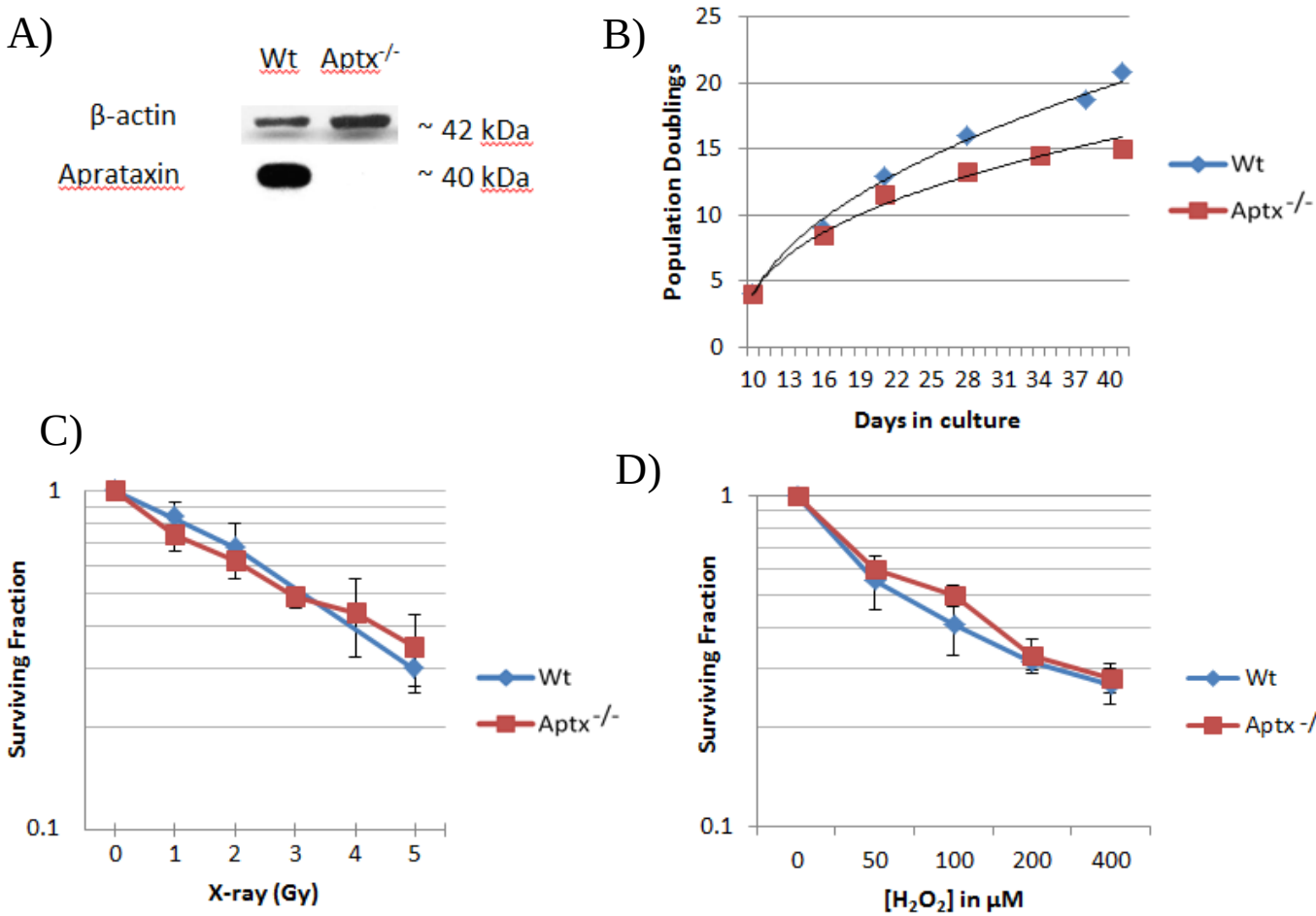

Figure 4.1: Aptx$^{-/-}$ MEFs show slightly slower growth but similar sensitivity to X-ray irradiation and H_2O_2 compared with Wt counterparts

A) Western blots of Wt and Aptx$^{-/-}$ MEF lysates confirmed lack of aprataxin expression in MEFs lacking the aprataxin gene.

B) Cells were counted at each passage. Population doublings were plotted against number of days in culture, showing that Aptx$^{-/-}$ MEFs grew more slowly in culture than Wt MEFs, from passage 1. The same trend was seen in MEFs cultured from a separate litter (Supp. Fig. 1 in Appendix II).

C) Wt and Aptx$^{-/-}$ MEFs were X-ray irradiated at the doses indicated and colonies were counted four days after treatment. The surviving fraction was plotted against X-ray irradiation dose.

D) Wt and Aptx$^{-/-}$ MEFs were treated with H_2O_2 at the doses indicated for ten minutes in the dark at RT. Colonies were counted four days after treatment. The surviving fraction was plotted against H_2O_2 dose.

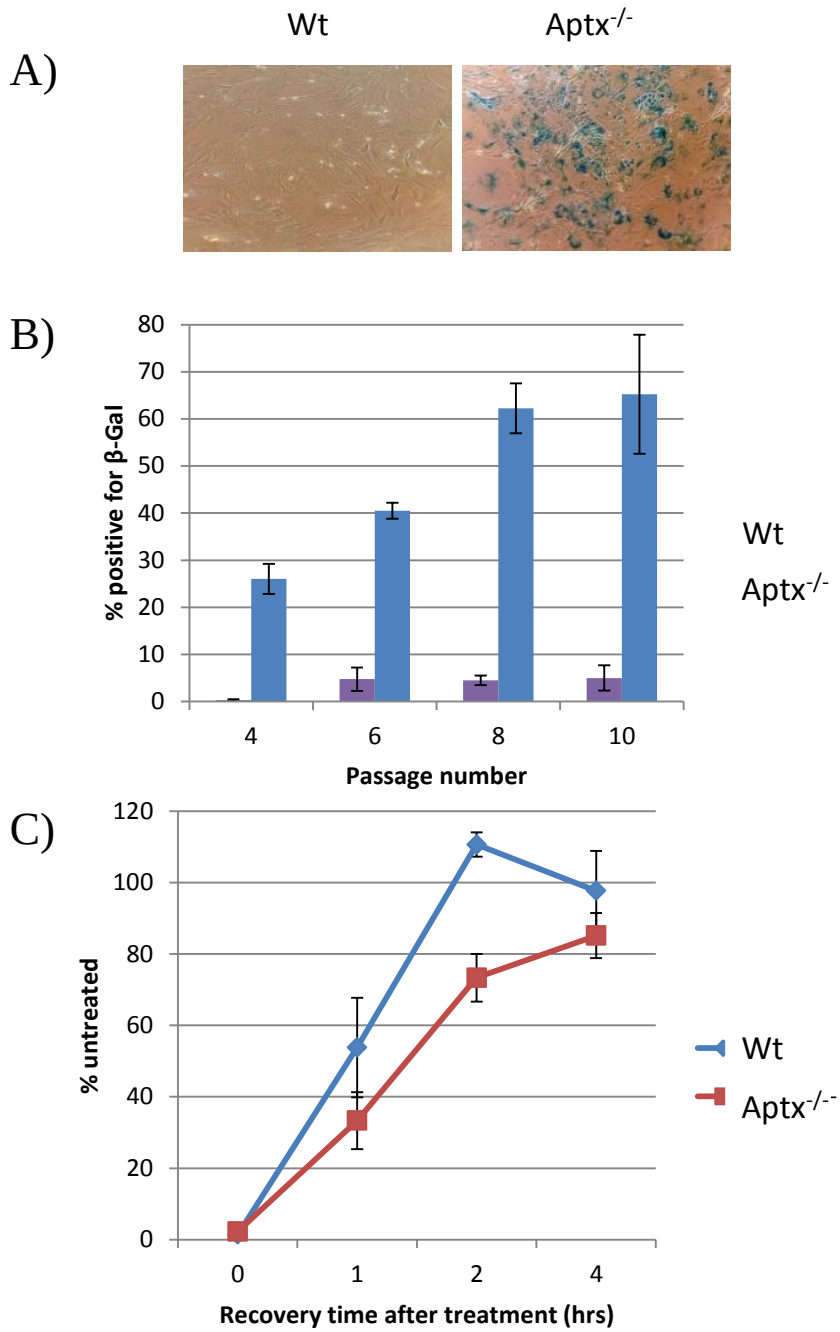

Figure 4.2: Aptx$^{-/-}$ MEFs have accelerated senescence phenotype compared to Wt

A) Representative image of β-Galactosidase at pH6 in Wt and Aptx$^{-/-}$ MEFs at passage 10. showed an accelerated passage-dependent senescence, relative to wild-type MEFs. Data were analysed by the two-way ANOVA statistical test. Significance was calculated to be $p < 0.01$.

B) RNA synthesis recovery was measured by incorporation of tritiated uridine over 15 mins in Wt and Aptx$^{-/-}$ MEFs after treatment with 50 μM H_2O_2 for 10mins, and plotted as a percentage of the RNA synthesis measured in untreated cells. MEF DNA was pre-labelled by incubation with ^{14}C-thymidine for 48 h in order to normalise RNA synthesis to DNA content.

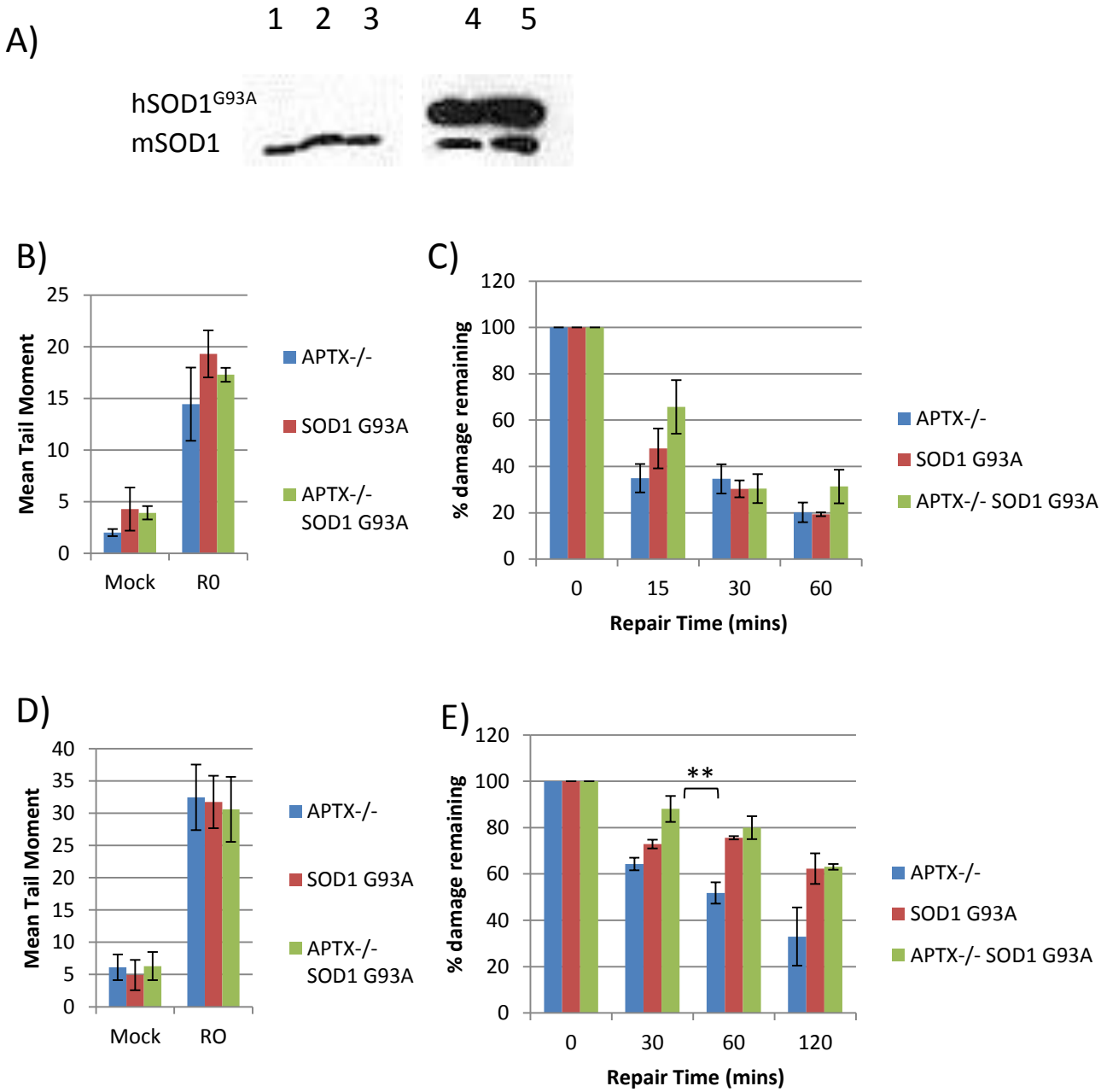

Figure 4.3: SOD1^{G93A} expression reveals defective oxidative repair in Aptx$^{-/-}$ MEFs

A) MEF lysates (1: Wild-type 2: Aptx$^{-/-}$ 3: Aptx$^{-/-}$ 4: SOD1^{G93A} 5: Aptx$^{-/-}$/SOD1^{G93A} show the presence of endogenous and mutant SOD1 by western blot.

Comet assays

B) All cell lines show similar damage induction with 20 Gy γ-radiation.

C) No significant difference in repair rate in Aptx$^{-/-}$ Sod1^{G93A} MEFs relative to SOD1^{G93A} MEFs.

D) All mutant cell lines used showed similar levels of DNA breaks induced with H_2O_2.

E) Aptx$^{-/-}$SOD1^{G93A} MEFs show synergistic repair defect at the 30 min repair time-point after H_2O_2 ($p < 0.001$). Data were analysed using a two-way ANOVA statistical test.

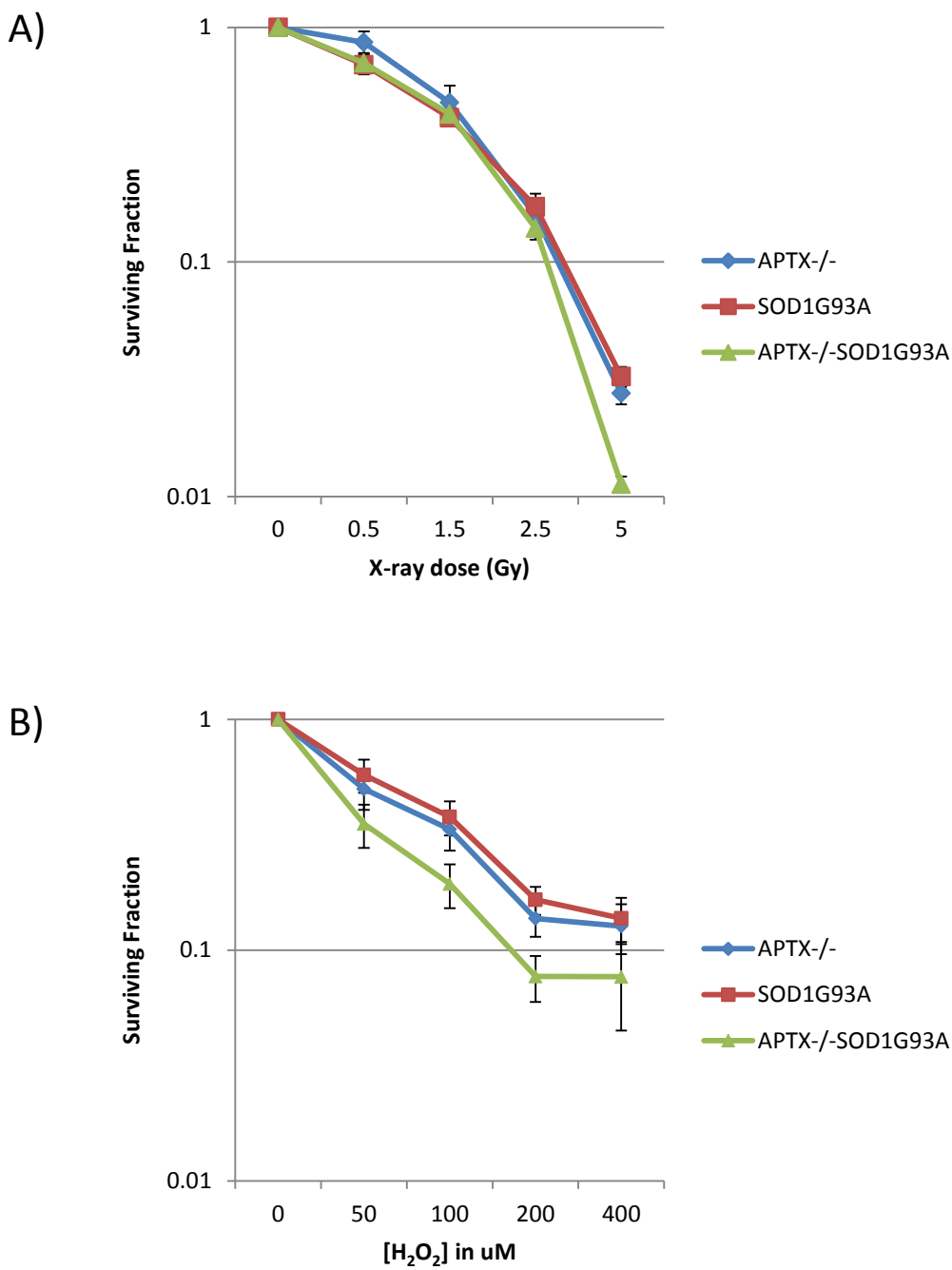

Figure 4.4 SOD1^{G93A} mutation reveals a survival defect in aprataxin-deleted MEFs following high doses of X-ray irradiation and moderate doses of H_2O_2

A) Aptx$^{-/-}$/SOD1^{G93A} MEFs showed synergistic survival defect at 5 Gy X-ray ($p = 0.03$).

B) Aptx$^{-/-}$/SOD1^{G93A} MEFs show synergistic survival defect at 100 μM ($p = 0.015$) and 200 μM ($p = 0.02$) H_2O_2. Statistical test used: Student's T-test.

Chapter Five

Results (3)

Analyses of the consequences of expression of a toxic form of SOD1 in aprataxin knockout models

Figures

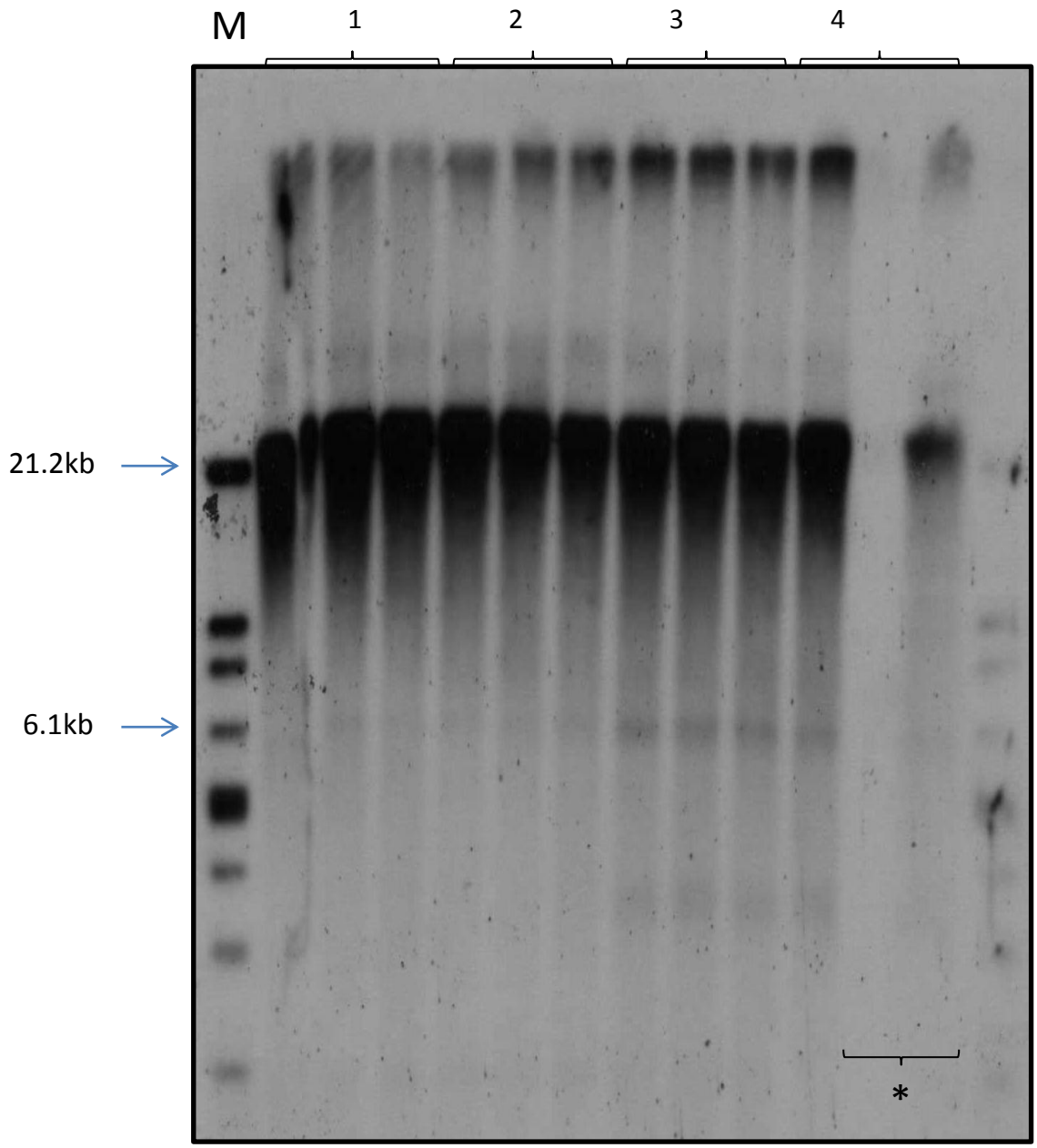

Figure 5.1 Southern blot comparing telomeric length in chromosomal MEF DNA

Assay was performed using the TeloTAGGG Telomere Length Assay® (Roche) and according to the instructions therein. Briefly, DNA was extracted from MEFs, digested by a Hinf I/Rsa I enzyme mixture for 2 h at 37°C. DNA was separated by gel electrophoresis and transferred to a positively charged nylon membrane by Southern blotting. DNA was fixed by UV-crosslinking at 120 mJ. A digoxigenin-labeled probe was used to bind to telomeric sequences. Subsequent incubation with Anti-DIG-AP for 30 min at RT, followed by substrate solution containing CDP-Star for 2-5 min at RT Lane produced chemiluminescent signal that was detected with X-ray film, indicating the length of telomeric sequences present in each sample. **M**: DNA size marker. Signal relates to telomeric sequences in eletrophoresed genomic DNA extracted from P8 MEFs **1:** Wt **2:** $Aptx^{-/-}$ **3:** $SOD1^{G93A}$ **4:** $SOD1^{G93A}/Aptx^{-/-}$

* The final two sample lanes were disrupted by a pierced well.

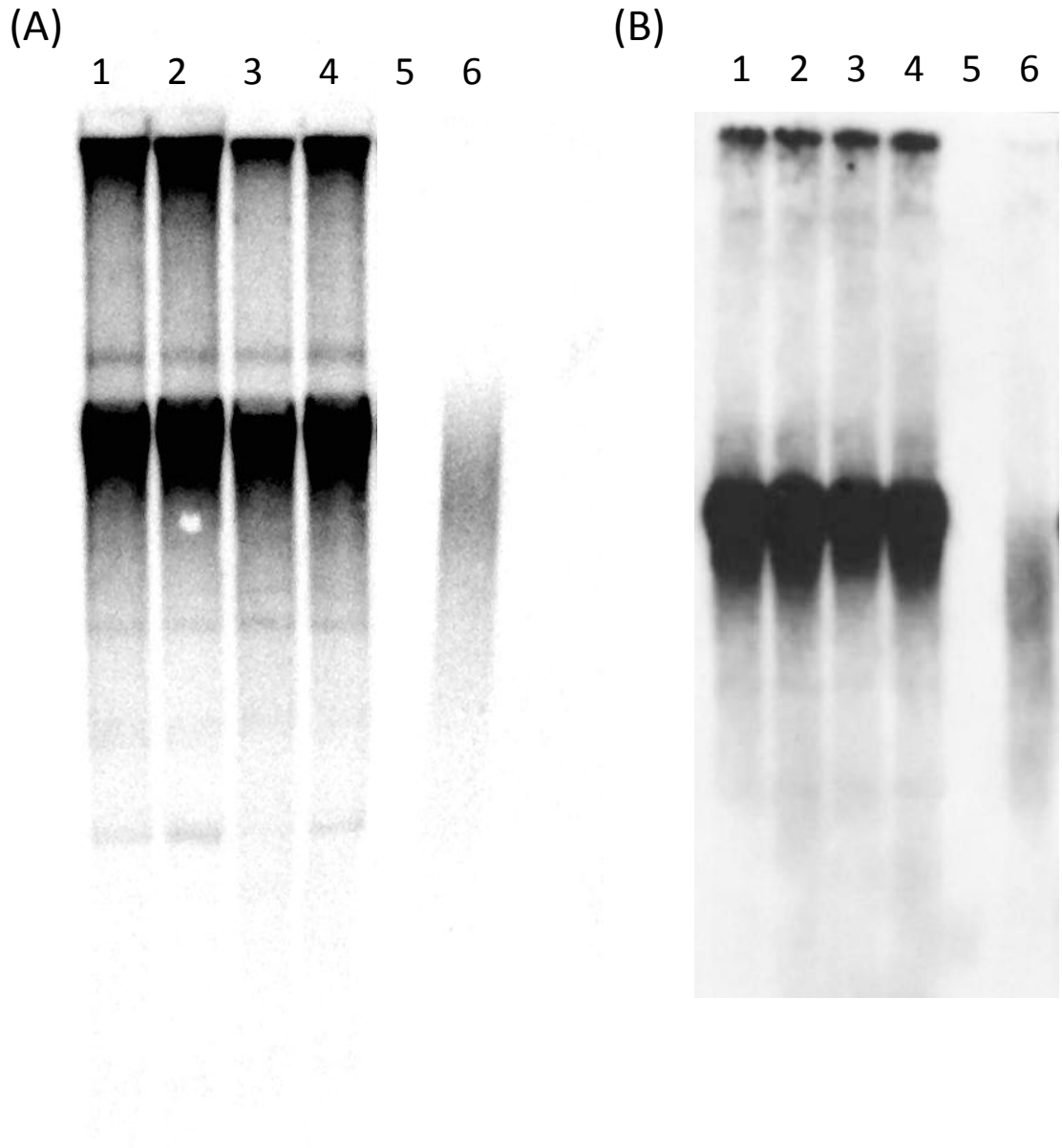

Figure 5.2 Southern blot reveals no significant difference in telomere stability with aprataxin deletion regardless of SOD1 background, with or without oxidative damage

A) Procedure as before (Figure 5.1) was carried out on genomic DNA extracted from P8 Wt and Aptx$^{-/-}$ MEFs without (-) or with (+) 50uM H_2O_2 treatment for 10 mins on three consecutive days. [lane 1 = Wt (-), lane 2 = Wt (+), lane 3 = Aptx$^{-/-}$ (-), lane 4 = Aptx$^{-/-}$ (+), lane 5 = blank, lane 6 = telomeric DNA control].

B) Procedure as before (Figure 5.1) was carried out on genomic DNA extracted from P8 MEFs without (-) or with (+) 50uM H_2O_2 treatment for 10 mins on three consecutive days [lane 1 = SOD1^{G93A} (-), lane 2 = SOD1^{G93A} (+), lane 3 = SOD1^{G93A}/Aptx$^{-/-}$ (-), lane 4 = SOD1^{G93A}/Aptx$^{-/-}$ (+), lane 5 = blank, lane 6 = telomeric DNA control].

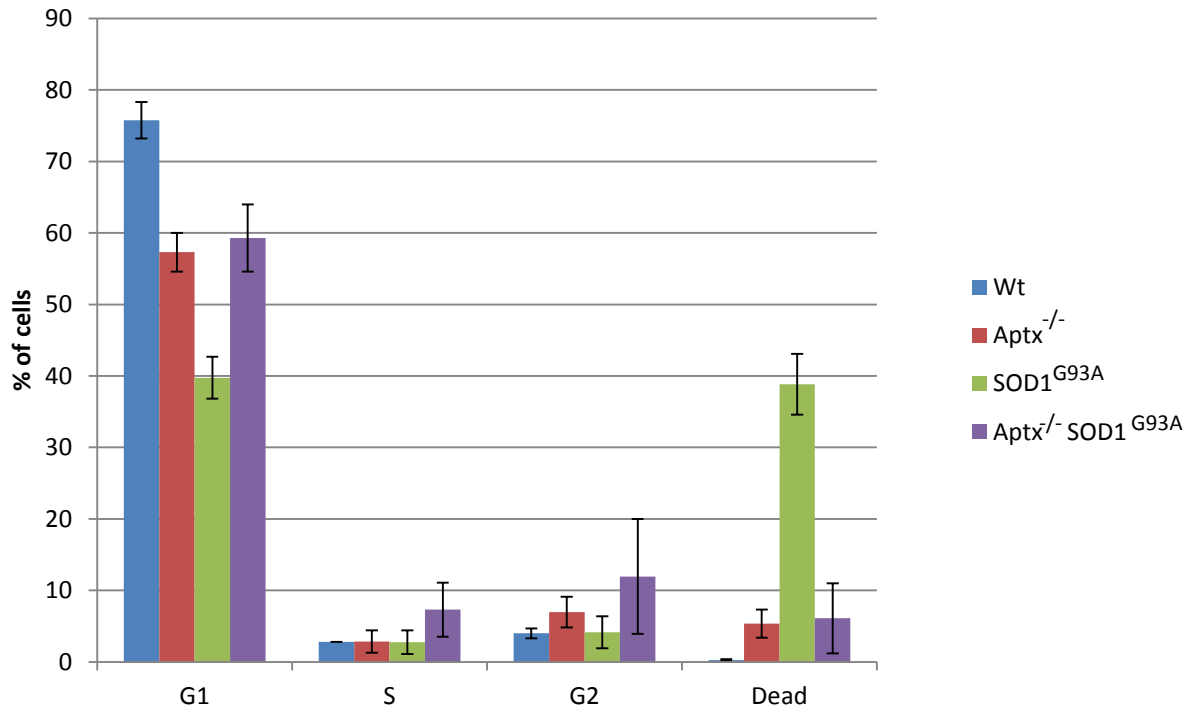

Figure 5.3. FACS analysis show a modest accumulation in S phase and a greater proportion of dead cells in the mutant cell populations compared with wild-type counterparts

FACS profiles of MEFs of each genotype: Wt, Aptx$^{-/-}$, SOD1^{G93A}, Aptx$^{-/-}$SOD1^{G93A}. Cells were sorted according to DNA density and cell size. The percentage of cells within gates 3, 4, 5 – relating approximately to cells in the G1, S and G2 phases of the cell cycle respectively, were plotted - as well as those cells with DNA density: cell size profiles suggesting that they were dead. The bar chart shows the combined data from two experiments using the same cultures, at passage 3 and 4. Raw data is provided in Figure 5.4 A and B.

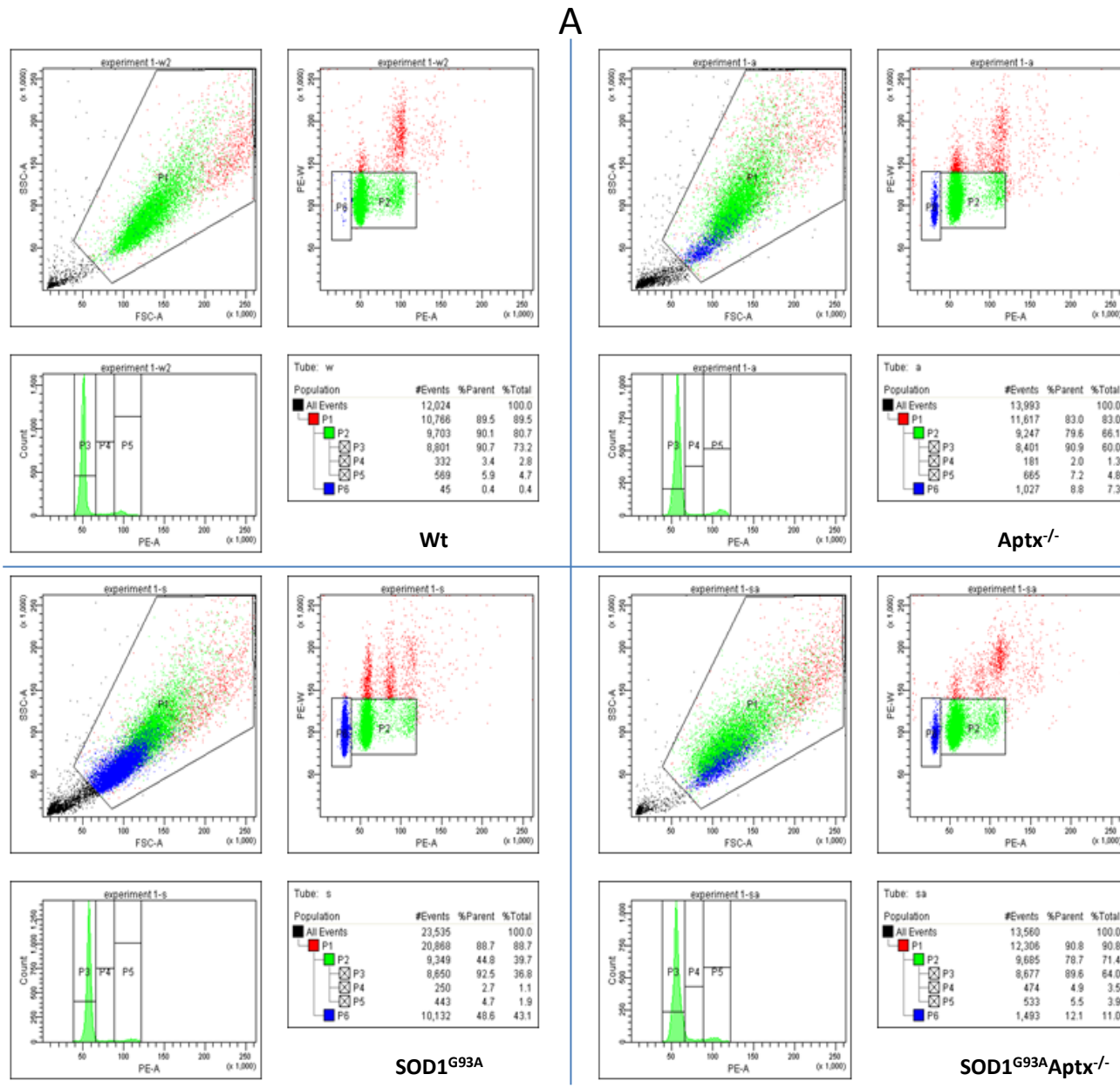

Figure 5.4 A FACS analysis show a modest accumulation in S phase and a greater proportion of dead cells in the mutant cell populations compared with wild-type

FACS profiles of MEFs of each genotype: Top left: Wt, top right: Aptx$^{-/-}$, bottom left: SOD1^{G93A}, bottom right: Aptx$^{-/-}$SOD1^{G93A}. FACS analysis profiles of MEFs of each genotype from separate cultures gave similar results (Figure 5.4). P3 = approx. proportion of cells in S phase, P4 = approx. proportion of cells in S phase, P5 = approx. proportion of cells in G2 phase.

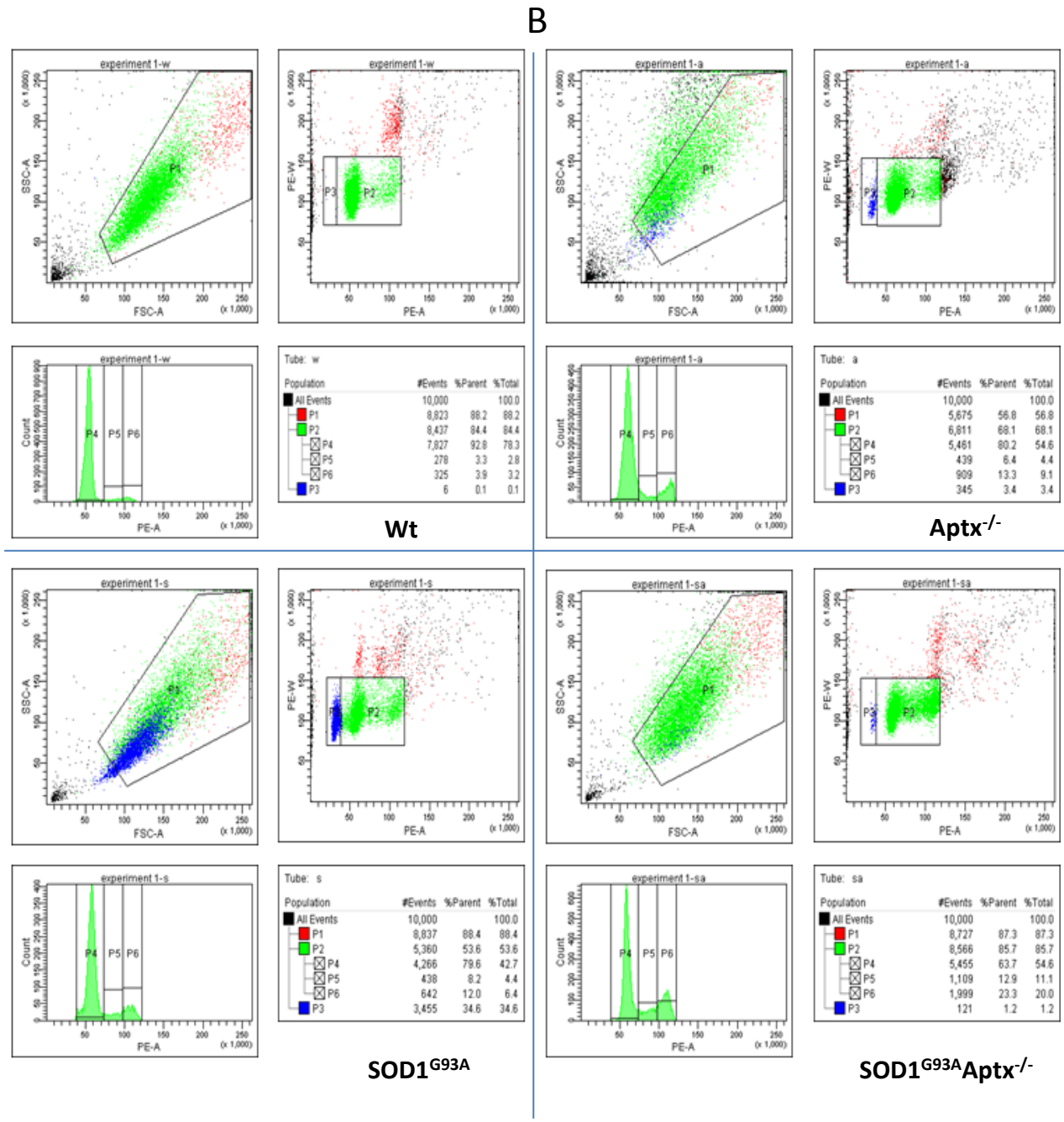

Figure 5.4. B FACS analysis show a modest accumulation in S phase and a greater proportion of dead cells in the mutant cell populations compared with wild-type

FACS analysis profiles of MEFs of each genotype: Top left, Wt, top right Aptx$^{-/-}$, bottom left SOD1^{G93A}, bottom right SOD1^{G93A}. P3 = approx. proportion of cells in S phase, P4 = approx. proportion of cells in S phase, P5 = approx. proportion of cells in G2 phase.

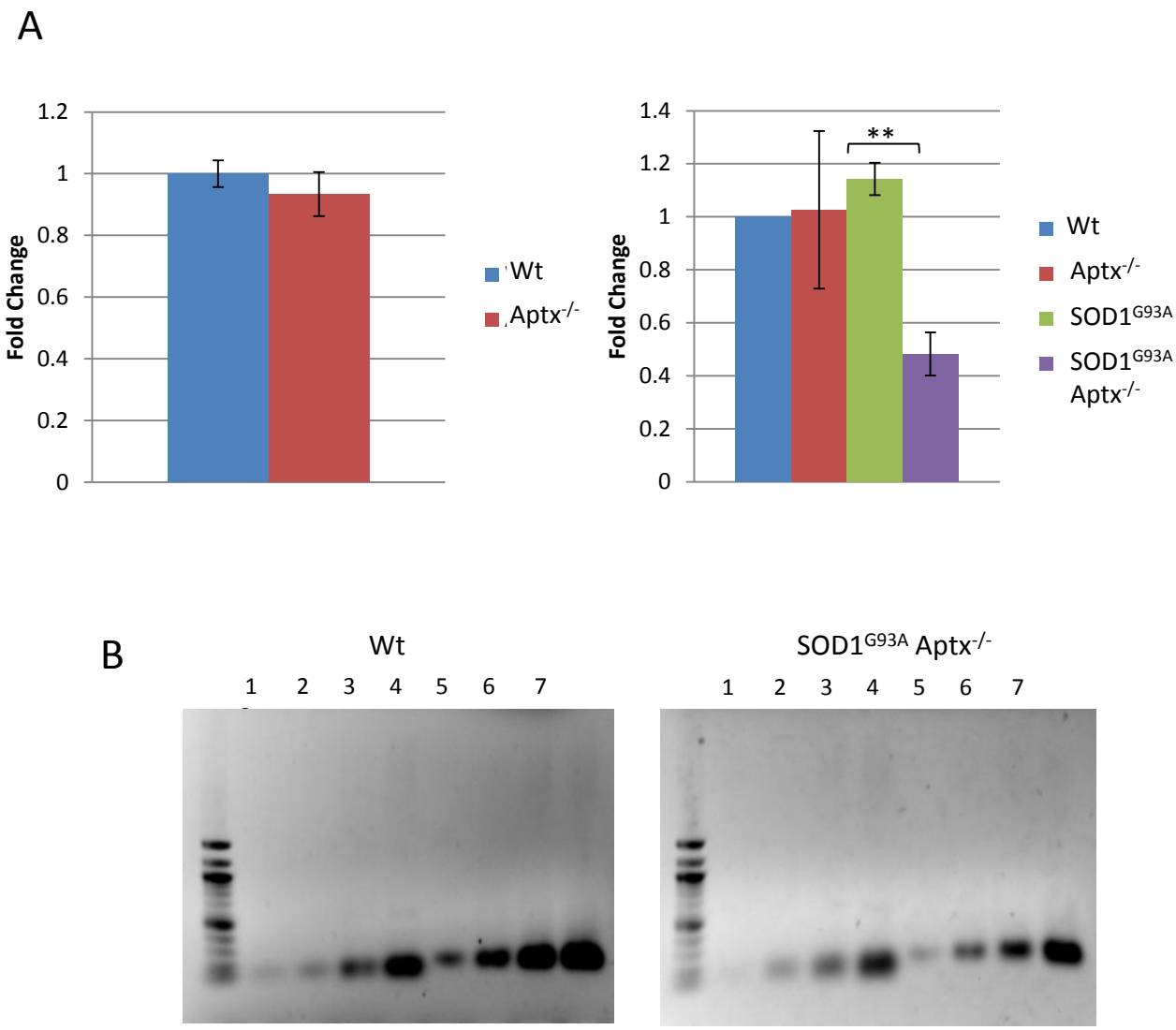

Figure 5.5 IGF-1 expression is down-regulated in SOD1^{G93A}Aptx$^{-/-}$ mouse liver

A) RNA was extracted using an RNeasy Plus Mini Kit (Qiagen) in triplicate from at least two livers from each genotype. cDNA was generated with the Promega reverse transcription system. SYBR Green master mix and a Stratagene Mx4000 qPCR system was used for analysis. qPCR analysis revealed no significant difference between wild-type and either of the single mutants - aprataxin-deleted or SOD1^{G93A}, but a marked down-regulation of IGF-1 was revealed in SOD1^{G93A}Aptx$^{-/-}$ double mutants relative to wild-type ($p < 0.01$) and SOD1^{G93A} mutants ($p < 0.001$). Data was analysed across experiments by Student's T-Test.

B) cDNA generated as above was amplified by PCR using Taq DNA polymerase (Roche) with either β-actin primers (reactions 1-4) or IGF-1 primers (reactions 5-8). Separate reactions were stopped at 24,27,30 and 33 cycles and run on a 0.8% agar gel.

Chapter Six

Discussion

Figures

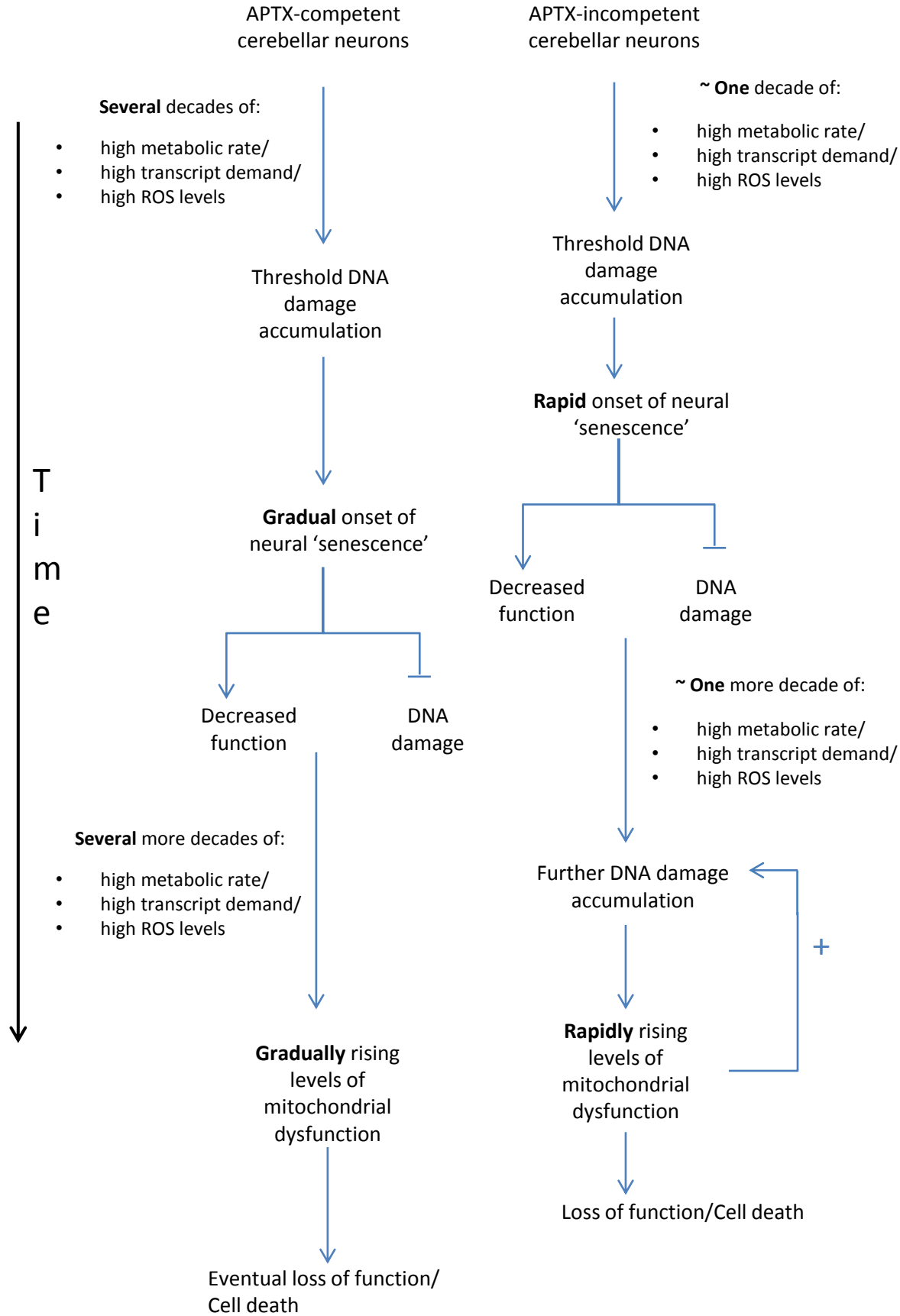

Figure 6.1 Model for AOA1 as a cerebellar-specific progeroid disorder

A schematic model of AOA1 disease progression, in which symptoms arise as the results of reiterative cycles of DNA damage and response – leading to increasing loss of function and eventual cell death.